

AD-A189 714

AN EXPERIMENTAL INVESTIGATION OF ROCKET RAMJET NOZZLE
ASSEMBLY BASE PRESSURES(U) AIR FORCE INST OF TECH
WRIGHT-PATTERSON AFB OH T R WESLING DEC 87

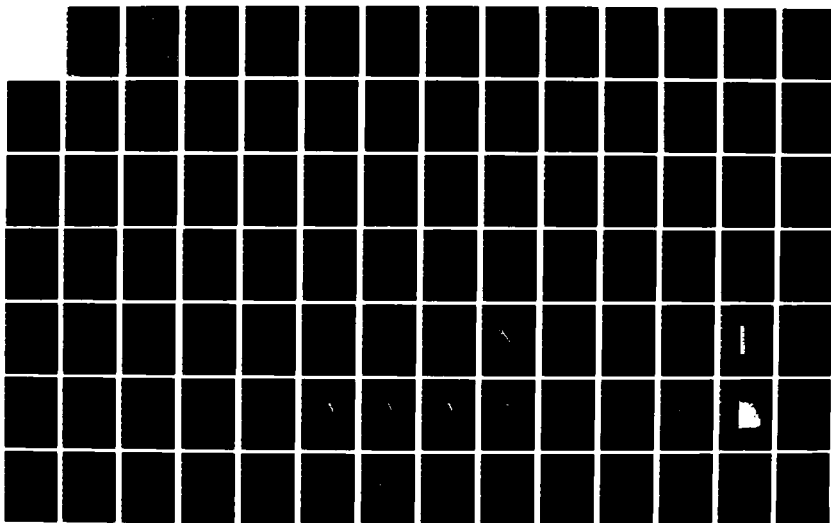
1/2

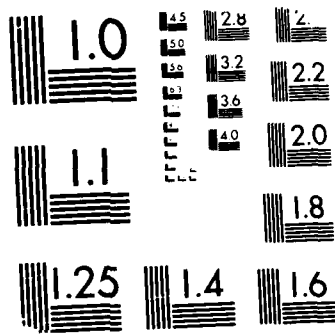
UNCLASSIFIED

AFIT/GA/AA/87D-9

F/G 21/8

NL





MICROCOPY RESOLUTION TEST CHART
NATIONAL BUREAU OF STANDARDS 1963-A

DTIC FILE COPY

AD-A189 714



AN EXPERIMENTAL INVESTIGATION OF
ROCKET RAMJET NOZZLE
ASSEMBLY BASE PRESSURES

THESIS

Timothy R. Wesling
Captain, USAF

AFIT/GA/AA/87D-9

DTIC

TE

MAR 07 1988

DEPARTMENT OF THE AIR FORCE
AIR UNIVERSITY

AIR FORCE INSTITUTE OF TECHNOLOGY

Wright-Patterson Air Force Base, Ohio

DISTRIBUTION STATEMENT A

Approved for public release;
Distribution Unlimited

88 3 01 063

AFIT/GA/AA/87D-9

AN EXPERIMENTAL INVESTIGATION OF
ROCKET RAMJET NOZZLE
ASSEMBLY BASE PRESSURES

THESIS

Timothy R. Wesling
Captain, USAF

AFIT/GA/AA/87D-9

DTIC

MAR 07 1988

CA H

Approved for public release; distribution unlimited

AN EXPERIMENTAL INVESTIGATION OF
ROCKET RAMJET NOZZLE
ASSEMBLY BASE PRESSURES

THESIS

Presented to the Faculty of the School of Engineering
of the Air Force Institute of Technology
Air University
In Partial Fulfillment of the
Requirements for the Degree of
Master of Science in Astronautical Engineering

Timothy R. Wesling
Captain, USAF

December 1987

Approved for public release; distribution unlimited

Preface

I selected my topic with three purposes in mind. My first intention is to put to actual practice what I am learning in my academic program at AFIT. My course sequence in rocket propulsion fits in well with an experimental thesis on rocket ramjets. The second purpose is to use what I had learned at the Air Force Rocket Propulsion Laboratory during my first assignment in the Air Force . My experimental work there was an appropriate lead in to an experimental thesis here at AFIT. My third aim is to augment my class room studies with hands-on experience that will help me gain interesting future assignments. This study on rocket ramjet nozzles has met these objectives in an outstanding fashion.

This successful effort was due entirely to the selfless and dedicated efforts of my thesis advisor, Dr. W. C. Elrod. He gave as much time as was possible and was always helpful and thoughtful. His technical and engineering expertise were invaluable. Dr. Elrod is one professor I will always remember for the way he made a sometimes arduous task enjoyable. The other members of my committee, Dr. M. Franke and Lt Planeaux, each made important contributions to this project. I appreciate their support and advice.

The laboratory technicians have my deepest appreciation for their assistance with this project. Messrs. Nick Yardich, Leroy Canon and Gerald Hild provided invaluable assistance and solutions to technical problems. Thanks also go to the people in the Technical Photo Branch of the Aeronautical Systems Division. I would also like to recognize Mr. John Brohas from the AFIT Model Shop. Mr. Brohas took crude drawings and

A vertical strip of 14 small images showing the progression of a 15-puzzle from an initial state to a solved state. The images are arranged in a single column, with the initial state at the top and the solved state at the bottom. The puzzle is a 4x4 grid with 15 numbered tiles and one empty space. The tiles are numbered 1 through 15, and the empty space is represented by a black square. The sequence shows the tiles being moved around the grid until they are in their correct positions.

U.S. CUSTOMS
INSPECTOR
1

[illegible]

Table of Contents

	Page
Preface	ii
List of Figures	vi
List of Tables	xi
List of Symbols	xii
Abstract	xiv
I. Introduction	1
Objectives	2
Scope	3
Approach	3
II. Theory	5
Rockets	5
Ramjets	8
Combined Rocket-Ramjet Engine Operation	9
III. Experimental Apparatus	12
Flow System	12
Test Sections	13
Nozzles	18
Nozzle Assembly Configurations Investigated	18
Instrumentation	21
Schlieren System	23
IV. Data Acquisition and Reduction System	25
V. Experimental Procedure	33
Calibration	33
Experiment Run Procedure	35
VI. Results and Discussions	41
Baseline and Types of Comparisons	44
Unshrouded Baseline, Rocket Flow Only	45
Unshrouded, Close Ramjet Nozzle, Low/Low AR	49
Unshrouded, Close Ramjet Nozzle, High/High AR	57
Unshrouded, Far Ramjet Nozzle, Low/Low AR	63

	Page
Unshrouded, Far Ramjet Nozzle, High/High AR	71
Close Shrouded Baseline, Rocket Flow Only	78
Close Shrouded, Close Ramjet Nozzle, Low/Low AR	80
Close Shrouded, Close Ramjet Nozzle, High/High AR	91
Shrouded, Far Ramjet Nozzle, Low/Low AR	98
Shrouded, Far Ramjet Nozzle, High/High AR	101
Shrouded, Close Ramjet Nozzle, Low/Low AR	114
Shrouded, Close Ramjet Nozzle, High/High AR	121
VII. Conclusions	130
VIII. Recommendations	133
Bibliography	134
Vita	136

List of Figures

Figure	Page
1. Nozzle Operating Diagram	6
2. Performance of Basic Cycles	10
3. Blowdown Wind Tunnel Flow System	14
4. Far Ramjet Nozzle Cluster Assembly	16
5. Transducer Locations	17
6. Schlieren System	24
7. Hardware Components	27
8. HP 6901S System Schematic	28
9. Data Flow Path	30
10. HP 6901S Menu Utilities Operational Diagram	31
11. Transducer Calibration Hardware	34
12. Transducer Null Adjustment Circuitry	37
13. Potentiometer Amplifier	38
14. Typical Recirculation in the Model Base Area	43
15. P3, P4, P5 and P6 Vs Time for Baseline, Rocket Flow Only, Unshrouded Base Pressures	47
16. Typical Back Pressure Curve	48
17. P3, P4, P5 and P6 Vs Time for Unshrouded, Close Ramjet Nozzle, Low/Low AR; $P_{rjp} = 42$ psia	50
18. Typical Flow Pattern for Unshrouded, Close Ramjet Nozzle, Low/Low AR	51
19. P3, P4, P5 and P6 Vs Time for Unshrouded, Close Ramjet Nozzle, Low/Low AR; $P_{rjp} = 52$ psia	53
20. P3, P4, P5 and P6 Vs Time for Unshrouded, Close Ramjet Nozzle, Low/Low AR; $P_{rjp} = 62$ psia	54

Figure	Page
21. P3, P4, P5 and P6 Vs Time for Unshrouded, Close Ramjet Nozzle, Low/Low AR; $P_{rjp} = 72$ psia	55
22. P3, P4, P5 and P6 Vs Time for Unshrouded, Close Ramjet Nozzle, Low/Low AR; $P_{rjp} = 87$ psia	56
23. P3, P4, P5 and P6 Vs Time for Unshrouded, Close Ramjet Nozzle, High/High AR; $P_{rjp} = 42$ psia	58
24. P3, P4, P5 and P6 Vs Time for Unshrouded, Close Ramjet Nozzle, High/High AR; $P_{rjp} = 52$ psia	59
25. P3, P4, P5 and P6 Vs Time for Unshrouded, Close Ramjet Nozzle, High/High AR; $P_{rjp} = 62$ psia	60
26. P3, P4, P5 and P6 Vs Time for Unshrouded, Close Ramjet Nozzle, High/High AR; $P_{rjp} = 72$ psia	61
27. P3, P4, P5 and P6 Vs Time for Unshrouded, Close Ramjet Nozzle, High/High AR; $P_{rjp} = 87$ psia	62
28. P3, P4, P5 and P6 Vs Time for Unshrouded, Far Ramjet Nozzle, Low/Low AR; $P_{rjp} = 42$ psia	64
29. Typical Flow Pattern for Unshrouded, Far Ramjet Nozzle, Low/Low AR	65
30. P3, P4, P5 and P6 Vs Time for Unshrouded, Far Ramjet Nozzle, Low/Low AR; $P_{rjp} = 52$ psia	67
31. P3, P4, P5 and P6 Vs Time for Unshrouded, Far Ramjet Nozzle, Low/Low AR; $P_{rjp} = 62$ psia	68
32. P3, P4, P5 and P6 Vs Time for Unshrouded, Far Ramjet Nozzle, Low/Low AR; $P_{rjp} = 72$ psia	69
33. P3, P4, P5 and P6 Vs Time for Unshrouded, Far Ramjet Nozzle, Low/Low AR; $P_{rjp} = 87$ psia	70
34. P3, P4, P5 and P6 Vs Time for Unshrouded, Far Ramjet Nozzle, High/High AR; $P_{rjp} = 42$ psia	72
35. P5 and P6 Vs Time for Unshrouded, Low/Low and High/ High AR, Far Ramjet Nozzle; $P_{rjp} = 42$ psia	73

Figure	Page
36. P3, P4, P5 and P6 Vs Time for Unshrouded, Far Ramjet Nozzle, High/High AR; $P_{rjp} = 52$ psia	74
37. P3, P4, P5 and P6 Vs Time for Unshrouded, Far Ramjet Nozzle, High/High AR; $P_{rjp} = 62$ psia	75
38. P3, P4, P5 and P6 Vs Time for Unshrouded, Far Ramjet Nozzle, High/High AR; $P_{rjp} = 72$ psia	76
39. P3, P4, P5 and P6 Vs Time for Unshrouded, Far Ramjet Nozzle, High/High AR; $P_{rjp} = 87$ psia	77
40. P4 and P5 Vs Time for Unshrouded, Far Ramjet Nozzle, High/High AR: Effect of Increasing P_{rjp}	79
41. P3, P4, P5 and P6 Vs Time for Baseline, Rocket Flow Only, Close Shrouded Base Pressures . . .	81
42. P3 Vs Time for Baseline Unshrouded and Close Shrouded Configurations	82
43. P3, P4, P5 and P6 Vs Time for Close Shrouded, Close Ramjet Nozzle, Low/Low AR; $P_{rjp} = 42$ psia	83
44. Typical Flow Pattern for Close Shrouded, Close Ramjet Nozzle, Low/Low AR	84
45. P3 Vs Time for Low P_{rjp} Unshrouded and Close Shrouded, Close Ramjet Nozzle, and Low/Low AR Configurations	86
46. P3, P4, P5 and P6 Vs Time for Close Shrouded, Close Ramjet Nozzle, Low/Low AR; $P_{rjp} = 52$ psia	87
47. P3, P4, P5 and P6 Vs Time for Close Shrouded, Close Ramjet Nozzle, Low/Low AR; $P_{rjp} = 62$ psia	88
48. P3, P4, P5 and P6 Vs Time for Close Shrouded, Close Ramjet Nozzle, Low/Low AR; $P_{rjp} = 72$ psia	89
49. P3, P4, P5 and P6 Vs Time for Close Shrouded, Close Ramjet Nozzle, Low/Low AR; $P_{rjp} = 87$ psia	90
50. Typical Flow Pattern for Close Shrouded, Close Ramjet Nozzle, High/High AR	92
51. P3, P4, P5 and P6 Vs Time for Close Shrouded, Close Ramjet Nozzle, High/High AR; $P_{rjp} = 42$ psia	93

Figure	Page
52. P3, P4, P5 and P6 Vs Time for Close Shrouded, Close Ramjet Nozzle, High/High AR; $P_{rjp} = 52$ psia	94
53. P3, P4, P5 and P6 Vs Time for Close Shrouded, Close Ramjet Nozzle, High/High AR; $P_{rjp} = 62$ psia	95
54. P3, P4, P5 and P6 Vs Time for Close Shrouded, Close Ramjet Nozzle, High/High AR; $P_{rjp} = 72$ psia	96
55. P3, P4, P5 and P6 Vs Time for Close Shrouded, Close Ramjet Nozzle, High/High AR; $P_{rjp} = 87$ psia	97
56. P3, P4, P5 and P6 Vs Time for Shrouded, Far Ramjet Nozzle, Low/Low AR; $P_{rjp} = 42$ psia	99
57. Typical Flow Pattern for Shrouded, Far Ramjet Nozzle, Low/Low AR	100
58. P3, P4, P5 and P6 Vs Time for Shrouded, Far Ramjet Nozzle, Low/Low AR; $P_{rjp} = 52$ psia	102
59. P3, P4, P5 and P6 Vs Time for Shrouded, Far Ramjet Nozzle, Low/Low AR; $P_{rjp} = 62$ psia	103
60. P3, P4, P5 and P6 Vs Time for Shrouded, Far Ramjet Nozzle, Low/Low AR; $P_{rjp} = 72$ psia	104
61. P3, P4, P5 and P6 Vs Time for Shrouded, Far Ramjet Nozzle, Low/Low AR; $P_{rjp} = 87$ psia	105
62. P3, P4, P5 and P6 Vs Time for Shrouded, Far Ramjet Nozzle, High/High AR; $P_{rjp} = 42$ psia	106
63. P6 Vs Time for Shrouded, Far Ramjet Nozzle, Low/Low and High/High AR	108
64. P6 Vs Time for Unshrouded, Far Ramjet Nozzle, Low/Low and High/High AR	109
65. P3, P4, P5 and P6 Vs Time for Shrouded, Far Ramjet Nozzle, High/High AR; $P_{rjp} = 52$ psia	110
66. P3, P4, P5 and P6 Vs Time for Shrouded, Far Ramjet Nozzle, High/High AR; $P_{rjp} = 62$ psia	111

67.	P3, P4, P5 and P6 Vs Time for Shrouded, Far Ramjet Nozzle, High/High AR; $P_{rjp} = 72$ psia	112
68.	P3, P4, P5 and P6 Vs Time for Shrouded, Far Ramjet Nozzle, High/High AR; $P_{rjp} = 87$ psia	113
69.	P3, P4, P5 and P6 Vs Time for Shrouded, Close Ramjet Nozzle, Low/Low AR; $P_{rjp} = 42$ psia	115
70.	Typical Flow Pattern for Shrouded, Close Ramjet Nozzle, Low/Low AR	116
71.	P3, P4, P5 and P6 Vs Time for Shrouded, Close Ramjet Nozzle, Low/Low AR; $P_{rjp} = 52$ psia	117
72.	P3, P4, P5 and P6 Vs Time for Shrouded, Close Ramjet Nozzle, Low/Low AR; $P_{rjp} = 62$ psia	118
73.	P3, P4, P5 and P6 Vs Time for Shrouded, Close Ramjet Nozzle, Low/Low AR; $P_{rjp} = 72$ psia	119
74.	P3, P4, P5 and P6 Vs Time for Shrouded, Close Ramjet Nozzle, Low/Low AR; $P_{rjp} = 87$ psia	120
75.	P3, P4, P5 and P6 Vs Time for Shrouded, Close Ramjet Nozzle, High/High AR; $P_{rjp} = 42$ psia	122
76.	Typical Flow Pattern for Shrouded, Close Ramjet Nozzle, High/High AR	123
77.	P3, P4, P5 and P6 Vs Time for Shrouded, Close Ramjet Nozzle, High/High AR; $P_{rjp} = 52$ psia	124
78.	P3, P4, P5 and P6 Vs Time for Shrouded, Close Ramjet Nozzle, High/High AR; $P_{rjp} = 62$ psia	125
79.	P3, P4, P5 and P6 Vs Time for Shrouded, Close Ramjet Nozzle, High/High AR; $P_{rjp} = 72$ psia	126
80.	P3, P4, P5 and P6 Vs Time for Shrouded, Close Ramjet Nozzle, High/High AR; $P_{rjp} = 87$ psia	127

List of Tables

Table	Page
I. Nozzle Dimensions.	19
II. Nozzle Assembly Configurations Investigated	20
III. Transducer Type and Location	22
IV. Instrumentation Hardware Components	26
V. Experimental Itinerary	46

List of Symbols

<u>Symbol</u>	<u>Definition</u>
A_e	nozzle exit plane area (in^2)
AR	nozzle area ratio
D.C.	direct current (volts)
F	thrust (lb_f)
F_n	net thrust (lb_f)
F_r	ram drag (lb_f)
ft	feet
h^*	nozzle throat height (in)
Hg	mercury
HP	Hewlett Packard
IB	interface bus
in	inches
lb_f	pounds force
lb_m	pounds mass
m	mass flow rate (lb_m per second)
mm	millimeter
P	pressure
P_a	ambient or back pressure (psia)
P_e	nozzle exit plane pressure (psia)
P_{rjp}	ramjet plenum pressure (psia)
psi	pounds force per inch squared
psia	pounds force per inch squared absolute
psig	pounds force per inch squared gage
PVS	portable vacuum system

<u>Symbol</u>	<u>Definition</u>
P1	rocket plenum pressure (psia)
P2	ramjet plenum pressure (psia)
P3	base pressure above upper ramjet (psia)
P4	base pressure below upper ramjet (psia)
P5	base pressure above upper rocket (psia)
P6	base pressure below upper rocket (psia)
P8	back pressure (psia)
sec	seconds
u_e	nozzle exit plane velocity (feet per sec)
V_∞	free stream velocity (feet per sec)

<u>Subscript</u>	<u>Definition</u>
a	air or ambient
e	nozzle exit plane
f	fuel or force
m	mass
n	net
r	ram
rjp	ramjet plenum
∞	free stream

Abstract

This research project involves the investigation of base pressures of clustered rocket-ramjet nozzles under shrouded and unshrouded conditions. Twelve combinations of expansion ratios and shrouds for rocket-ramjet nozzle clusters in cold flow were investigated. Pressure measurements were made along the base of the rocket-ramjet cluster under simulated conditions ranging in altitudes up to 70,000 feet and flight Mach numbers to just over 3.0. Comparisons were made of the effects on nozzle base pressures of altitude, ramjet plenum pressure, nozzle geometry and shrouding.

Results of this investigation show a potential increase in base pressure thrust for certain nozzle geometries is possible. As the ramjet nozzle exit distance from the centerline of the nozzle assembly increases for unshrouded cases, the base pressure thrust also increases. This appears to be due to recirculation of exhaust gases. There appear to be variations in performance caused by changes in the distance of the shroud from the nozzle assembly centerline. Also, there is a pressure gradient between nozzles in the base region which is affected by configuration and which has an important effect on evaluating the base pressures.

AN EXPERIMENTAL INVESTIGATION OF ROCKET RAMJET NOZZLE ASSEMBLY BASE PRESSURES

I. Introduction

The combination of rockets and ramjets on a vehicle in the single-stage-to-orbit fully reusable flight arena may offer increased performance compared to present day launch vehicles. This is because this propulsion combination may require less propellant resulting in a lower gross weight vehicle than a vehicle propelled solely by rocket propulsion.

This study looks at rocket-ramjet nozzles in clustered, shrouded and unshrouded configurations. Studies on clustered rocket nozzles have been going on for some time now. Some of the earliest studies performed at Arnold Engineering Development Center showed promise for clustered nozzle assemblies and configurations with shrouds (11,13). Most launch vehicles such as Delta, the Space Shuttle, the Saturn V and Minuteman III have some type of clustered rocket nozzle arrangement. System studies on the subject of combined rocket-ramjet operation at the Defense Advanced Research Projects Agency and the Air Force Wright Aeronautical Laboratories have had such promise that the National Aerospace Plane is likely to have rockets and ramjets in combination for its source of propulsion. Also, a single-stage-to-orbit vehicle would probably have rocket-ramjet propulsion.

A single-stage-to-orbit vehicle would be ideally suited to performing resupply missions in which a great many flights to low earth

orbit are required. Possible future programs could include the proposed manned space station or the building on the Moon of a manned vehicle to Mars. In order to exploit the potential benefits of clustered rocket-ramjet nozzles, the research done at AFIT by Bjurstrom (7), Moran (3), Rodgers (2) and Maxwell (1) has been expanded in this study.

Objectives

At AFIT, there have been a number of studies on clustered and shrouded rocket nozzles. In 1984, Bjurstrom (7) performed a study with rocket nozzles in which their separation distance was variable. That study was expanded by Moran (3) in 1985 to include variable shrouds. Rodgers (2) furthered the work of Moran in 1986 by including three dimensional rocket nozzles. Preliminary studies on rocket-ramjet nozzles in combination have been completed by Maxwell (1) in late 1986 and early 1987.

In this research, rocket-ramjet nozzle combinations were simulated in an experimental apparatus under low to medium altitude conditions, with these objectives:

1. To experimentally evaluate fundamental pressure effects in the base region of clustered rocket ramjet nozzles due to plume interaction,
2. To study the effect on the nozzle base pressures of varying the separation distance of the ramjets from the nozzle cluster centerline, and
3. To study the effect of shrouding the model on the nozzle base pressures.

Scope

The important difference between this investigation and previous work is that this research not only combines much of the work done by Bjurstrom (7), Moran (3), Rodgers (2), and Maxwell (1), but also expands their work to consider the above objectives. All of this is done in light of using rocket-ramjets with a more realistic number and arrangement of nozzles and including many more pressure ratios (ratio of plenum pressure to local ambient pressure) by extending to higher ramjet plenum pressure.

In the present study, the work by Maxwell has been expanded to include a more realistic configuration of rocket and ramjet nozzles for a single-stage-to-orbit vehicle. The ramjets are assumed to be annular around the outside of the vehicle and thus can be approximated by a two-dimensional model. The number of two dimensional rocket nozzles in this study has been increased to three. This study investigates the variance in performance due to differences in the distance of the ramjet nozzle centerline from the model centerline. Shrouded and unshrouded models were also investigated. The change in separation distance of the ramjet from the model center furthers the work of Moran (3), and the shroud work extended the efforts of Rodgers (2).

Approach

The approach taken in this study was to use a two-dimensional model which can utilize either of two sets of nozzles for the rocket ramjet clusters. Each set had three rocket nozzles and two ramjet nozzles. The flow was kept two-dimensional by using plexiglass panes downstream of the nozzle exit planes. All nozzles were designed using the method of

characteristics as in Shapiro (8:462-528). The five nozzle stack consisted of three rocket nozzles bounded on top and bottom by a ramjet nozzle. Nozzle Set 1 had a rocket area ratio (AR) of 4.0 to 1.0 and a ramjet area ratio of 1.9 to 1.0. Set 2 had a rocket AR of 7.32 to 1.0 and a ramjet AR of 4.0 to 1.0. Each set was tested with a rocket plenum pressure of 100 pounds force per square inch absolute (psia) and a range of ramjet plenum pressures from 42 to 87 psia. Each set of nozzles was used in two separate modes, the "far ramjet nozzle" mode and the "close ramjet nozzle" mode (referring to ramjet nozzle location). In the far ramjet nozzle mode the ramjets were 2.125 inches from the nozzle cluster centerline. In the close ramjet nozzle mode, the ramjets were 1.688 inches from the nozzle cluster centerline. In each of these modes, the nozzles were tested unshrouded and then with a four inch shroud 2.5 in from the nozzle cluster centerline. Additionally, for the close ramjet nozzle mode only, experiments were done when the shroud was 2.0 in from the centerline.

II. Theory

Rockets

Rockets provide propulsion force as described by the momentum equation. The governing thrust equation for rockets as derived from the momentum equation is:

$$F = m u_e + (P_e - P_a) A_e, \quad (1)$$

where

F = thrust (lb_f)

m = mass flow rate (lb_m/sec)

u_e = exit velocity of exhaust gases at nozzle exit plane (ft/sec)

P_e = exit pressure at nozzle exit plane (lb_f/in^2)

P_a = local ambient pressure (lb_f/in^2)

A_e = nozzle exit plane area (in^2)

This equation shows that thrust is made up of two parts. The first is the momentum flux which is the product of the mass flow rate and the exit velocity of the exhaust gases. This term accounts for the majority of the thrust. The second term is pressure thrust and is the product of the difference between the nozzle exit plane and local ambient pressures and the nozzle exit plane area. Ordinarily, nozzles are designed to spend most of their flight regime with P_e greater than P_a .

A rocket nozzle progresses through three important operating regimes. They are the overexpanded region, the optimum operating point and the underexpanded region, in terms of ascending altitude. The various flow regimes can be seen in Figure 1 (4:8). Optimum operation occurs when the local ambient pressure and the exhaust pressure are the

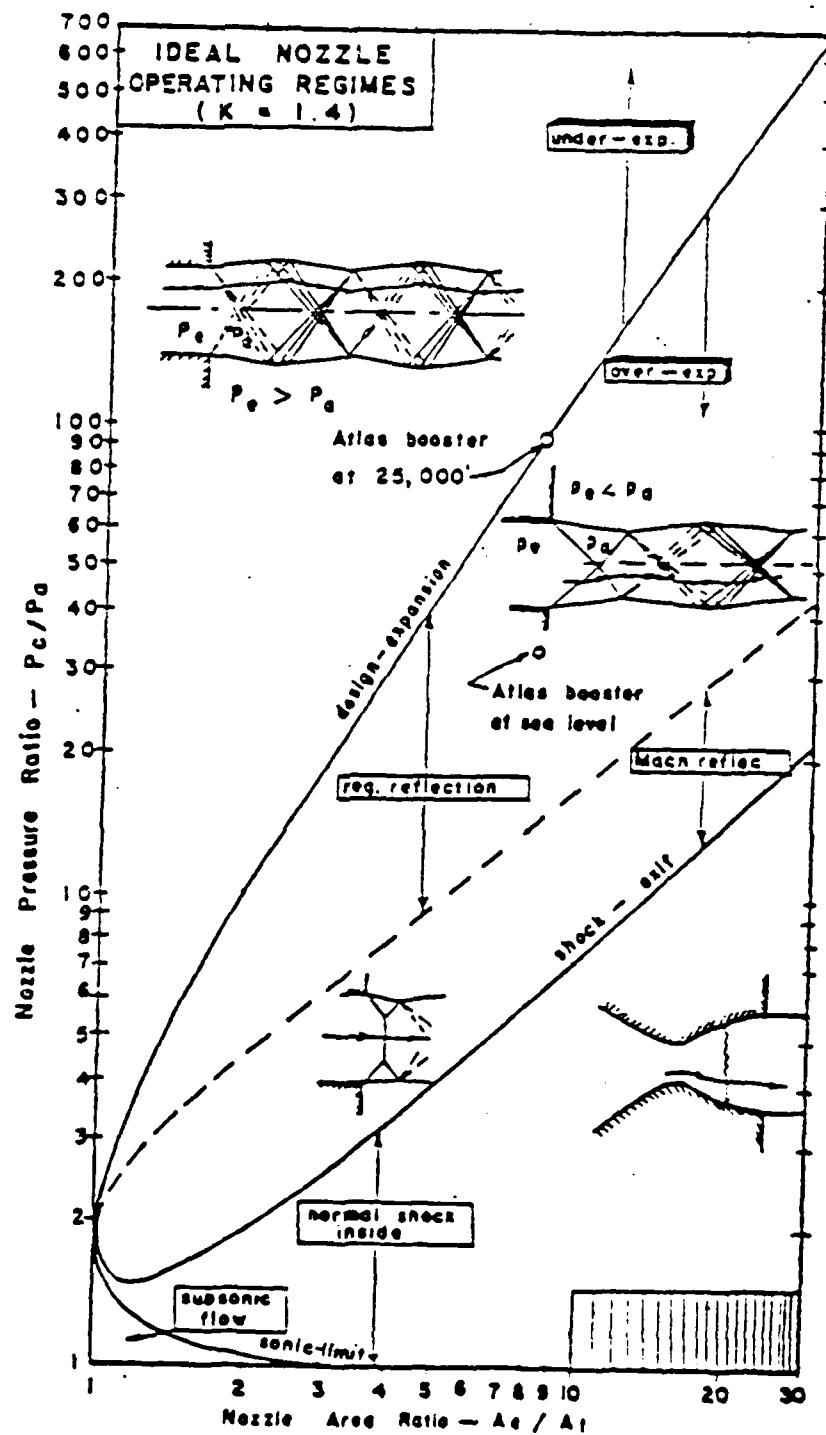


Figure 1. Nozzle Operating Diagram (4:8)

same. In Figure 1, this is the line called design expansion. The optimum case could be maintained at more than a single point by the use of nozzles with variable exit geometries or it could be approximated by using multiple fixed geometry nozzles having separate distinct geometries.

A nozzle is underexpanded if the exit pressure is greater than the local ambient pressure since the exit flow is capable of further expansion (5:410-412). The flow within the nozzle remains undisturbed by pressure differences downstream of the nozzle exit plane. The pressure must adjust to the local ambient conditions and this adjustment occurs beyond the exit plane via a series of expansion waves whose initial influence begins at the exit Mach angle. The expansion waves reflect from the jet boundary in the form of compression waves which may actually converge to form a shock. This familiar diamond pattern of alternating expansion and compression waves is repeated downstream of the nozzle. It dissipates the pressure difference between the nozzle exit plane and the local ambient pressures.

For overexpanded flow, the local ambient pressure is greater than the nozzle exit pressure, making the flow in the nozzle susceptible to disturbances under certain conditions. As in the underexpanded flow regime, the nozzle exit pressure must adjust to the local ambient conditions. In this case, the diamond pattern is started with an oblique shock. The shock angle is determined by the pressure ratio P_a/P_e and the exit Mach number.

A rocket engine system has two main points of interest when compared with an air-breathing system. The first is the rocket's high thrust-to-

weight ratio which is a point in its favor. The second point is a low specific impulse which is an unfavorable factor. Ramjets in conjunction with rockets is considered in an attempt to improve performance in this area.

Ramjets

The ramjet has a very high specific impulse but should be boosted to supersonic speeds by some other device such as a rocket. The reason for its high specific impulse is that the ramjet carries no oxidizer on board. The ramjet gets all its oxidizer from the air surrounding it. The greater the length of time of ramjet operation in an optimized trajectory, the greater the performance gains will be in terms of specific impulse and overall propulsion system performance.

The performance of the ramjet nozzle (like that of a rocket nozzle), is measured by the amount of thrust produced when a fluid is accelerated through the nozzle. The thrust of the ramjet engine is also derived from the momentum equation and is given by (6:87-90):

$$F = (m_a + m_f)u_e + (P_e - P_a)A_e \quad (2)$$

where

m_a = mass flow of air (lb_m/sec)

m_f = mass flow of fuel (lb_m/sec)

F = gross thrust (lb_f)

The engine net thrust is the gross thrust adjusted to account for the ram drag to give the overall thrust.

The ram drag is given by

$$F_r = m_a V_\infty \quad (3)$$

where

F_r = ram drag (lb_f)

V_∞ = free stream velocity

and the net thrust for the ramjet engine is

$$F_n = F - F_r \quad (4)$$

where

F_n = net thrust of the ramjet engine (lb_f)

Combined Rocket-Ramjet Engine Operation

The combination of rockets and ramjets may be able to greatly increase the vehicle specific impulse over a vehicle solely propelled by rockets. The best performing booster engine currently available is the Space Shuttle main engine with a vacuum delivered specific impulse of 453.5 seconds. If that were combined with a ramjet, which produces a specific impulse of up to 3000 seconds, an impressive increase in overall specific impulse could be achieved. Figure 2 compares rockets and ramjets, showing how they could complement each other in terms of specific impulse and propulsive unit thrust-to-weight. For example, the rocket's high engine thrust to weight ratio can offset the ramjet's low engine thrust to weight ratio. Conversely, the ramjet's high specific impulse at low Mach number can be used to compensate for the low specific impulse of the rocket.

PERFORMANCE OF BASIC CYCLES

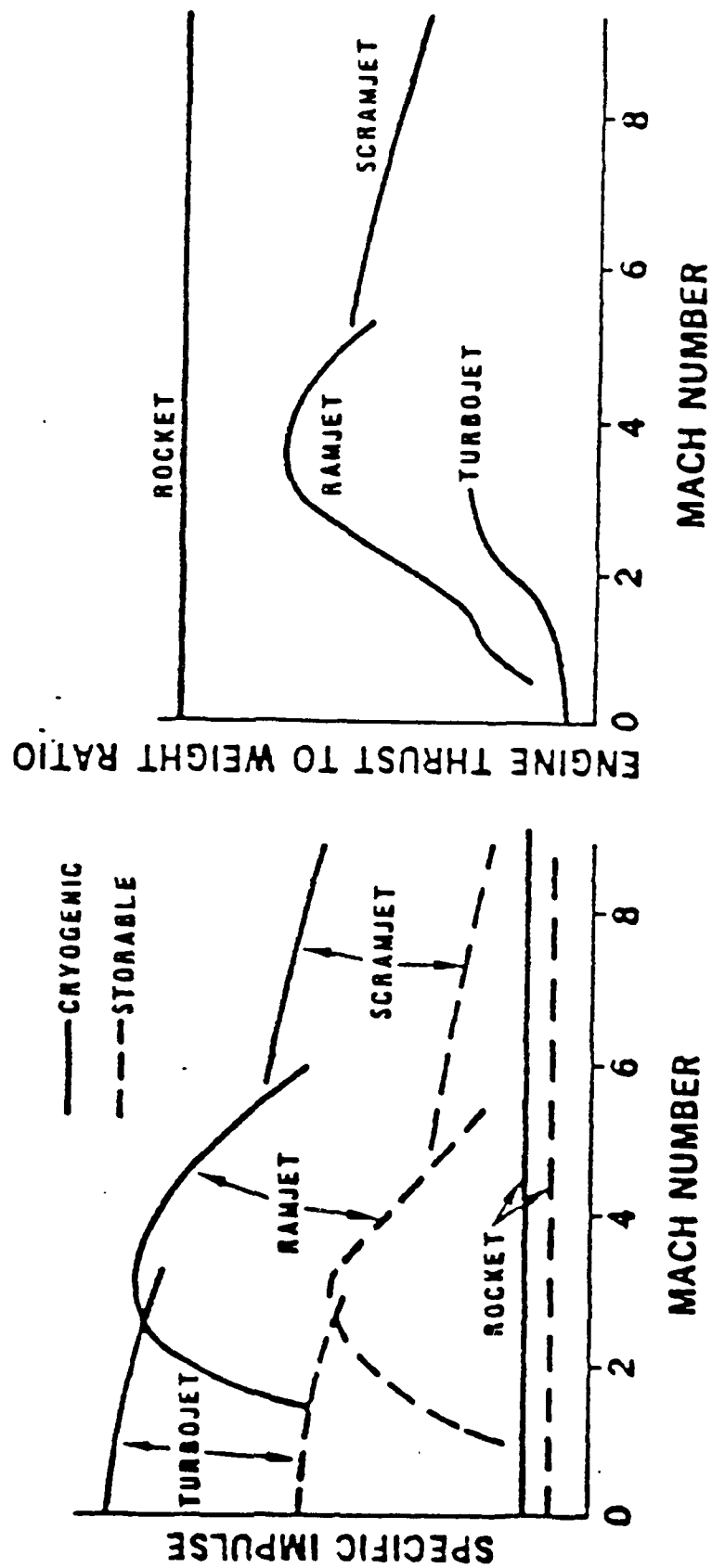


Figure 2. Performance of Basic Cycles (1:8)

Nozzle arrangements of several rockets and ramjets in a clustered configuration do not alter internal operation of each individual thrust chamber. However, system concerns such as exhaust flow patterns, nozzle arrangement geometry and propellant plumbing are important vehicle considerations which could be affected by using both rockets and ramjets in the same vehicle.

Clustered nozzles may create an intense recirculation of the exhaust gases at the vehicle base, thereby imparting a significant additional thrust component. To determine conditions under which the base pressure thrust may become important comprises a large part of this study. Shrouds around the assembly will modify the recirculation pattern. The remaining parts of this study are to investigate the effects of adding a shroud to the rocket-ramjet nozzle cluster assembly and to see what effect the ramjet nozzle location has on the base pressures.

III. Experimental Apparatus

This study was done using the AFIT blowdown wind tunnel. The wind tunnel, vacuum tank and the air supply are all components of the flow system. The test sections and nozzles which were designed and fabricated specifically for this study were inside the vacuum tank during the experimental runs. Different nozzles and test sections made up the twelve separate configurations which were investigated. The pressure transducers (one of the instrumentation items) which measured the nozzle base pressures were attached to the test sections. Additionally, the test sections were built with plexiglass windows to use a schlieren flow visualization system.

Flow System

Air was supplied to the blowdown facility at 100 pounds force per square inch (psi) and room temperature. This was the pressure available to the rocket-ramjet plenums. As in any flow system, particulates and moisture had to be removed. In this system, a cyclone separator using centrifugal forces was the first step in cleaning the air. The second step was a paper filter located just downstream of the cyclone separator. Finally, another paper filter was placed before the rocket-ramjet plenums. The cyclone separator was emptied as often as three times a day. The paper filters were changed bimonthly.

The supply air was fed to a 3-inch diameter line which forked just downstream of a manually operated disk type on-off valve. One path fed the air into the rocket plenum and the other path was for the ramjet

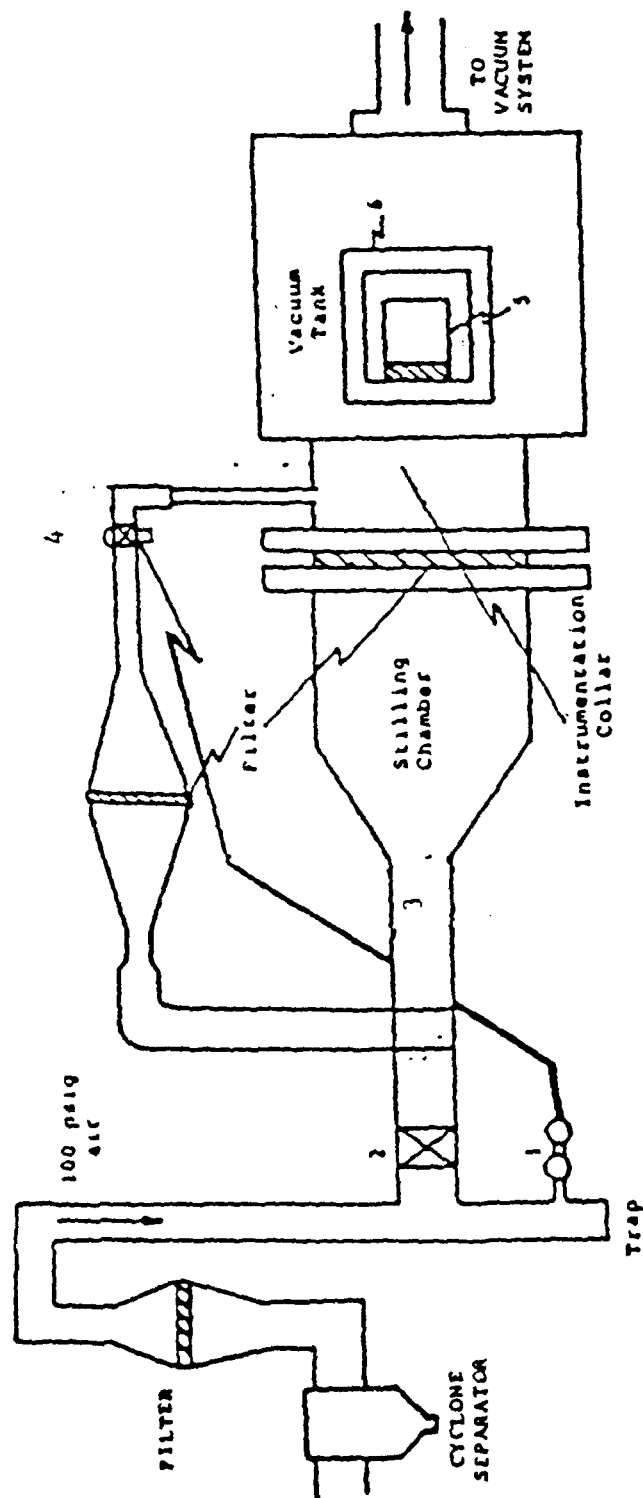
plenum. The rockets were always supplied air at 100 psi, but the ramjet plenum pressure was adjusted by the use of a Grove regulator and dome valve. The range of the regulator was 0-100 psi and the dome valve was capable of controlling air at up to 3000 psi. The flow system is shown in Figure 3. In previous work there was more than one rocket plenum and they were supplied air by slightly different routes and this led to slightly different rocket plenum pressures. In this study, the ramjets were supplied air through a common plenum specifically designed for this investigation. The ramjets bound the rocket assembly which more nearly simulates a future launch vehicle than the rockets surrounding the ramjet as in previous studies at AFIT.

The test section containing the nozzles was installed in the 535 ft³ vacuum chamber. Three vacuum pumps reduced the pressure in the chamber to .25 psia and allowed for test runs of approximately 30 seconds. A fourth vacuum pump was used to establish a reference of 0.1 millimeter of mercury (mm Hg) absolute for the transducers located in the base region of the nozzle assemblies. This permitted the output of the transducers to be considered absolute pressure.

The vacuum tank has 10 in square optical quality glass windows to allow schlieren photography for still and motion pictures.

Test Sections

The test section used consisted of five nozzles. There were three simulated rocket nozzles, one on the model centerline and one each at equidistances above and below the centerline. The other two nozzles, simulating ramjet engine nozzles, were placed outside the rocket nozzle assembly, one on top and one on bottom at equidistances from the



- | | |
|--------------------------|-----------------------|
| 1 Grove Regulator | 4 Hand Operated Valve |
| 2 Hand Operated Valve | 5 Test Section |
| 3 Rocket Nozzle Air Flow | 6 Optical Window |

Figure 3. Blowdown Wind Tunnel Flow System

centerline. The ramjet nozzles were placed at two different distances from the model centerline during the test matrix. The first distance was 2.125 in, and the second was 1.688 in. The longer distances are referred to as the "far ramjet nozzle" experiments and the shorter distances are referred to as the "close ramjet nozzle" experiments. All nozzles were one inch wide. The far ramjet nozzle test section may be seen in Figure 4, and a close up of transducer location is in Figure 5.

During these experiments, the nozzles were shrouded by a 4 in long shroud. For the far ramjet nozzle experiments, the shroud was at 2.5 inches from the model centerline. For the close ramjet nozzle experiments, the shroud was placed at two distances from the centerline. The longer distance was at 2.5 in and is referred to as the "far shrouded" experiments. The shorter distance is 2.0 in from the model centerline and is referred to as the "close shrouded" experiments. The nozzle assembly is shown in Figure 4 with the far shroud installed.

The air flow to the rockets was delivered by the main line directly through the rockets to the vacuum chamber. For the ramjet nozzles, however, the air flow was from the main line to a dome valve and then to a plenum which supplied the air to each ramjet at the same pressure.

Plexiglass windows downstream of the nozzles allowed the use of a schlieren photography system to record the wave interactions downstream of the nozzle exits.

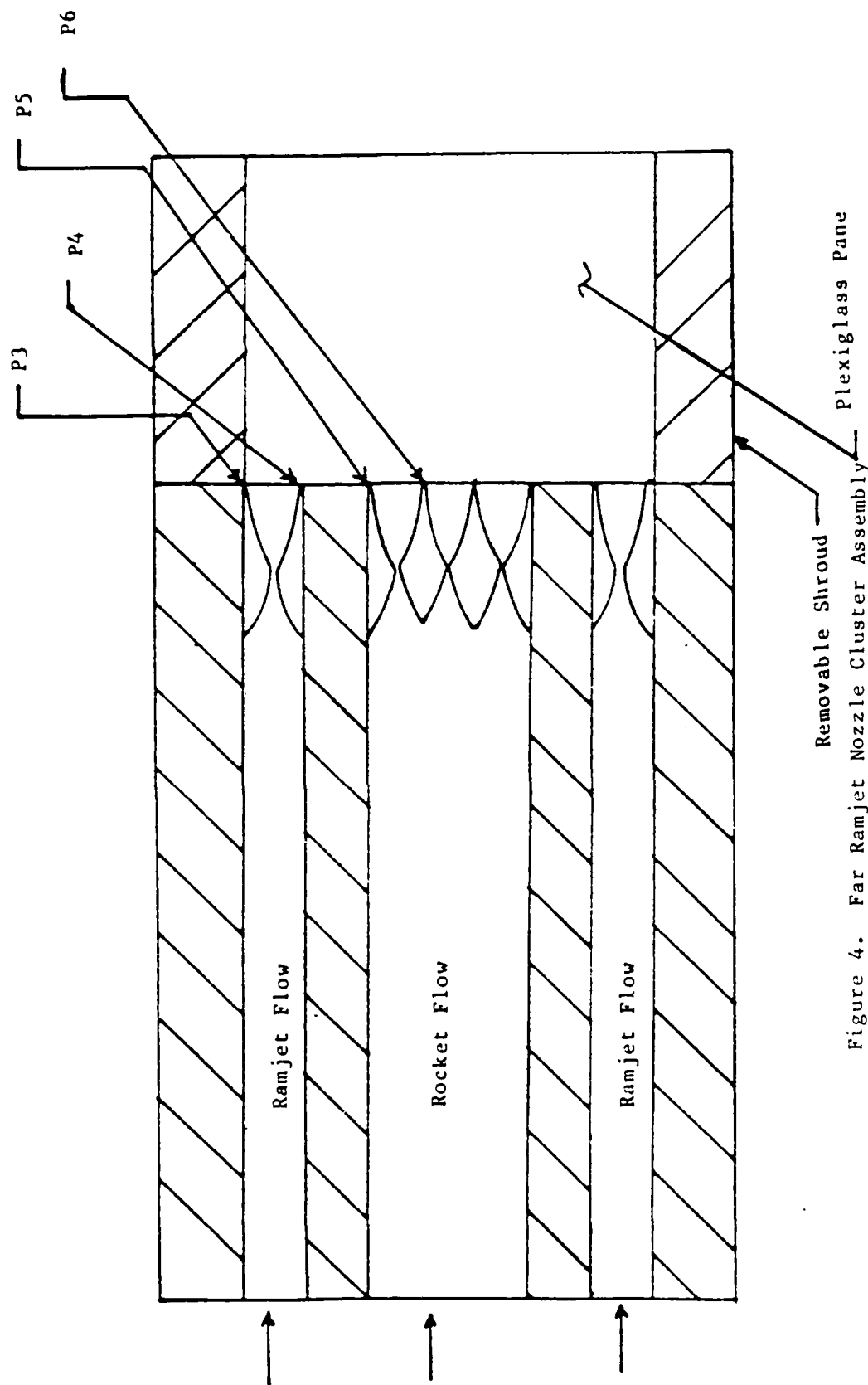


Figure 4. Far Ramjet Nozzle Cluster Assembly

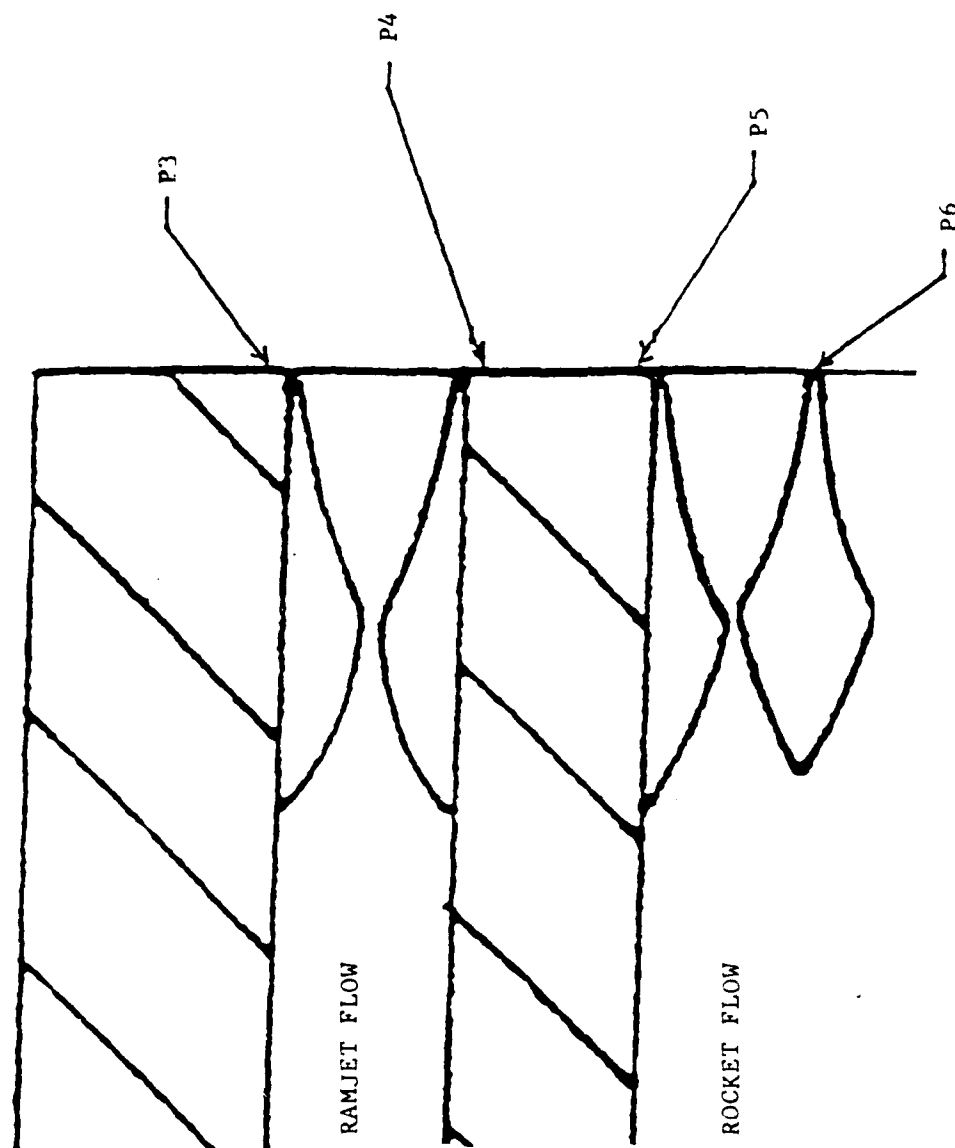


Figure 5. Transducer Location

Nozzles

Two different rocket and ramjet nozzle configurations were studied. The dimensions, area ratios and exit Mach numbers are given in Table I. The nozzle area ratios used were chosen so comparisons could be drawn between this work and earlier work (1:21). The combination of rocket AR = 4.0 and ramjet AR = 1.9 is referred to as the "low/low AR" nozzles. The combination of rocket AR = 7.32:1 and ramjet AR = 4.0:1 is referred to as the "high/high AR" nozzles. These ratios were chosen as the extremes of previous work by Maxwell. In all cases, the nozzles were two-dimensional. The throat dimensions of 0.050 inches for the rockets and 0.100 inches for the ramjets were held constant.

These nozzles were designed using the method of characteristics as shown by Shapiro (8:462-528). All the nozzles were sharp corner nozzles with inlet radius based on 3 times the throat height (h^*) as in the Mulenburg (9:15) study. Although Mulenburg showed the faired ellipse subsonic contour to be a slightly better performer in terms of total pressure loss, the constant radius contour was chosen to facilitate fabrication.

Nozzle Assembly Configurations Investigated

The various configurations of nozzles and shrouds that were investigated are shown in Table II. The configurations were chosen to represent the extremes of previous work so that significant changes in the operation of the nozzles and the wave interactions that result from the change of nozzle arrangement could be detected. The shrouds and the plexiglass windows of each configuration were designed so that the next

Table I. Nozzle Dimensions

Nozzle Set	Nozzle	A/A*	Throat Width (inches)	Throat to Exit Length (inches)	Exit Mach Number
Low/Low AR	Rocket	4.00:1.0	0.050	0.500	3.00
	Ramjet	1.90:1.0	0.100	0.500	1.50
High/High AR	Rocket	7.32:1.0	0.050	0.500	3.59
	Ramjet	4.00:1.0	0.100	0.500	3.00

Table II. Nozzle Assembly Configurations Investigated

Shroud Location	Ramjet Nozzle Location	Nozzle AR
None	None ^a	Low/Low
None	Close ^b	Low/Low
None	Close	High/High
None	Far ^c	Low/Low
None	Far	High/High
Closed ^d	None	Low/Low
Close	Close	Low/Low
Close	Close	High/High
Far ^e	Far	Low/Low
Far	Far	High/High
Far	Close	Low/Low
Far	Close	High/High

(a) Rocket flow only

(b) Ramjet nozzle 1.6875 in from model centerline

(c) Ramjet nozzle 2.125 in from model centerline

(d) Shroud 2.0 in from model centerline

(e) Shroud 2.5 in from model centerline

logical step in this area of research would be to instrument these areas with pressure transducers.

Instrumentation

Eight pressure transducers were used to measure the data for all configurations and all experiments. The base pressures above the upper ramjet, below the upper ramjet, above the upper rocket and below the upper rocket were measured by four Endevco 8506-B transducers. These transducers have a range of 0-5 pounds per square inch gauge (psig). The pressures were assumed to be symmetrical on the lower half of the model. This assumption was determined to be valid when the pressure transducers were mounted on the bottom half of each configuration and the pressures were within just a few tenths of a percent of the pressures from the top half of the model. The base pressure transducers are numbers 3, 4, 5, and 6. These transducers were used to measure absolute pressure (psia). A near absolute vacuum was connected to the rear face of each transducer diaphragm through a tube vent. This vacuum became the reference to which the pressure acting on the external side of the diaphragm was compared.

Transducers 2 and 7 were Endevco 8530A-100 with a 0-100 psia range. These were used to measure the upstream pressure in the ramjets. Transducer 1, also an Endevco 8530A-100, was used to measure the upstream pressure of the rocket nozzle. Downstream of the test section, a Bell and Howell transducer with a 0-5 psia range was used. Table III shows the transducers by number type and location. Figure 5 details the locations of the base pressure transducers.

In addition to the electronic transducers, two mercury manometers were used during the experiments. One manometer was connected to the

Table III. Transducer Type and Location

Item	Model Number	Location
Pressure Transducer	Endevco 8530A	Rocket Plenum (P1)
Pressure Transducer	Endevco 8530A	Ramjet Plenum (P2)
Pressure Transducer	Endevco 8506B-5	Base above upper ramjet (P3)
Pressure Transducer	Endevco 8506B-5	Base below upper ramjet (P4)
Pressure Transducer	Endevco 8506B-5	Base above upper rocket (P5)
Pressure Transducer	Endevco 8506B-5	Base below upper rocket (P6)
Pressure Transducer	Endevco 8530A	Ramjet Plenum (P7)
Pressure Transducer	Bell and Howell	Back pressure (P8)

vacuum chamber to read the vacuum in the chamber prior to each experiment. The other manometer was attached to the transducer vacuum reference pump. This manometer was used to compare the vacuum being applied to the transducers with atmospheric pressure. A precision gauge, model FA160, was also attached to the reference pump to insure that a near absolute vacuum was attained and maintained as the reference for the pressure transducers.

Schlieren System

One goal of this research was to study the exit flow patterns 1) as the inlet stagnation pressure to the ramjet nozzles was varied and 2) as the exit conditions varied with simulated altitude in terms of the back pressure from the underexpanded to the overexpanded regimes. The schlieren system shown in Figure 6 was used to take still and motion pictures of these phenomena. Still photos were taken using a spark lamp with spark duration of less than 1 microsecond. The still photos were taken using Polaroid sheet film, type 57. Motion pictures were taken using a steady lamp and a 16 millimeter low speed camera which was operated by the personnel of the Technical Photo Branch of Aeronautical Systems Division.

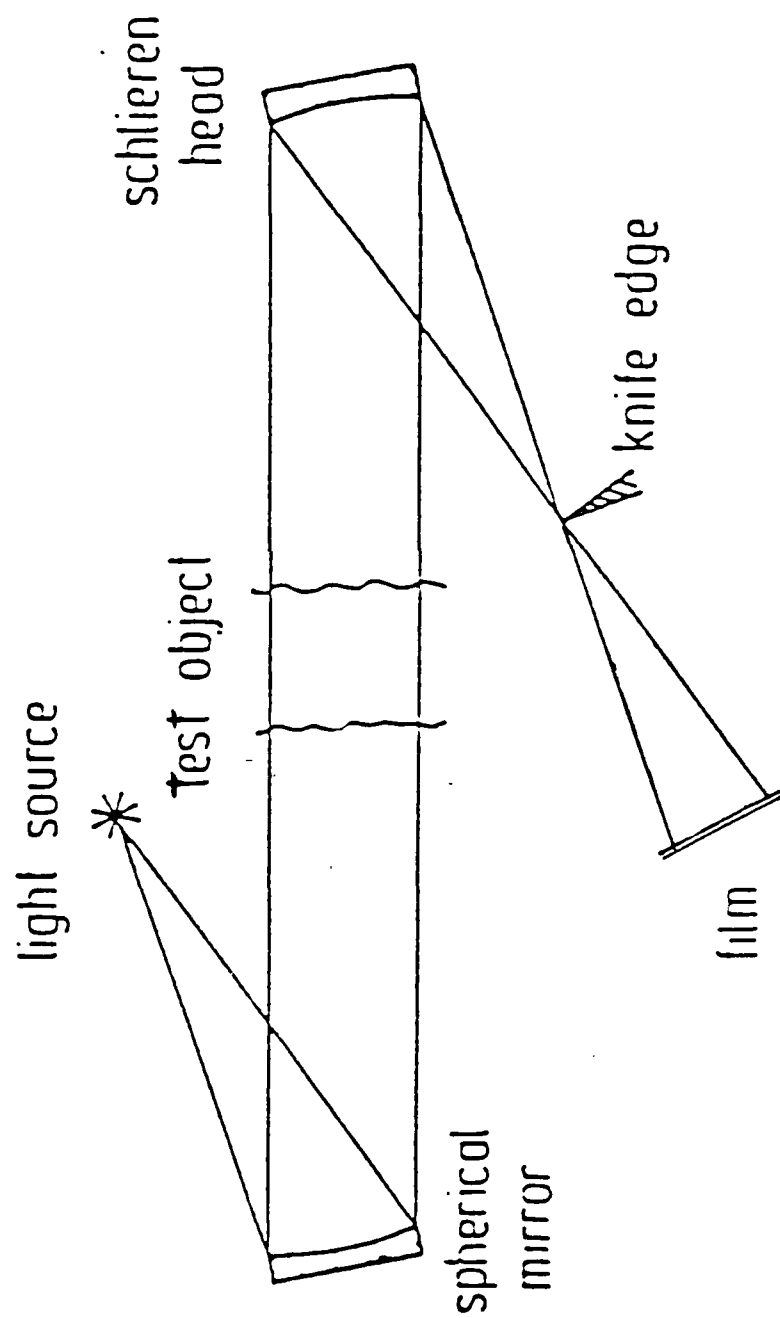


Figure 6. Schlieren System

IV. Data Acquisition and Reduction System

The Hewlett Packard (HP) 6901S Measurement and Analysis System is an automated digital system which was used to collect the raw analog data from the pressure transducers and reduce it to usable digital information. The experimental apparatus was designed to interface with the HP 6901S using the hardware components listed in Table IV. These components were interconnected as shown in Figure 7. The HP 6901S is a menu driven system which is controlled via the HP 9826 computer keyboard through the system software. All the hardware items were linked using the HP-IB interface bus which is the central coordination location for several external devices such as printers, plotters and disk drives. The HP-IB bus can selectively send data to individual devices and tailor the data flow rate to the requirements of each receiving device. The bus also controls the data flow in the other direction, i.e., from the peripheral devices to the computer.

The HP 6901S is a multiple channel data acquisition and reduction system. It can collect up to 264 channels of either analog or digital data with a total measurement capability of 4096 samples per experiment. A sample rate of 100,000 samples per second is possible when all 16 interface cards are installed in the HP 6901S. Figure 8 shows how the HP 6901S interfaces with the other operational hardware devices.

An HP 6942 multiprogrammer is installed internally within the HP 6901S. The HP 6942 multiprogrammer contains the memory cards, analog to digital converter, scanner relays and controller cards required for system operation. Data is collected through the HP 6901S terminal boards

Table IV. Instrumentation Hardware Components

Item	Model Number
Power Supply	HP 6205C
Multiprogrammer	HP 6942A
Computer	HP 9826
Plotter	HP 7470A
Printer	HP 2934A
Measurement and Analysis System	HP 6901S
Portable Vacuum Standard	PVS-2A-10000

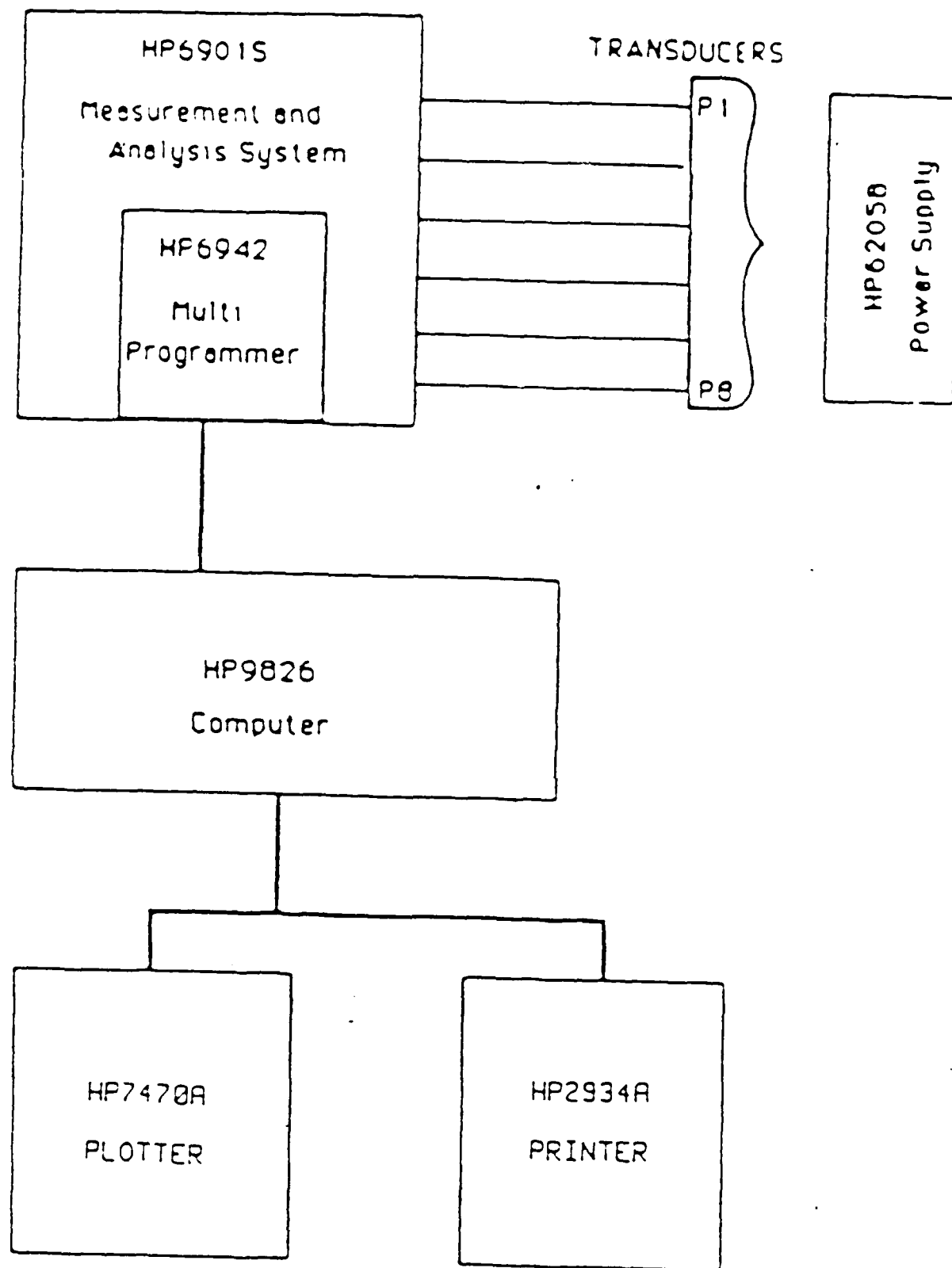


Figure 7. Hardware Components (3:16)

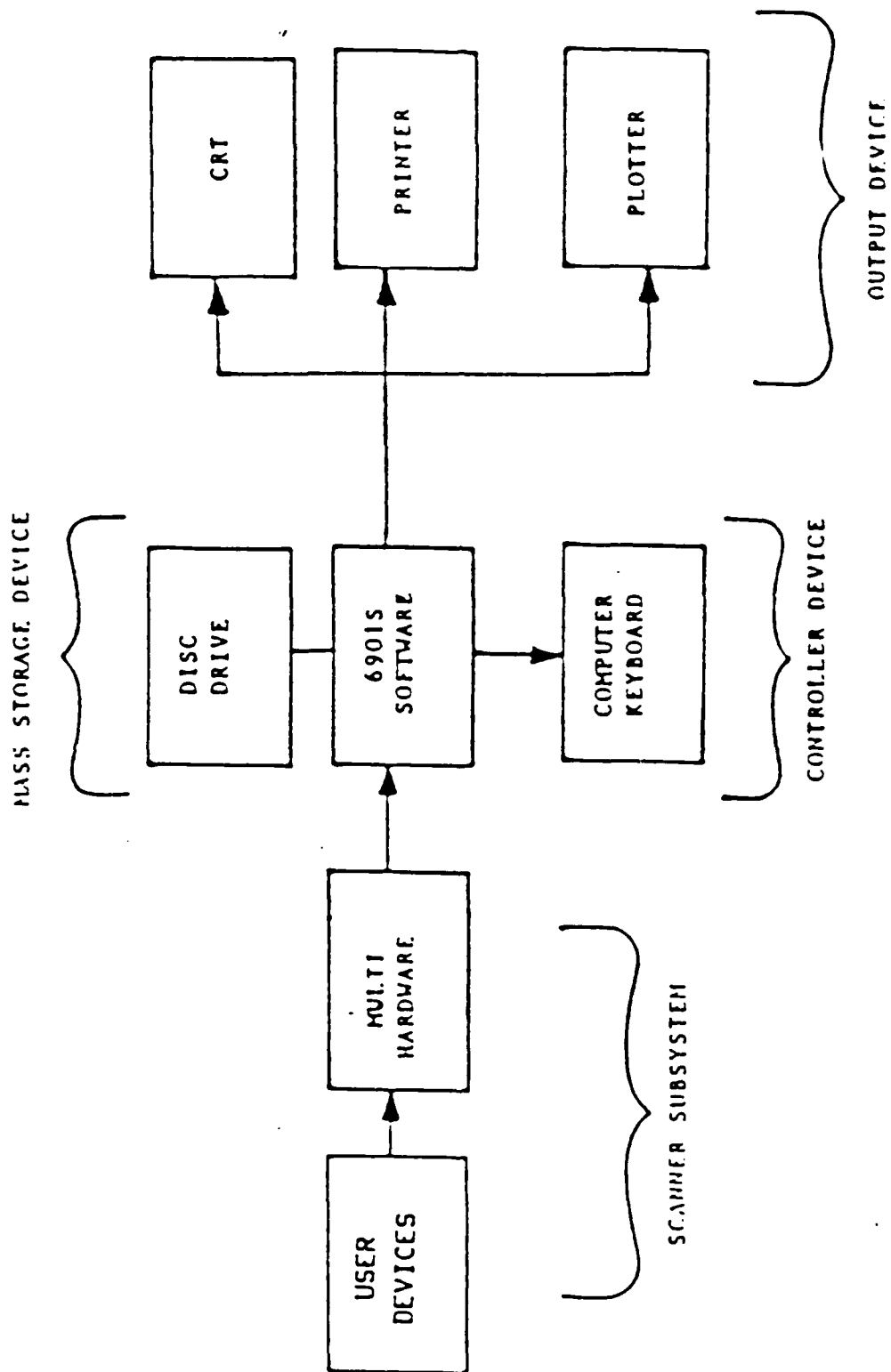


Figure 8. HP 6901S System Schematic (3:17)

and temporarily stored. This temporary storage is done so that the desired sampling rate can be achieved without exceeding the capacity of the analog to digital converter. The data is then recalled sequentially, converted to digital form and sent to the HP 9826 computer for storage on floppy disk. This flow of data is shown in Figure 9.

The HP 9826 computer is menu driven just like the HP 6901S. The menu utilities are presented in Figure 10. The menu entries are controlled via the keyboard and they provide the means for entering the experimental parameters required by the first five menus at the top of Figure 10. The experimental data acquisition parameters are entered using the HP 6901S software. These parameters are: the scan rate, total number of scans and the method of initiating the data acquisition.

For this research, the run time was approximately 30 seconds. The software was set appropriately to scan all 8 channels every .0589 seconds with 7350 microseconds between the start of reading one channel to the start of reading the next channel. The burst mode menu was the method of data collection selected (see middle of Figure 10). The high speed scanning capability of this mode allowed the input sources to be scanned nearly simultaneously. Transient events such as pressure changes could be most easily captured by using this mode. The software package of the HP 6901S and HP 9826 offered several data presentation options such as tables, graphs or histograms. Though tables were occasionally used, the normal method of data presentation was graphic. This menu option can display one channel, any grouping of channels, or all eight channels at one time. This menu also allowed windowing and zoom options for detailed views of the data. The data reduction process, with appropriate offset

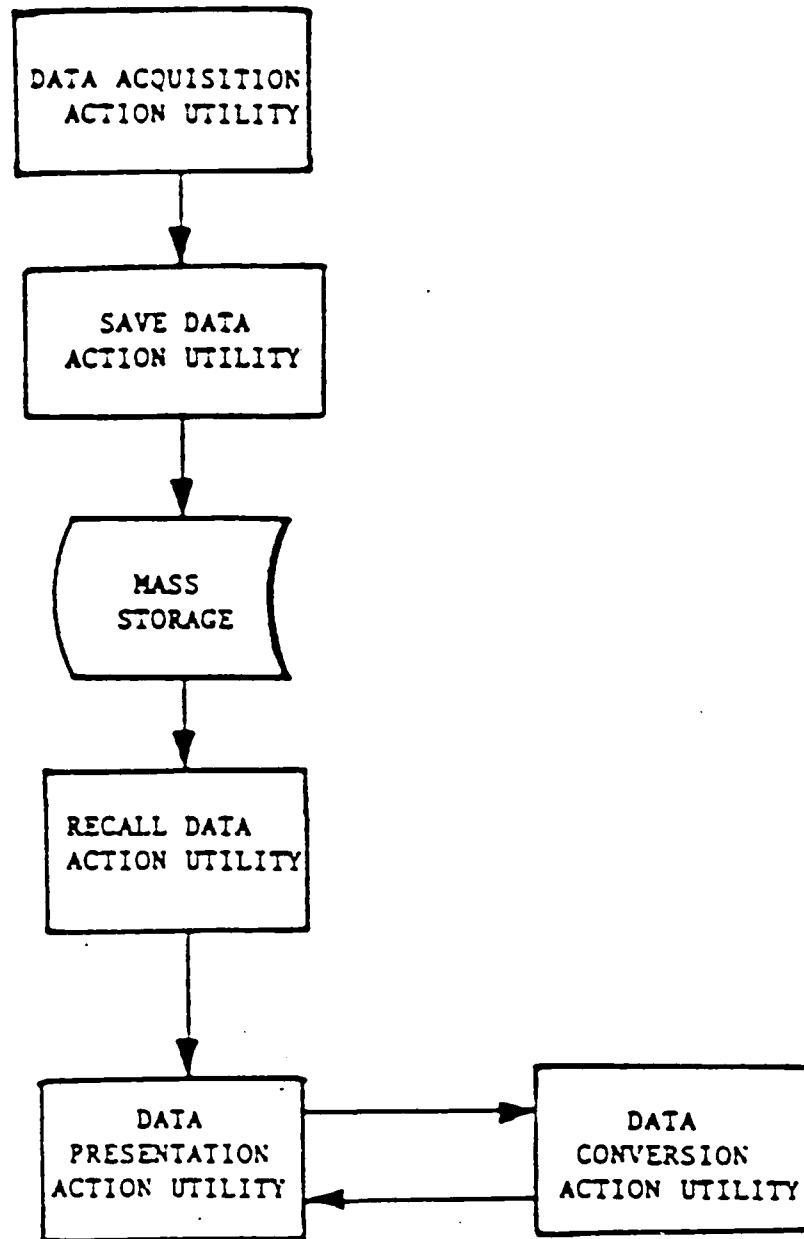


Figure 9. Data Flow Path (3:19)

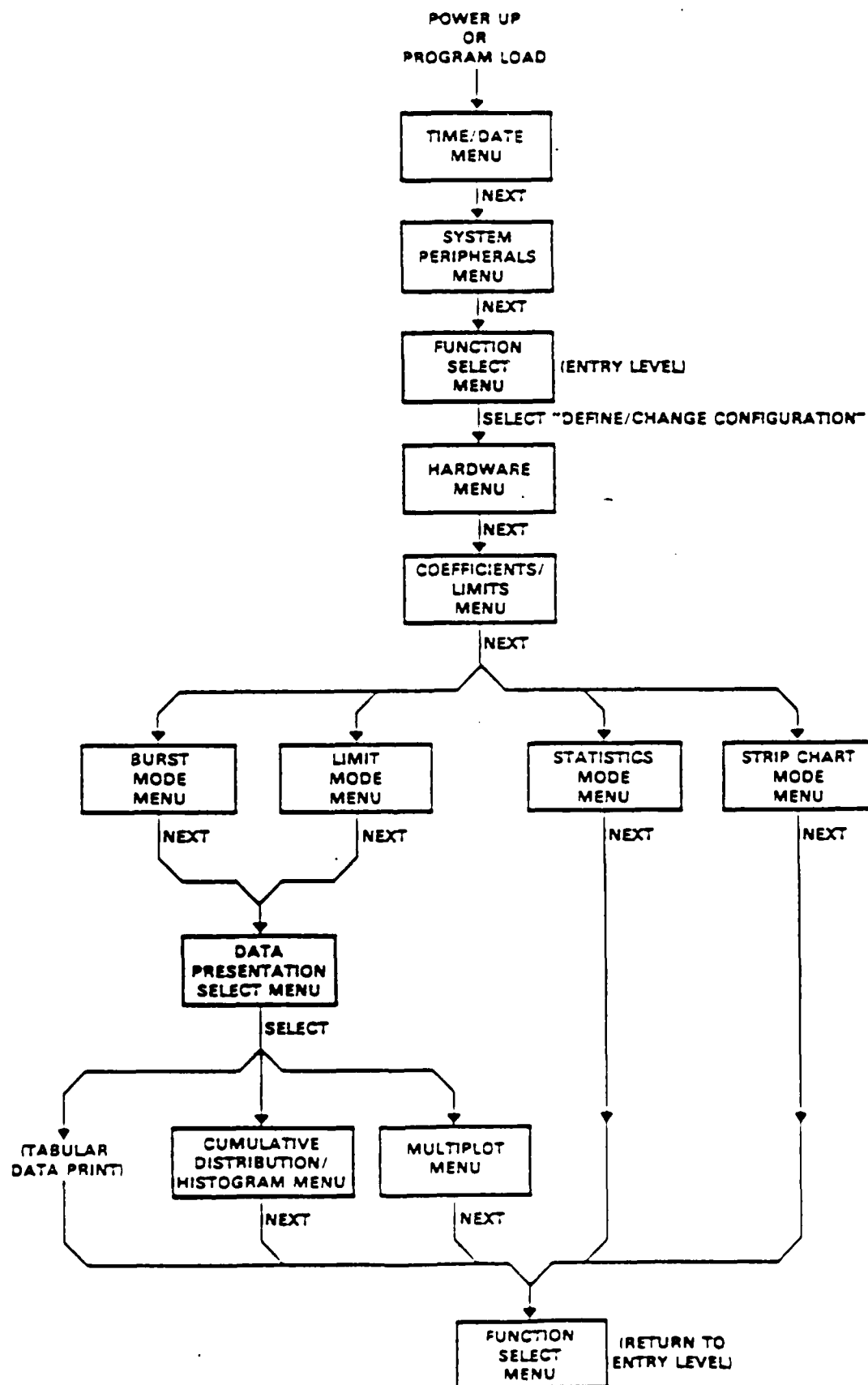


Figure 10. HP 6901S Menu Utilities Operational Diagram (14:2-4)

values inserted to scale the data, was accomplished prior to receiving the selected output presentation.

Several computer programs were used to obtain the desired graphical output. The plotting programs load the file by assigning input/output paths to translated data for plotting on the HP 7470 plotter. The data can then be presented in pressure versus time, pressure ratio versus time, pressure ratio versus pressure or in any other of a number of different ways.

The data acquisition and reduction systems used in this research are ideally suited to the blowdown wind tunnel facility. The pressure characteristics of the nozzles were adequately acquired, processed and formatted. This system is expandable for the next phases of research.

V. Experimental Procedure

There are three distinct phases of the experimental procedure. The first is the calibration and checkout of pressure transducers and electronics that precedes any data collection. This is done to reduce possible error or misinterpretation of data. The second part includes daily checkout of equipment to make sure it is functioning properly. The third component is comprised of the actual data runs.

Calibration

All of the Endevco 8506 and 8530 pressure transducers were calibrated using a Portable Vacuum System 2 (PVS-2). This PVS-2 provided a reference pressure for the transducer. The reference pressure on one side of the measurement diaphragm was compared with air pressure from a separate source acting on the other side of the diaphragm. This provided a pressure differential thereby producing a voltage differential. The pressure from the separate air source was increased in small increments over the transducer range. The voltage generated from this pressure difference was recorded on a digital voltmeter. Then, pressure versus voltage was recorded and the slope of this data gave the pressure transducer sensitivity in millivolts per psi. This sensitivity remained linear over the full range of the transducer, and is the scaling data used in the experimental procedure. The measured sensitivity was always within three percent of what the manufacturer claimed. The transducer calibration hardware is shown in Figure 11.

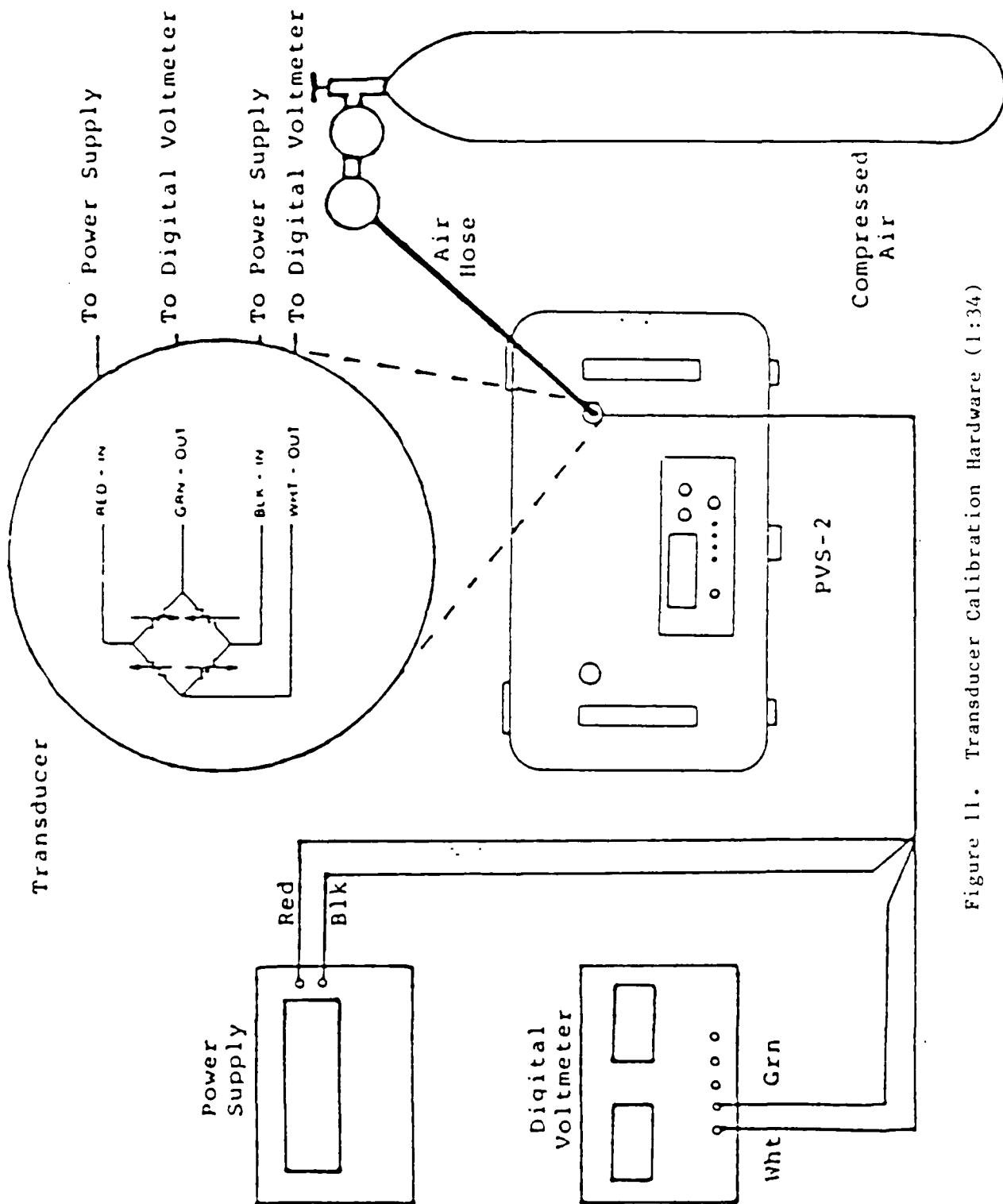


Figure 11. Transducer Calibration Hardware (1:34)

The remaining Bell & Howell transducer which measured the back pressure was calibrated in place on the vacuum chamber. This transducer measured absolute pressure so no separate reference pressure was required. The main vacuum pumps were used to lower the vacuum chamber pressure to approximately 0.25 psia as measured by the mercury manometer connected to the vacuum tank. The transducer was connected to a 10 volt D.C. power supply to provide the excitation voltage and to a digital voltmeter to record the voltage across the transducer. The vacuum tank was also connected to a 100 inch mercury manometer to record the vacuum chamber pressure. A valve connecting the vacuum tank to the atmosphere was used to vary the pressure inside the tank. The pressure was allowed to rise in small steps to atmospheric pressure. The mercury manometer reading was subtracted from the barometric pressure measurement to give the pressure value in the vacuum chamber. As the pressure in the tank changed, the voltage and pressure were recorded. The data were graphed to show the sensitivity of the transducer in millivolts per psi. The sensitivity of the transducer remained linear over its full range.

Experiment Run Procedure

The experimental procedure for all runs was the same. The power supply to the transducers was turned on. Using a digital voltmeter as a check on the power supply, an excitation voltage of 10 volts D.C. was applied to the transducers. At this time the reference pressure to the Endevco 8506B-5 pressure transducers at the nozzle base was applied. The reference pressure was approximately 0.1 mm Hg. The transducers were "nulled" or balanced by adjusting the potentiometer and insuring that the input voltage was identical to the output voltage received on the HP

6901S system. The balancing circuitry, shown in Figure 12, includes the differential amplifiers which have a gain of one between the potentiometer and the measured input voltage to reduce background noise. Figure 13 shows a close up of the potentiometer converting the two-wire transducer output into a one-wire output suitable for the HP 6901S. The mode rejection ratio characteristics of this circuit with its associated gain of one preserved the signal while simultaneously producing a cleaner transducer output.

Next, the three vacuum pumps were all turned on. As the vacuum increased in the tank, the HP 9826 computer was turned on and the Extended BASIC 2.1 was booted. The Shell software program of the HP 6901S Measurement and Analysis System was loaded. The time and date were entered to keep track of the data. The Shell program's "Run Current Configuration" option was selected from the Function Select Menu shown in Figure 10. This configuration for the computer is not to be confused with the model configuration in the test section of the vacuum chamber. This refers to two different and unassociated items. The current configuration included all transducer scaling information, data start information and the medium for presentation of reduced pressure data. The scaling information was discussed in the calibration part of this chapter. The data start information directs the HP 6901S to start taking data when the pressure upstream of the rocket nozzles reaches 5.5 psia. This occurs almost instantaneously after the air supply on-off valve is opened to allow air flow into the vacuum chamber. The medium used for initial examination of the data was the multichannel option which

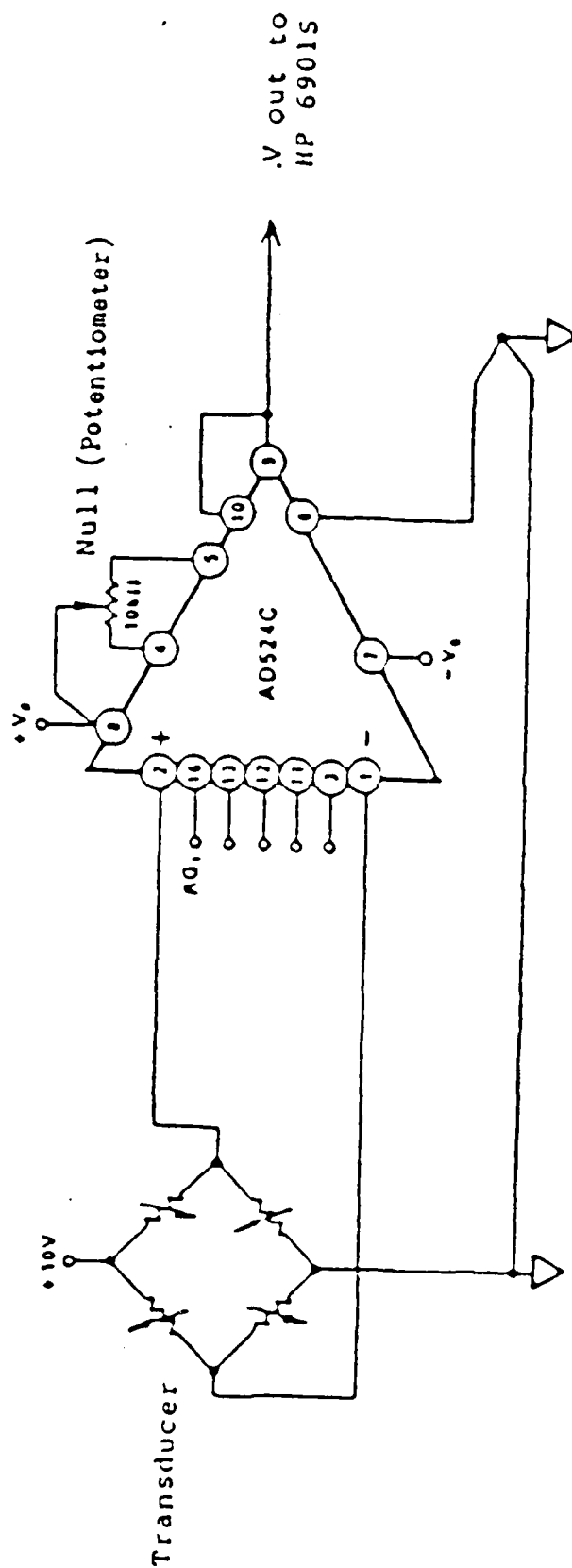


Figure 12. Transducer Null Adjustment Circuitry (1:37)

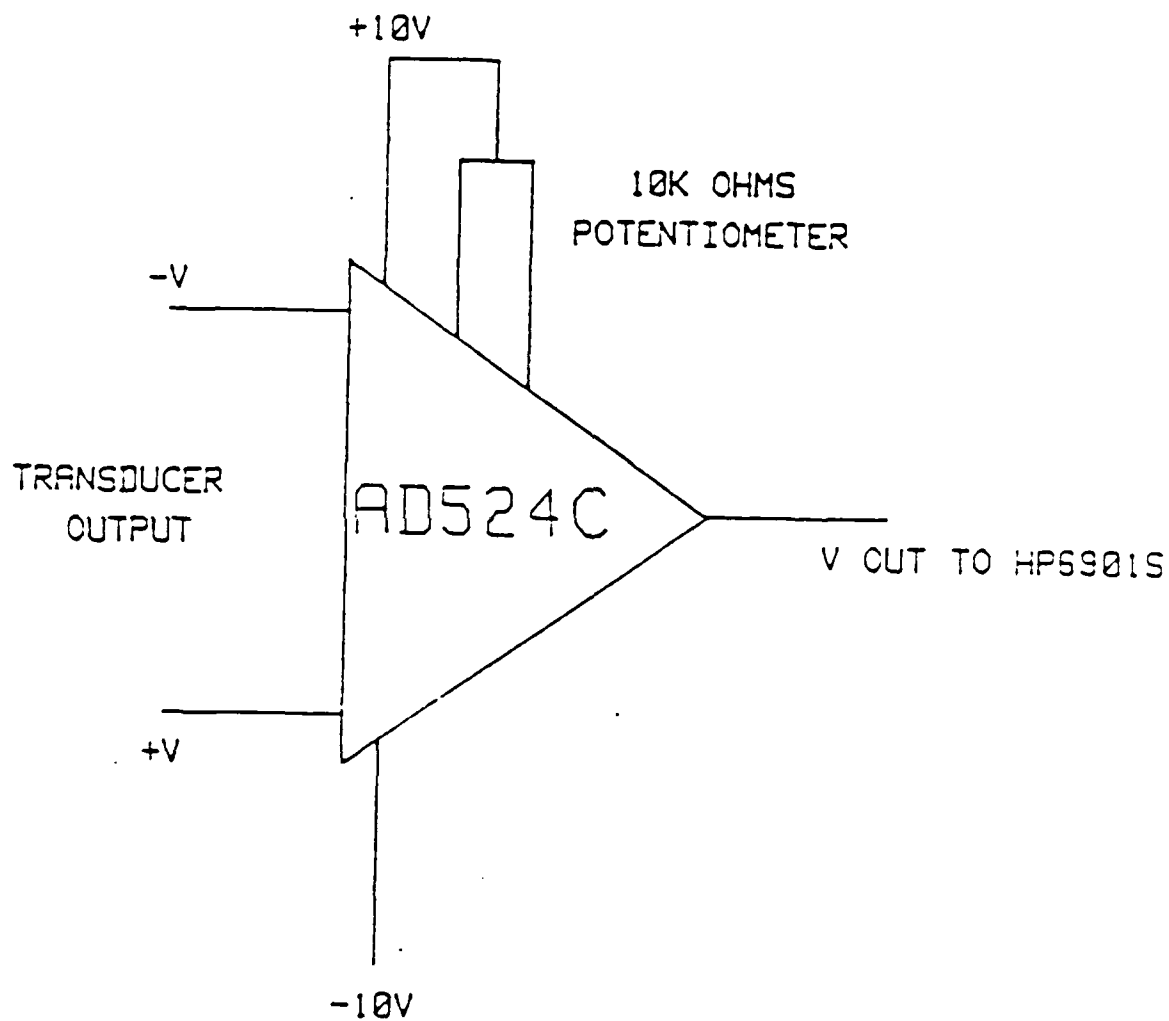


Figure 13. Potentiometer Amplifier (2:32)

presented all eight transducer pressure versus time plots on a single hard copy graph.

After choosing the "Run Current Configuration" option, a four-second self test of the HP 6901S occurred to ensure that all integrated circuit cards were in their proper places and that a severe hardware failure would not cause a malfunction of all or part of the HP 6901S system. Then a file name for data storage was selected and entered.

The main valve to the 100 psi air supply was opened. The ramjet stagnation pressure was established by setting the Grove regulator for the same valve at various values between 40 psi and 90 psi for each model configuration.

An experiment could be performed once the vacuum in the tank reached the necessary start condition of about 0.25 psia. Since the downstream pressure varied continuously during a run, the lowest possible back pressure was established before each run. Due to small leaks this value of the initial back pressure was limited to about 0.25 psia. This represented an altitude of about 75,000 feet and the underexpanded regime of flight operation for the nozzles being investigated.

Several experiments were performed for each model configuration. The ramjet nozzle stagnation pressures used were 42, 52, 62, 72 and 87 psi. The experimental run started when the on-off hand valve was opened. Once the pressure reached 5.5 psia upstream of the rockets the HP 6901S started the pressure data versus time acquisition. During the experimental run, the lights in the room were turned off and schlieren photographs were taken near the start of the run in the underexpanded region of the nozzle flow. After the experiment run time of about 30

seconds, the hand valve was closed thus terminating the experiment. The HP 9826 computer stored the data and produced it in hard copy form.

All runs were repeated and the conformity of results was very good. The conformity of the data from one run to another was checked by comparing individual channels of one run against other runs at the same ramjet stagnation pressure.

The individual pressure transducer channel hard copies of the pressure versus time data formed the basis of comparisons and determinations drawn in the sections on results and conclusions.

VI. Results and Discussions

The AFIT blowdown wind tunnel was used in experiments with twelve combinations of nozzle area ratio, ramjet nozzle spacing from the model centerline and shrouds. Normal rocket operation is from low altitude to high, corresponding to going from the overexpanded to the underexpanded regime of the nozzle through the optimum design point of the nozzle. Instead in this experimentation, the blowdown facility operating procedure began with each experiment at a simulated high altitude and proceeded toward low, corresponding to moving from the underexpanded regime to the overexpanded regime of the nozzles.

During an experimental run, the model was supplied a nearly constant 100 psi rocket plenum pressure. The ramjet nozzles in the model were supplied with different plenum pressures on separate runs. This was to simulate a range of altitudes and flight speeds for ramjet engines in combination with rockets. During a particular experiment, the nearly constant ramjet plenum pressure was 42, 52, 62, 72, or 87 psi.

The comparisons of the nozzle configurations are based on the base pressures which were measured directly as previously described. Due to symmetry of the nozzle configurations and shrouds, the experimental results were the same on either the top or bottom half of the model. Discussions are made referring to the top half of the model with the understanding that the bottom is the same. To backup the pressure measurements, schlieren photographic stills and motion pictures were taken. All time dependent discussions have been supported by the schlieren motion pictures.

The types of phenomena to be discussed include flow recirculation, flow entrainment which removes mass from the base regions, wave interaction, interaction between the ramjet plume and the shroud or the open top of the two dimensional model, interaction of the ramjet plume with the rocket plumes, the presence of a pressure differential in the base region between rockets and ramjet, and the effect of these phenomena on a launch vehicle. In the recirculation regions between the ramjet and the shroud and between ramjet and rockets, the base pressures are established by the flow recirculated into the base regions and balanced by flow entrainment across the flow streams bounding the flow recirculation regions.

The models used in this study were all two dimensional. This made it possible for plume interaction to cause recirculation areas as shown in Figure 14. This recirculation in the base region between rocket and ramjet exhaust waves was balanced by entrainment of flow across the flow streams. It will be shown in these discussions that depending on the configuration being discussed, the recirculation may cause the base pressure to be greater closer to either the rocket or the ramjet. This difference in pressure along the base region between rockets and ramjet is indicative of a pressure gradient in this region. However, not enough data has been collected in this study to discuss the magnitude of the gradient in any great detail. In upcoming discussions, the presence of a gradient will be referred to as a pressure differential.

This same type of recirculation is present between the ramjet and the shroud when a shroud is present. This recirculation will be shown to be of a lesser magnitude than in the area between the rockets and

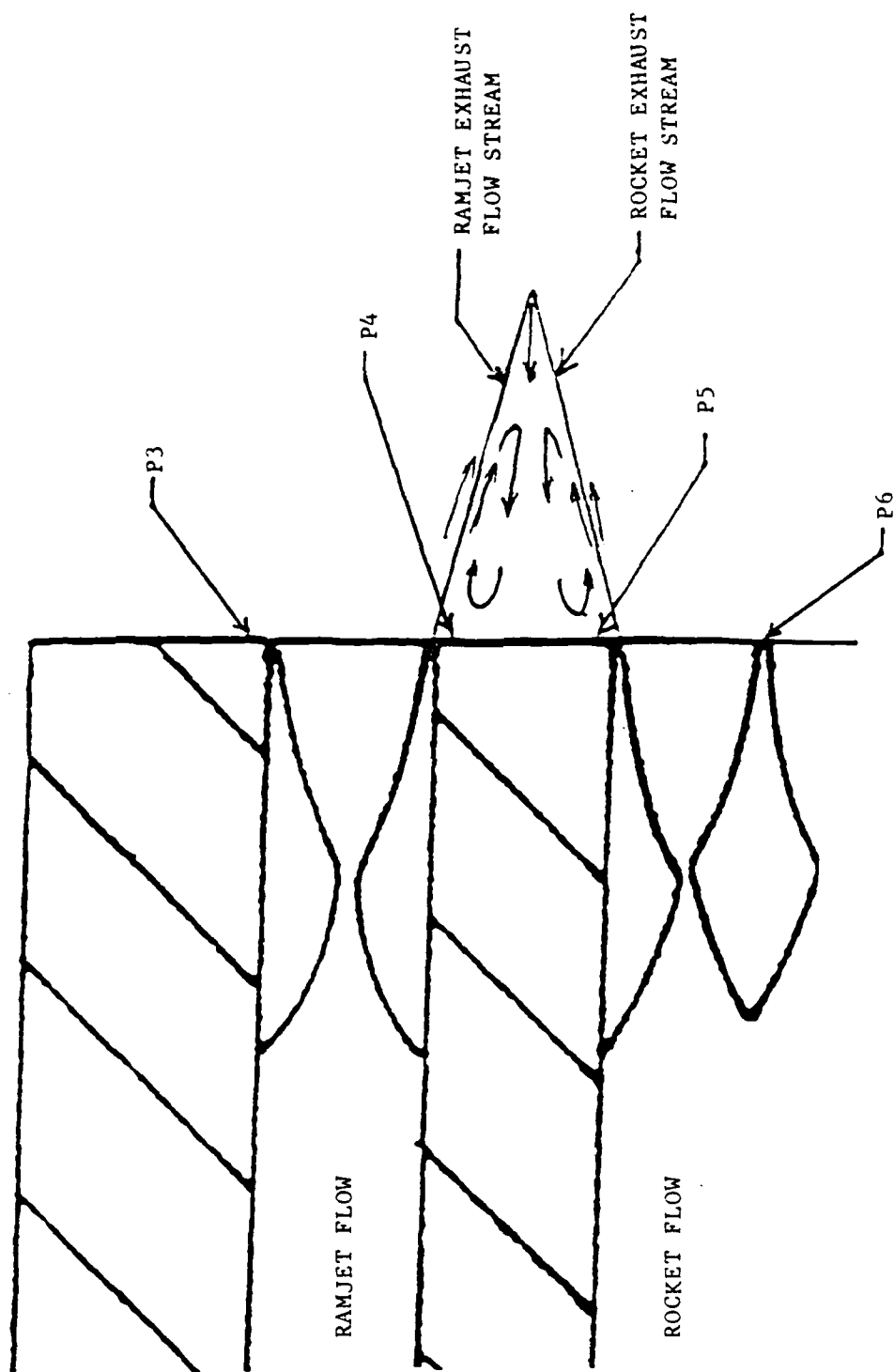


Figure 14. Typical Recirculation in the Model Base Area

the ramjet. However, the recirculation in the region above the ramjet may add to the thrust (15:10). During overexpanded operation when the ramjet exhaust waves are attached to the rocket plumes and not to the shroud an increase in thrust is possible due to the relationship between the base pressure and the back pressure. If the base pressure above the ramjet is greater than the back pressure then there could be additional positive thrust. Otherwise, the additional thrust may be zero or negative.

Baseline and Types of Comparisons

In order to evaluate the different configurations, a baseline model was established. The term baseline refers to a configuration consisting of rocket flow only, no ramjet flow. The model chosen for the baseline was the low area ratio (AR) rockets with no shrouds. The low area ratios were chosen since most booster rockets have relatively low AR nozzles. The case of no shrouds was chosen since no launch vehicle with a shroud exists. This low AR, no shroud model is the one most like current available boosters.

The various models were compared and evaluated on the basis of the magnitudes and trends shown in the measurements of the base pressures. For each model, the four base pressures were plotted on a single graph. Then the rockets only, unshrouded model (the baseline) was compared to other unshrouded models. A shroud was added to the baseline and this became a shrouded baseline configuration for comparison to other shrouded models. The baseline configurations were compared to various combinations of rocket-ramjet nozzle configurations in which the following could be traded off: low AR versus high AR nozzles, shrouded

versus unshrouded, ramjet nozzles close to or far from the model centerline, and in the case of the ramjet nozzles close to the centerline, the effect of shroud position is considered. Also, comparisons are made on the basis of increasing ramjet plenum pressure. A diagram of this is in Table V. These comparisons are contained in the following sections.

Unshrouded Baseline, Rocket Flow Only

In Figure 15 the four base pressures for the rockets only, unshrouded, low AR configuration are shown. The base pressures, except for between the rockets, are fairly low and begin to respond to the back pressure as the back pressure came up to 1.5 psia. The base pressure between the rockets (P6) is much higher in this region due to recirculation. The base pressure in this area is not affected by the back pressure until the back pressure has risen to almost 8 psia. This is since the wave structure around that area of the base is strong enough to keep the back pressure out of from between the rockets. A typical back pressure trace is shown in Figure 16. All references to back pressure refer to pressures as shown in this graph, not a back pressure ratio of plenum pressure to back pressure. The operation of a single nozzle in the various flow regimes has been well established (5:410-412). The effects of wave interactions for a multiple nozzle assembly is much less well understood. However, the pressure traces shown in Figure 15 correspond to what has been shown in previous work at AFIT on multiple rocket nozzles (7:22,23 and 7:39,40).

Table V. Experimental Itinerary (Bold Indicates Progression)

Baseline Unshrouded Rocket Flow Low/Low AR	→			Rocket/Ramjet Flow	Rocket/Ramjet Flow	Rocket/Ramjet Flow
				Unshrouded	Unshrouded	Unshrouded
				Close Ramjet Nozzle	Far Ramjet Nozzle	Far Ramjet Nozzle
				Low/Low AR	Low/Low AR	High/High AR
Baseline Close Shrouded Rocket Flow Low/Low AR	→			Rocket/Ramjet Flow	Rocket/Ramjet Flow	Rocket/Ramjet Flow
				Close Shrouded	Shrouded	Shrouded
				Close Ramjet Nozzle	Far Ramjet Nozzle	Far Ramjet Nozzle
				Low/Low AR	Low/Low AR	High/High AR
→						
			Rocket/Ramjet Flow	Rocket/Ramjet Flow	Rocket/Ramjet Flow	
			Shrouded	Shrouded	Shrouded	
			Close Ramjet Nozzle	Close Ramjet Nozzle	Close Ramjet Nozzle	
			Low/Low AR	High/High AR	High/High AR	

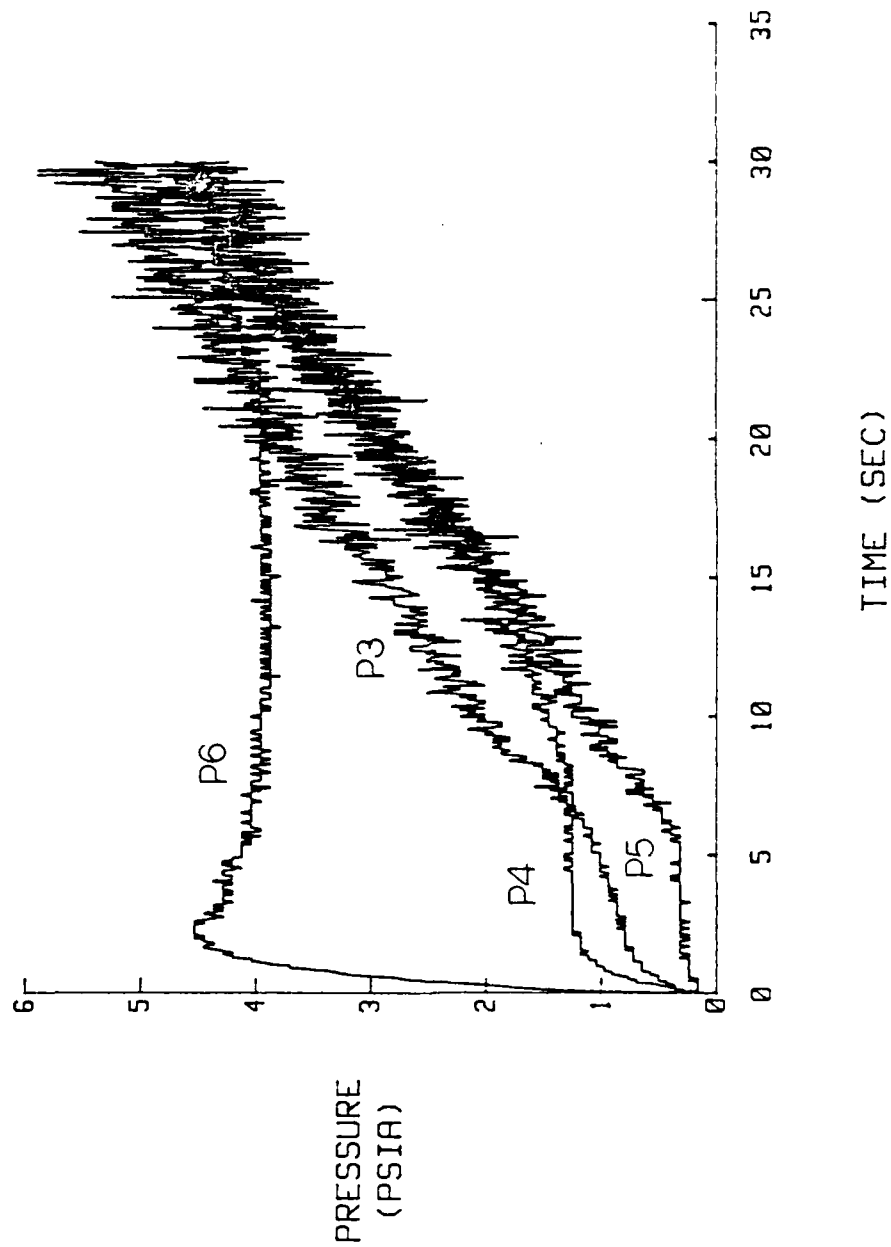


Figure 15. P3, P4, P5 and P6 Vs Time for
Baseline, Rocket Flow Only, Unshrouded Base Pressures

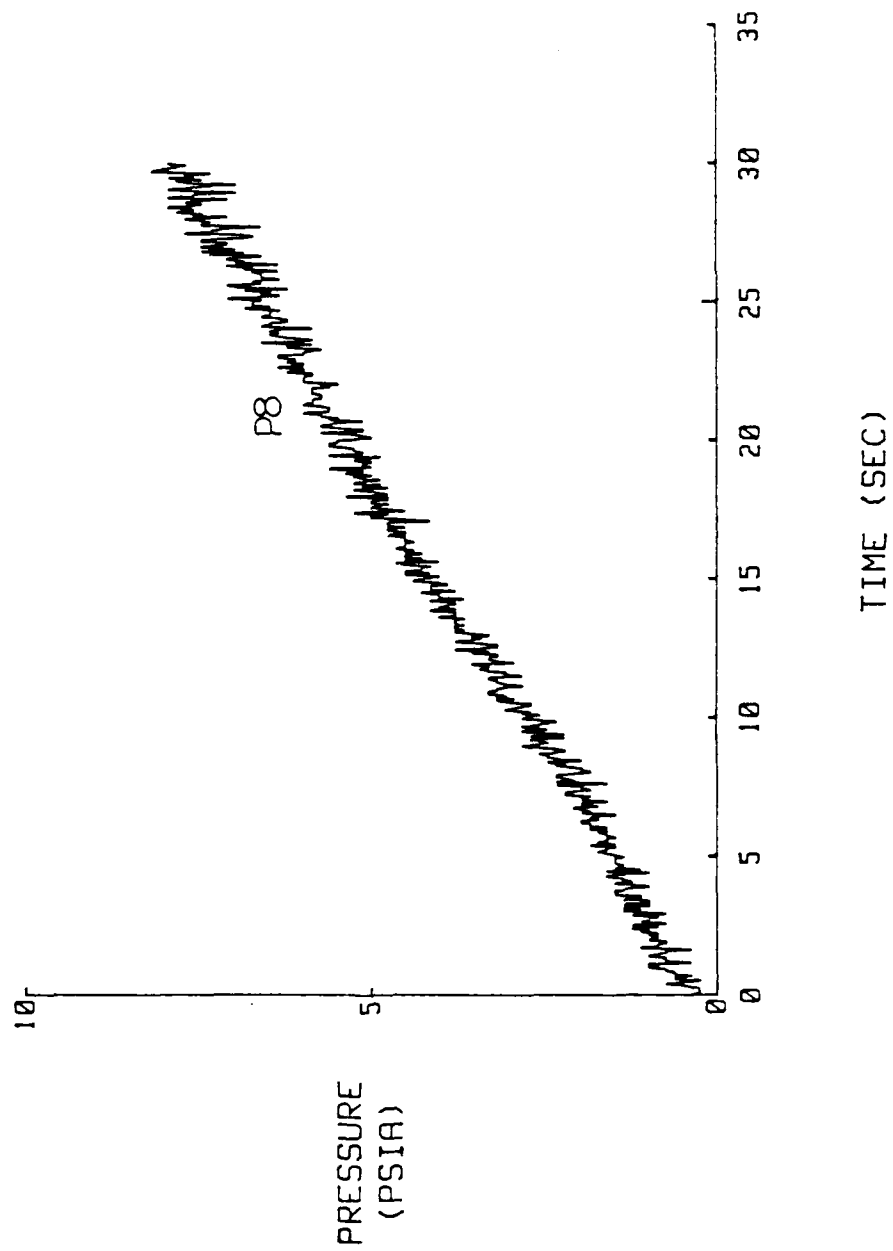


Figure 16. Typical Back Pressure Curve

Unshrouded, Close Ramjet Nozzle, Low/Low AR

The addition of ramjet nozzles and shrouds creates additional effects which are now examined. Rocket-ramjet base pressures for unshrouded, close ramjet nozzle and low/low AR operation are shown in Figure 17. Typical exhaust plume patterns are in Figure 18 for the underexpanded regime of the nozzles. The horizontal lines at the top and the bottom of the schlieren photograph are the top and bottom of the plexiglass sidewall panes. The initial pressure spikes in Figure 17 are startup pulses that the transducers detect and which occur due to the initial flow.

The addition of the ramjet flow has quite an effect on the base pressures (compare Figure 17 to Figure 15). The pressure between the rockets (P6) is not so high as before in rocket only operation due to the expansion waves from the ramjets interacting with the waves from the rockets. The interaction apparently modifies the recirculation zone between the rocket nozzles. The pressure between rockets and ramjet closer to the rocket (P5) is of the same magnitude as before when there was no ramjet flow except the back pressure is somewhat greater before it affects that area. This is because the interaction of the waves protects this area of the base from the back pressure better than rocket only operation. The pressure close to the ramjet and between the rockets and ramjet (P4) is much higher now since this area is isolated from the back pressure by the wave pattern. The pressure above the ramjet (P3) is higher in this case than in rocket only operation and this is due to a combination of recirculation and effects noted by Huband (15). Huband noted that the exit plane pressure may strongly indicate what the base

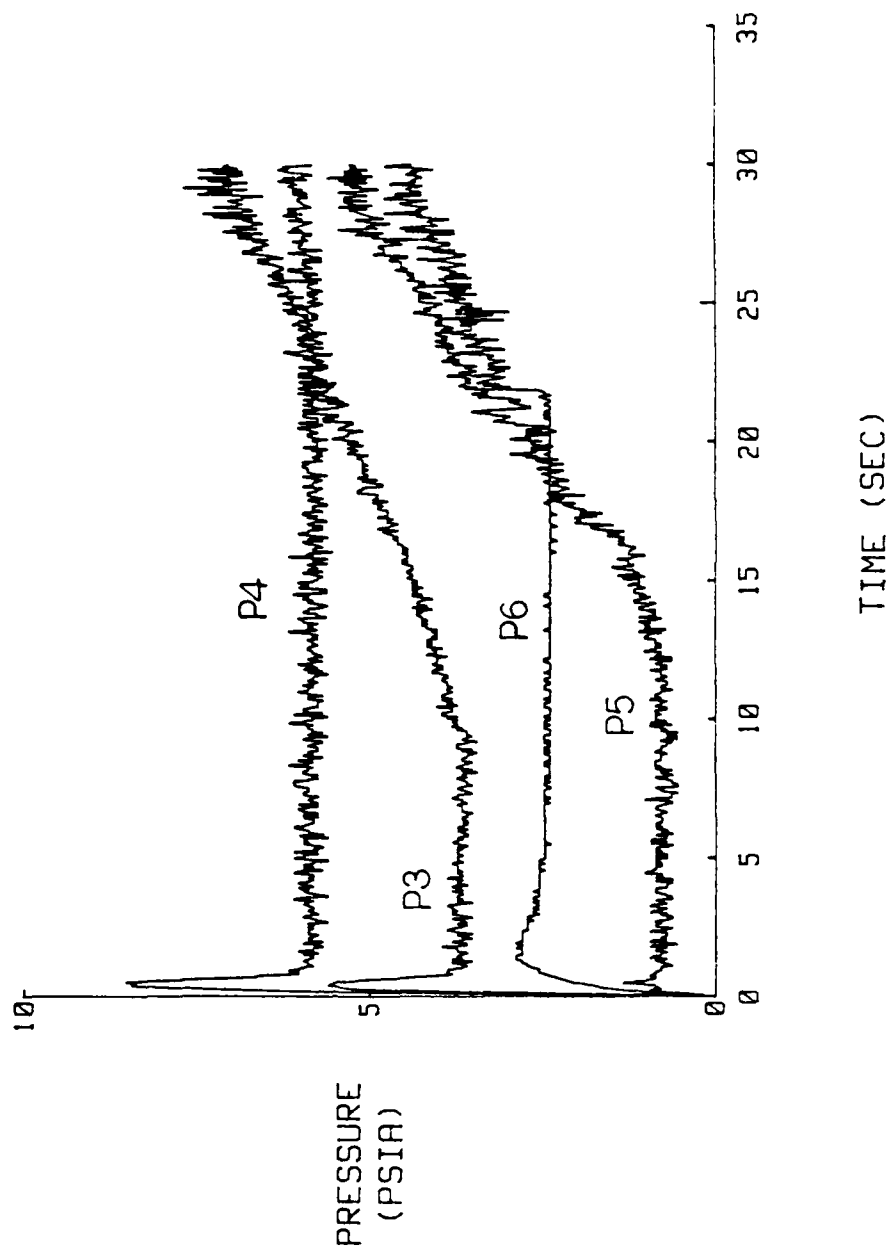


Figure 17. P3, P4, P5 and P6 Vs Time for Unshrouded,
Close Ramjet Nozzle, Low/Low AR; $P_{rjp} = 42$ psia

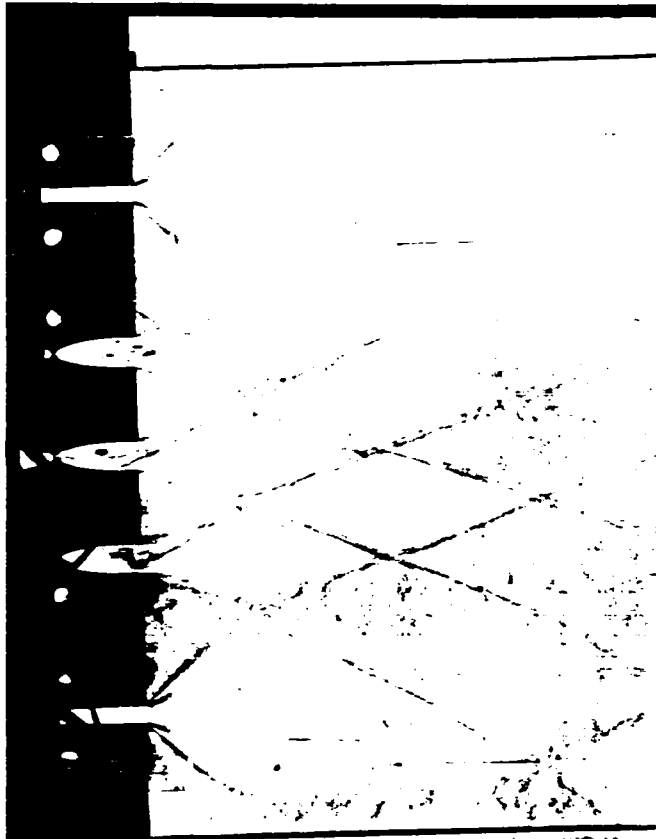


Figure 18. Typical Flow Pattern for Unshrouded,
Close Ramjet Nozzle, Low/Low AR

pressure adjacent to the nozzle exit may be. The back pressure must be increased to affect the base region and that may be noticed when the back pressure is about 6.5 psia. This is because the combination of rocket and ramjet flow produces a wave structure which is able to protect the base from higher back pressures than in the case of rocket only flow. This means that this configuration is able to operate against higher back pressures. It appears as though in the base region between the rocket and ramjet nozzles there is a pressure differential. The pressure differential along the base appears to be due to flow sharply expanding around the nozzle exit, the pressure due to recirculation and other effects previously mentioned which may produce an uneven pressure along the base. The pressure is sometimes highest near the rocket and at other times it is highest near the ramjet. Which location has higher pressure depends on the model configuration. In this case, the pressure is highest near the ramjet and lower close to the rocket. In Figures 19, 20, 21 and 22, the base pressures for increasing ramjet plenum pressure are shown. The general results for increasing the ramjet plenum pressure are to greatly increase the base pressures around the ramjet (P3 and P4) due to the effects noted by Huband (15). The pressures around the rockets (P5 and P6) are hardly affected by increasing ramjet plenum pressure in this configuration. This is because the main influence in the base region around the rockets is the rocket flow in this model. The pressure differential present in this model shows the pressure to be greater near the ramjet as a result of increasing the ramjet plenum pressure giving greater pressures in the region around the ramjet.

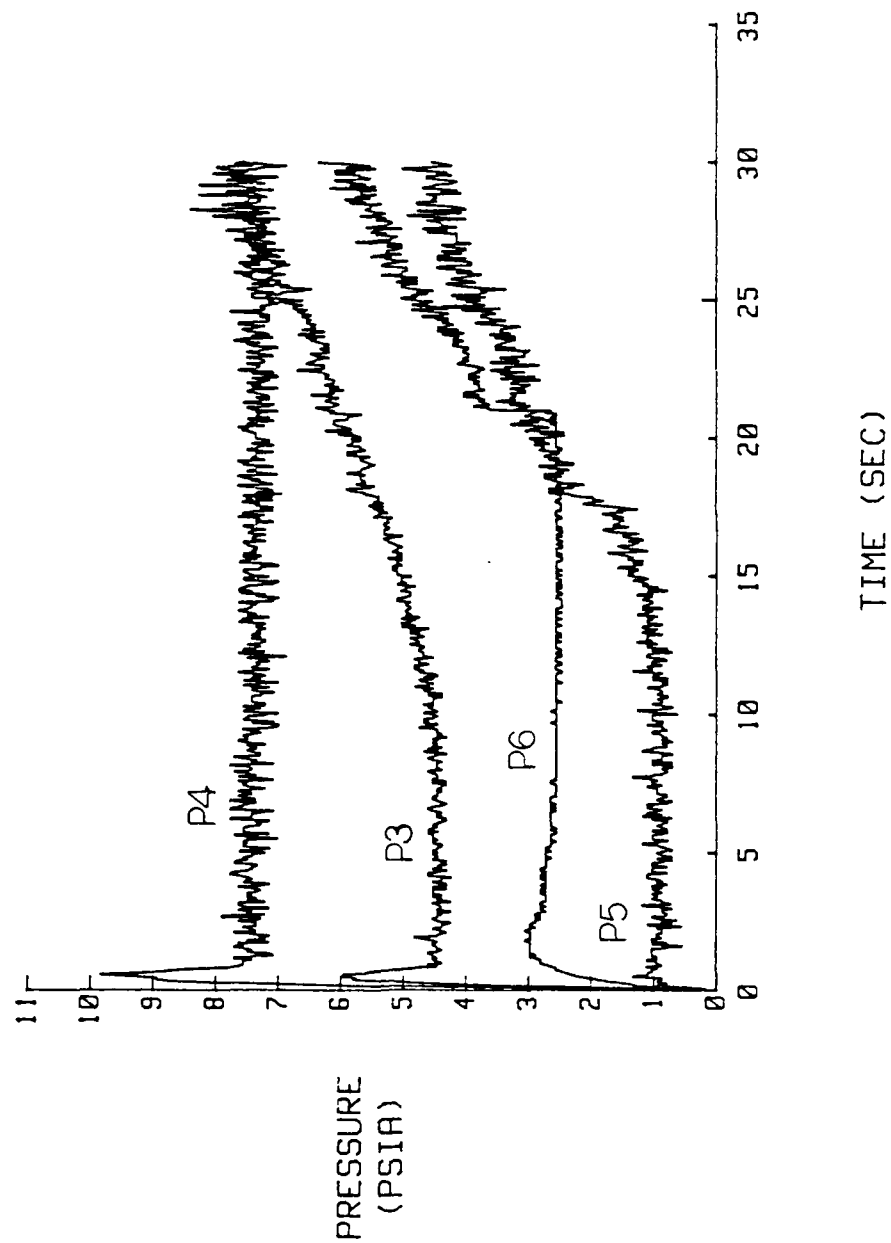


Figure 19. P3, P4, P5 and P6 Vs Time for Unshrouded,
Close Ramjet Nozzle, Low/Low AR; $P_{rjp} = 52$ psia

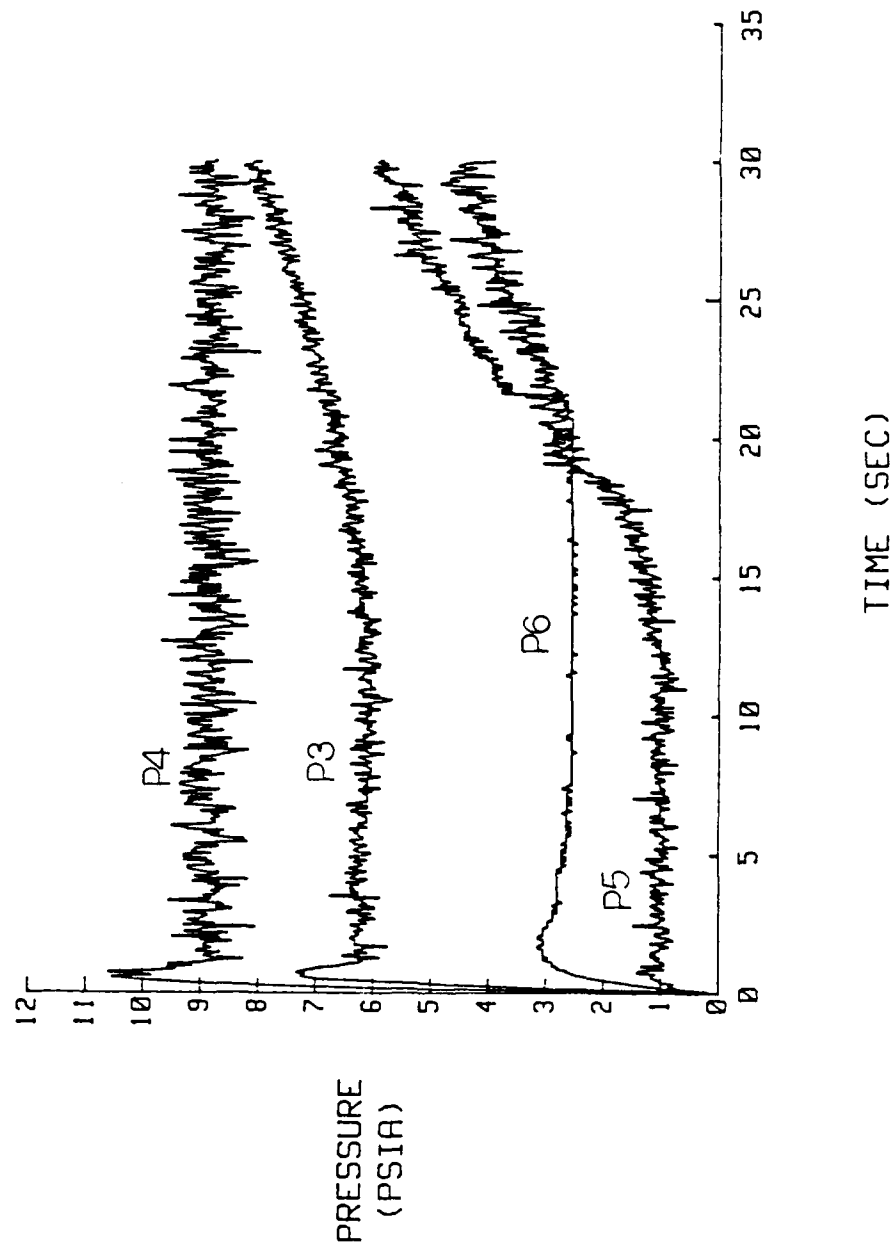


Figure 20. P3, P4, P5 and P6 Vs Time for Unshrouded,
Close Ramjet Nozzle, Low/Low AR; $P_{rjp} = 62$ psia

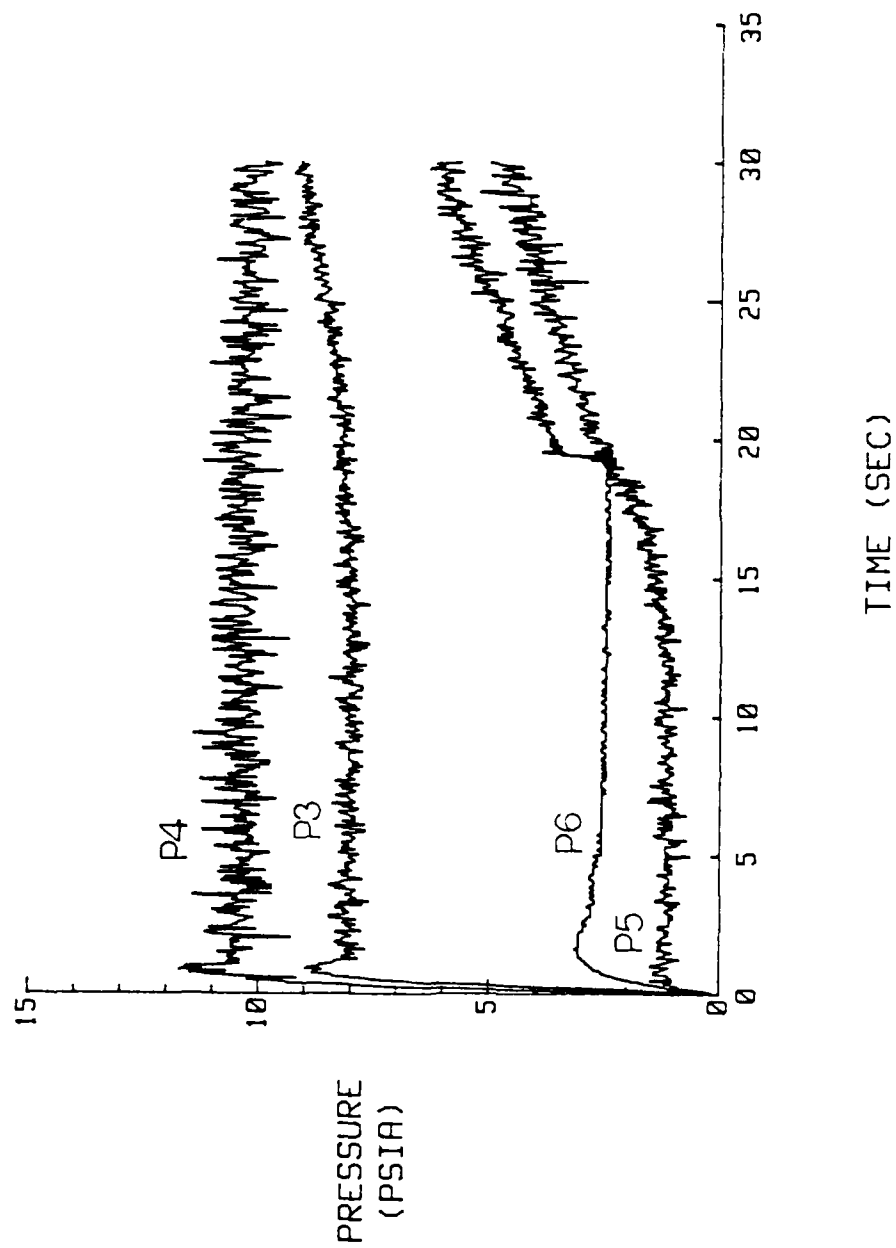


Figure 21. P3, P4, P5 and P6 Vs Time for Unshrouded,
Close Ramjet Nozzle, Low/Low AR; $P_{rjp} = 72$ psia

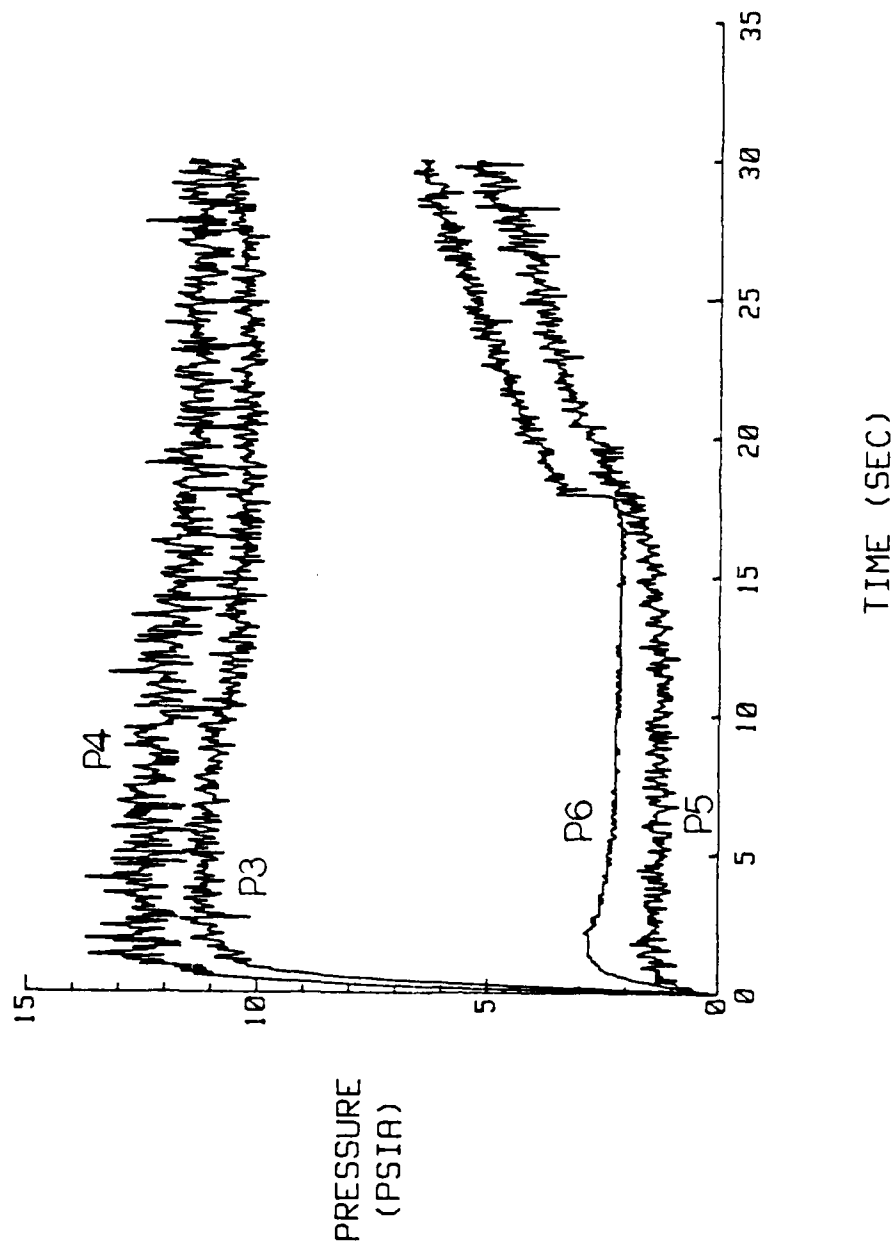


Figure 22. P3, P4, P5 and P6 Vs Time for Unshrouded,
Close Ramjet Nozzle, Low/Low AR; $P_{rjp} = 87$ psia

Unshrouded, Close Ramjet Nozzle, High/High AR

In this configuration, unshrouded, close ramjet nozzles, when the high AR nozzles are used, the base pressures around the rockets are decreased significantly compared to the previous configuration with the low AR nozzles. This is due to the lower exit plane pressures of the high AR nozzles. The base pressures for this model are shown in Figure 23. The ramjet base pressures also are lower due to the same effect of lower exit plane pressure for a higher AR nozzle. The back pressure first affects the base pressure above the ramjet (P3) and after a slight increase in the back pressure, it begins to affect the base pressure between the rockets and ramjet closer to the rockets (P5). This is due to the fact that the base pressures closer to the center of the model are better protected from the effects of the back pressure by the interaction of the rocket and ramjet exhaust waves in this configuration. P3 is least protected from the effects of back pressure and the base pressure between the rockets (P6) is best protected. In Figures 24, 25, 26 and 27, the base pressures for increasing ramjet plenum pressure are shown. From these graphs it can be seen that increasing the ramjet plenum pressure has little effect on the base pressures near the rockets. This is due to the wave structure produced by this configuration. The wave structure in the area between the rockets and just above the rockets between rockets and ramjet protects this area from influences created by increasing the ramjet plenum pressure. The most important increases in base pressure for this configuration occur around the ramjet nozzle as the ramjet plenum pressure is increased. This is due to the effect on base pressures of increased nozzle exit plane pressures at higher ramjet

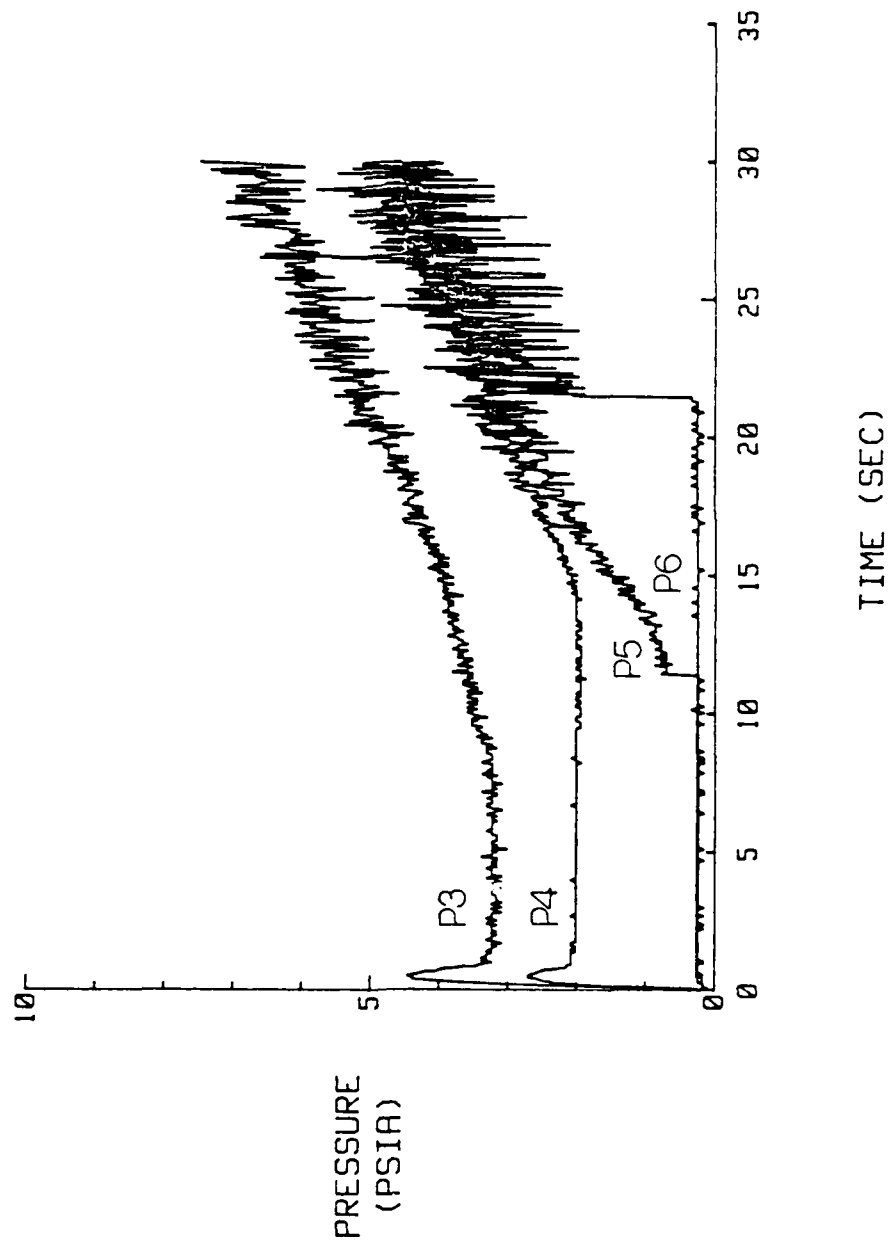
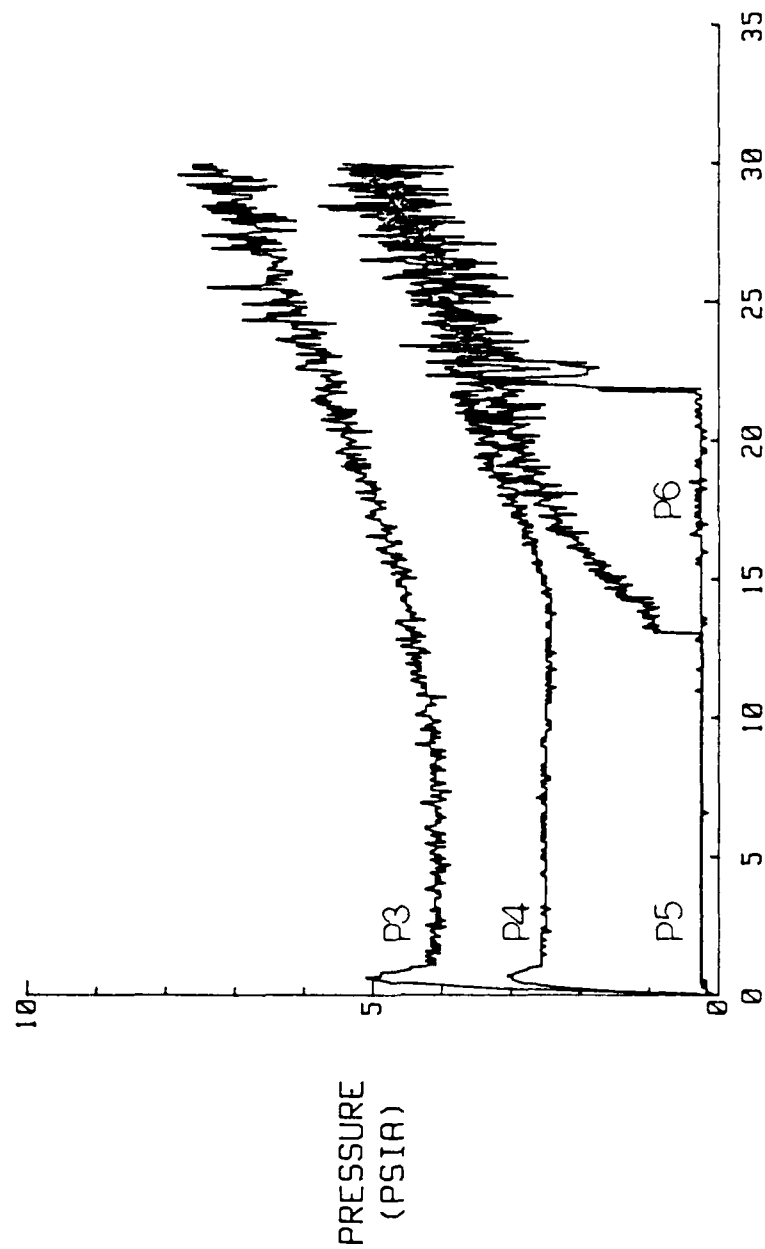


Figure 23. P3, P4, P5 and P6 Vs Time for Unshrouded,
Close Ramjet Nozzle, High/High AR; $P_{rjp} = 42$ psia



TIME (SEC)

Figure 24. P3, P4, P5 and P6 Vs Time for Unshrouded,
Close Ramjet Nozzle, High/High AR; $P_{rjp} = 52$ psia

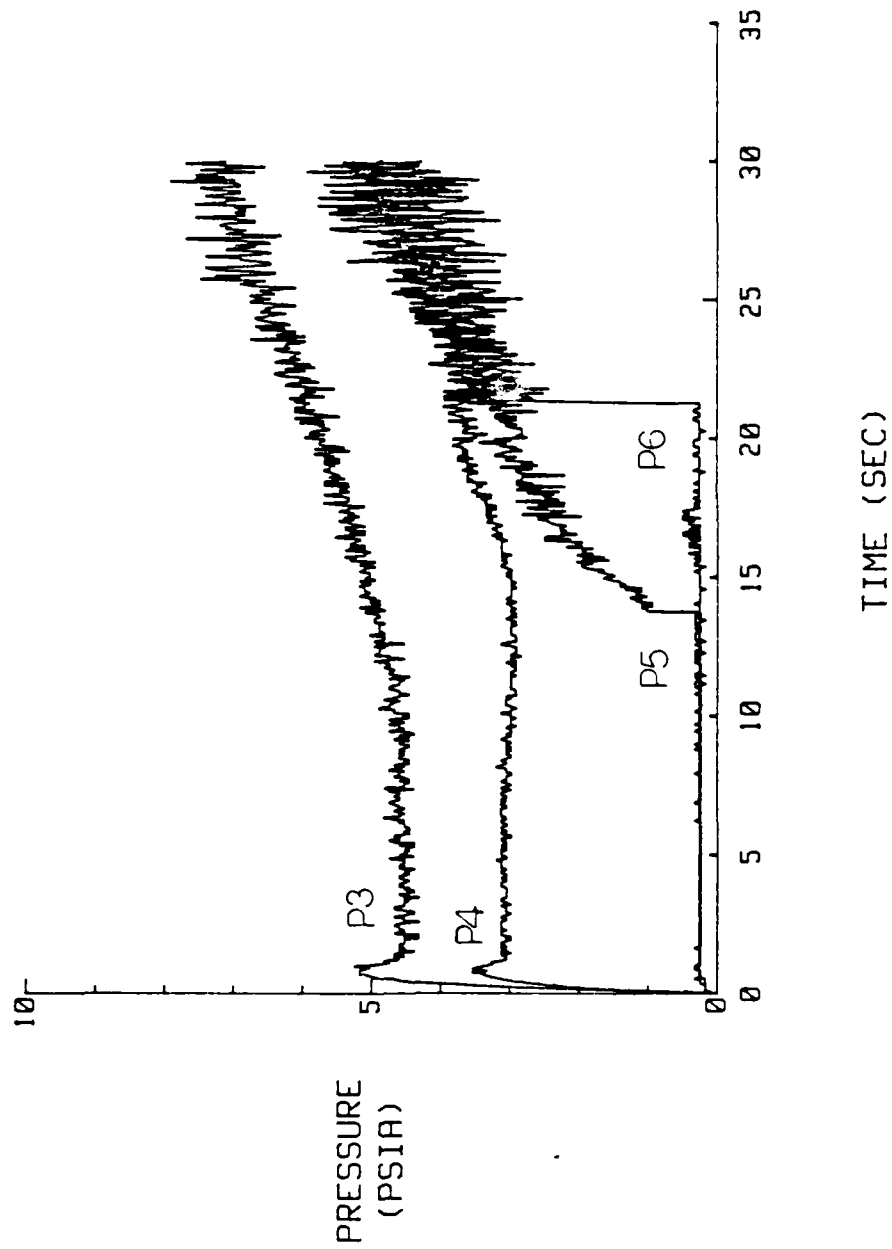


Figure 25. P3, P4, P5 and P6 Vs Time for Unshrouded,
Close Ramjet Nozzle, High/High AR; $P_{rjp} = 62$ psia

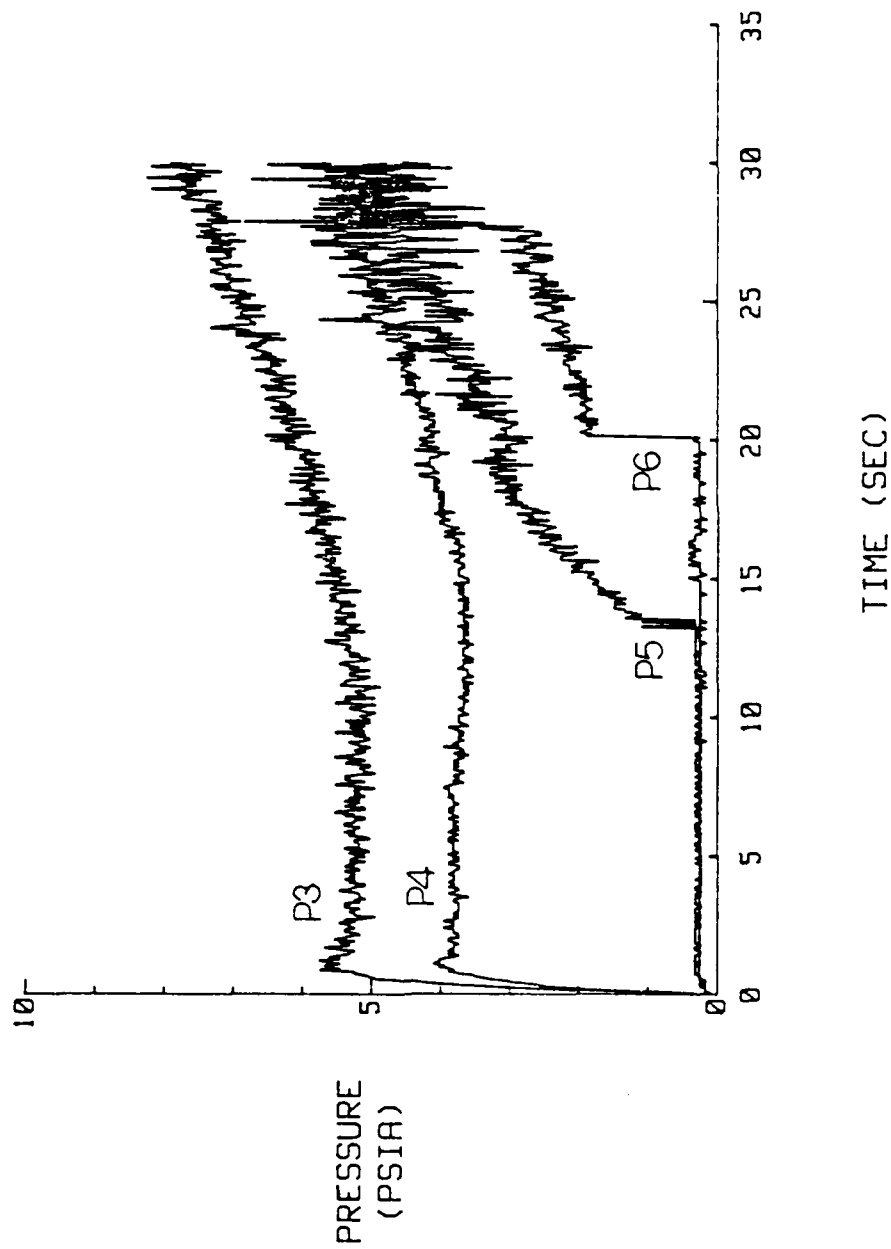
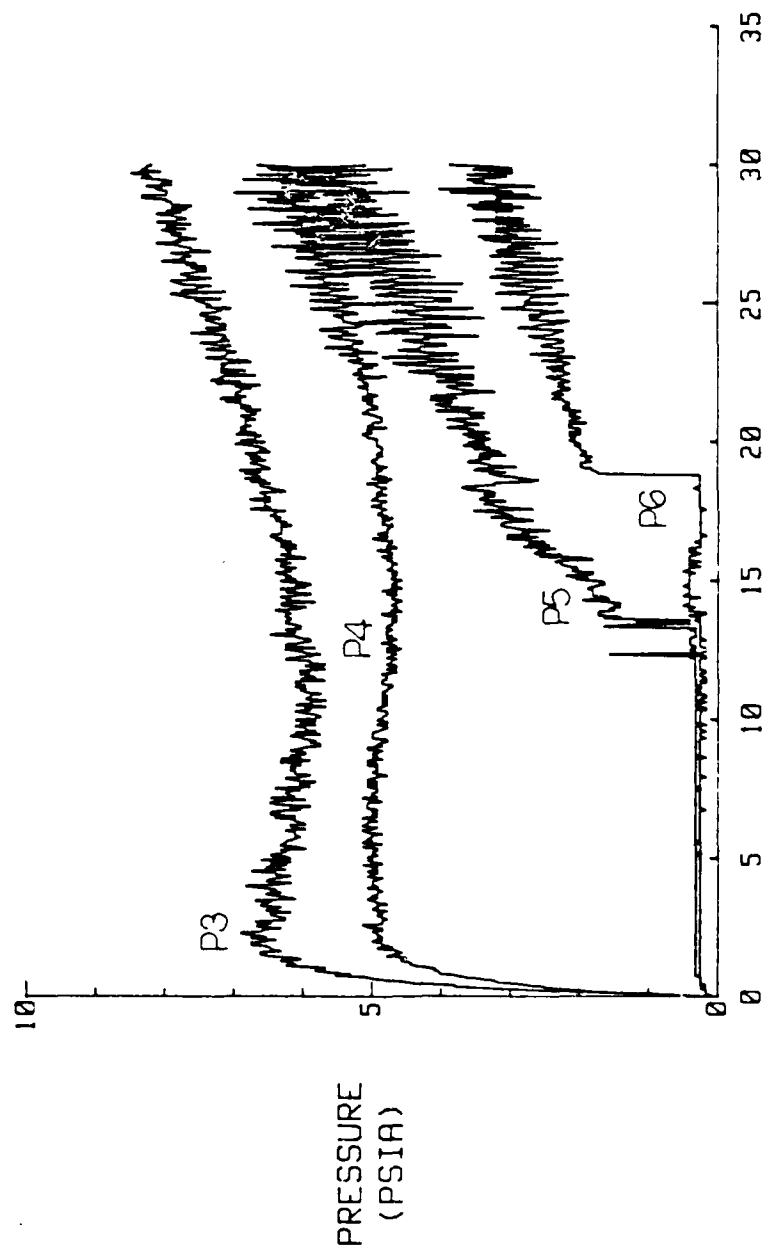


Figure 26. P3, P4, P5 and P6 Vs Time for Unshrouded, Close Ramjet Nozzle, High/High AR; $P_{rjp} = 72$ psia



TIME (SEC)

Figure 27. P3, P4, P5 and P6 Vs Time for Unshrouded, Close Ramjet Nozzle, High/High AR; $P_{rjp} = 87$ psia

plenum pressures as described by Huband (15). For this configuration, the differential of pressure between the rockets and ramjet is again showing the base pressure to be greatest near the ramjet and least near the rockets. This is true regardless of the ramjet plenum pressure. However, as the ramjet plenum pressure increases, the pressure gets higher close to the ramjet.

Unshrouded, Far Ramjet Nozzle, Low/Low AR

For the next configuration, the ramjet nozzles have been placed at the far distance from the model centerline. This is the unshrouded, far ramjet nozzle, low/low AR configuration. The base pressures for this model are shown in Figure 28. The base pressures are much greater here than in any previous configuration. The exhaust flow pattern for this configuration is presented in Figure 29. The high base pressure for P5 is due to recirculation from the rocket and ramjet exhausts interacting. This high pressure has been previously discussed by Huband (15). In his work, Huband suggests the exit pressure may strongly indicate what the base pressure in a region adjacent to the nozzle exit plane might be. However, for this AR the exit plane pressure of the rocket ought to be about three psia. This is far below the 20 psia indicated for P5 in Figure 28. Therefore the high pressure around P5 must be due to recirculation being directed into that area. The change in location of the ramjet nozzle changes the recirculation zone so as to increase P5. The least effect of recirculation is noted on P4, when compared to the case where the ramjet nozzles are close in. This is due to the ramjet exhaust waves protecting that area close to the ramjet and the effect of interaction with the rockets is felt mostly around the area of the rocket

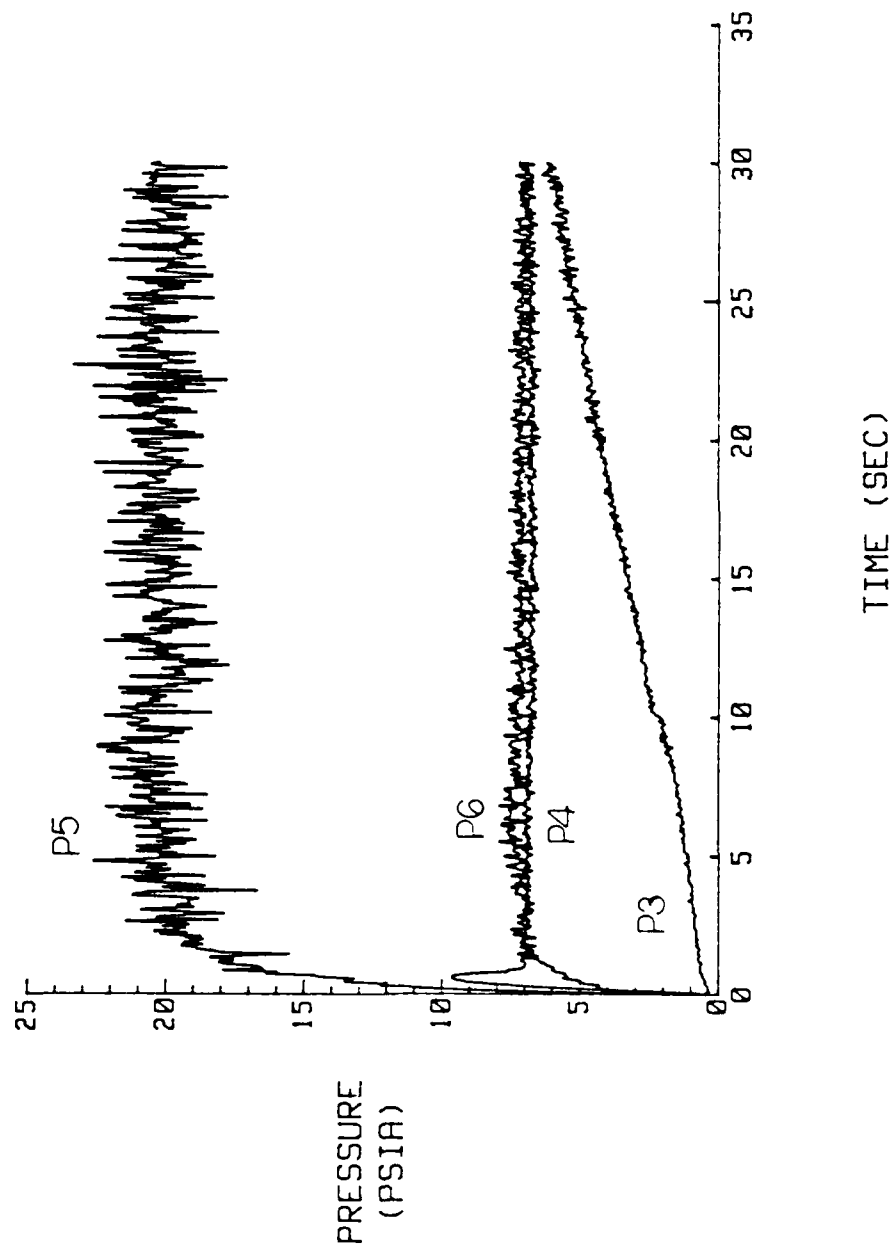


Figure 28. P3, P4, P5 and P6 Vs Time for Unshrouded, Far Ramjet Nozzle, Low/Low AR; $P_{rjp} = 42$ psia

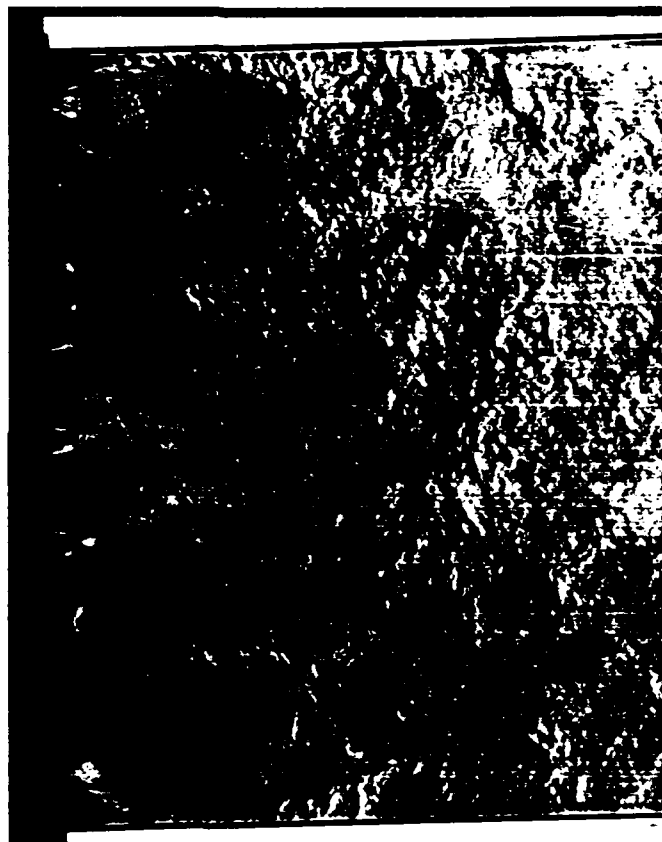


Figure 29. Typical Flow Pattern for Unshrouded,
Far Ramjet Nozzle, Low/Low AR

base (between the rockets and the ramjet close to the rockets). The back pressure effect on P3 is almost immediate. This can be seen in the steady rise almost from the start of the P3 curve and is due to the rockets attracting the ramjet exhaust toward the model centerline and away from the top of the model. P6 is somewhat higher than in the close ramjet case due to greater recirculation. The pressure differential in this model shows the base pressures are greatest near the rocket and lowest near the ramjet at low ramjet plenum pressure. The effects of increasing ramjet plenum pressure can be seen in Figures 30, 31, 32 and 33 for this configuration. One of the effects is the differences in P3 which show the effects of the back pressure. The plateau in P3 of Figure 33 shows the back pressure takes effect at about two psia. This is a lower simulated altitude than the corresponding altitude at which the back pressure is felt by P3 at lower ramjet plenum pressures. This delay is due to the increasing strength of the ramjet exhaust waves with increasing ramjet plenum pressure giving the area above the ramjet protection from the back pressure. P6 between the rockets sees only slightly more recirculation due to the increased ramjet plenum pressure so it only goes up a little. The increasing ramjet plenum pressure greatly affects the base pressure between the rockets and ramjet close to the ramjet (P4) to where P4 and P5 are nearly equal. This is because the increasing ramjet plenum pressure increases the ramjet nozzle exit plane pressure and in turn that increases the base pressure in the area of P4 as described by Huband (15). The result of P4 and P5 being nearly equal is that the pressure differential shows the differences in pressures between the two nozzles is lessened with increasing ramjet plenum

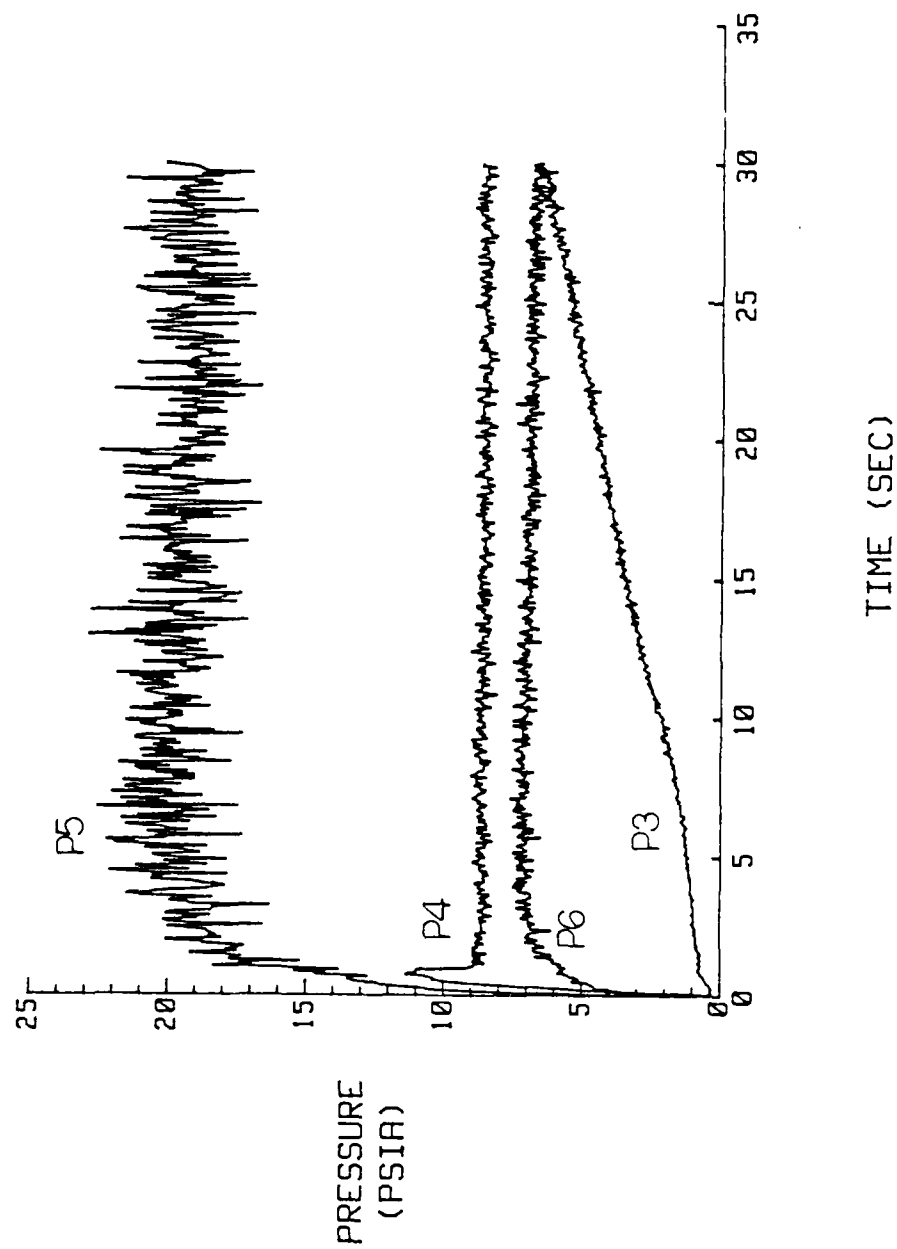
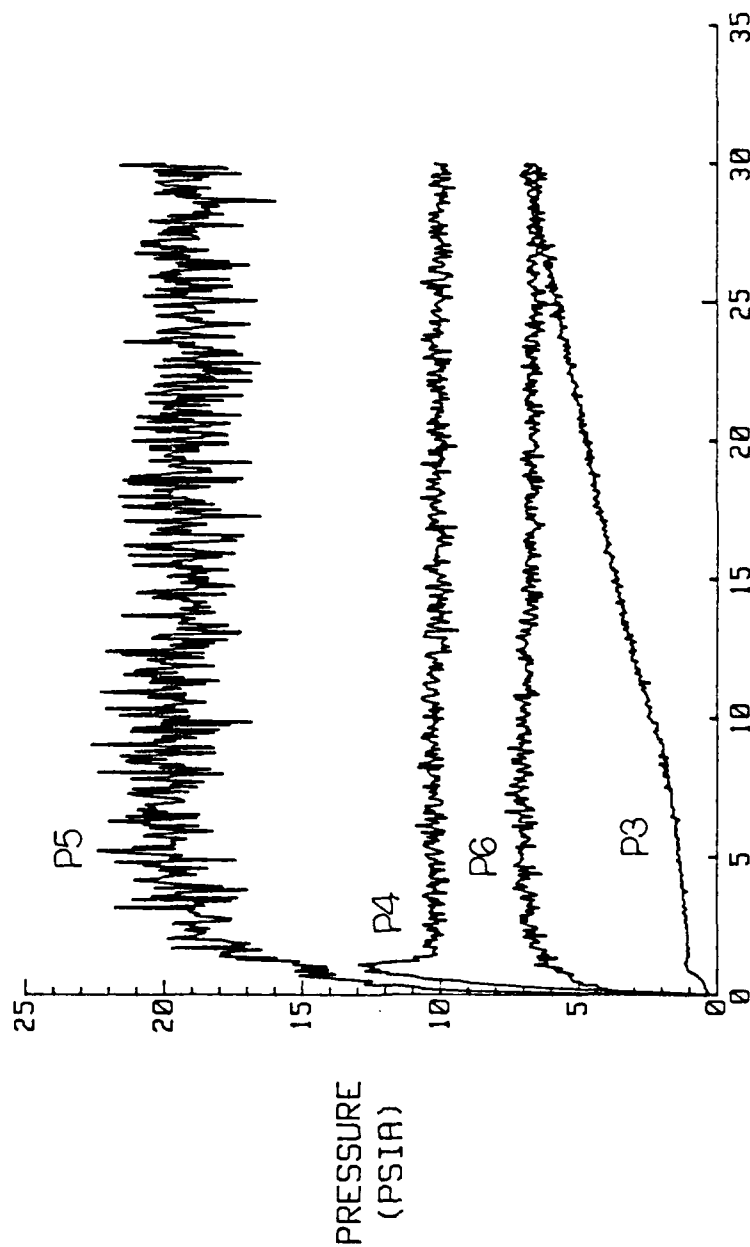


Figure 30. P3, P4, P5 and P6 Vs Time for Unshrouded,
Far Ramjet Nozzle, Low/Low AR; $Pr_{jp} = 52$ psia



TIME (SEC)

Figure 31. P3, P4, P5 and P6 Vs Time for Unshrouded, Far Ramjet Nozzle, Low/Low AR; $P_{rjp} = 62$ psia

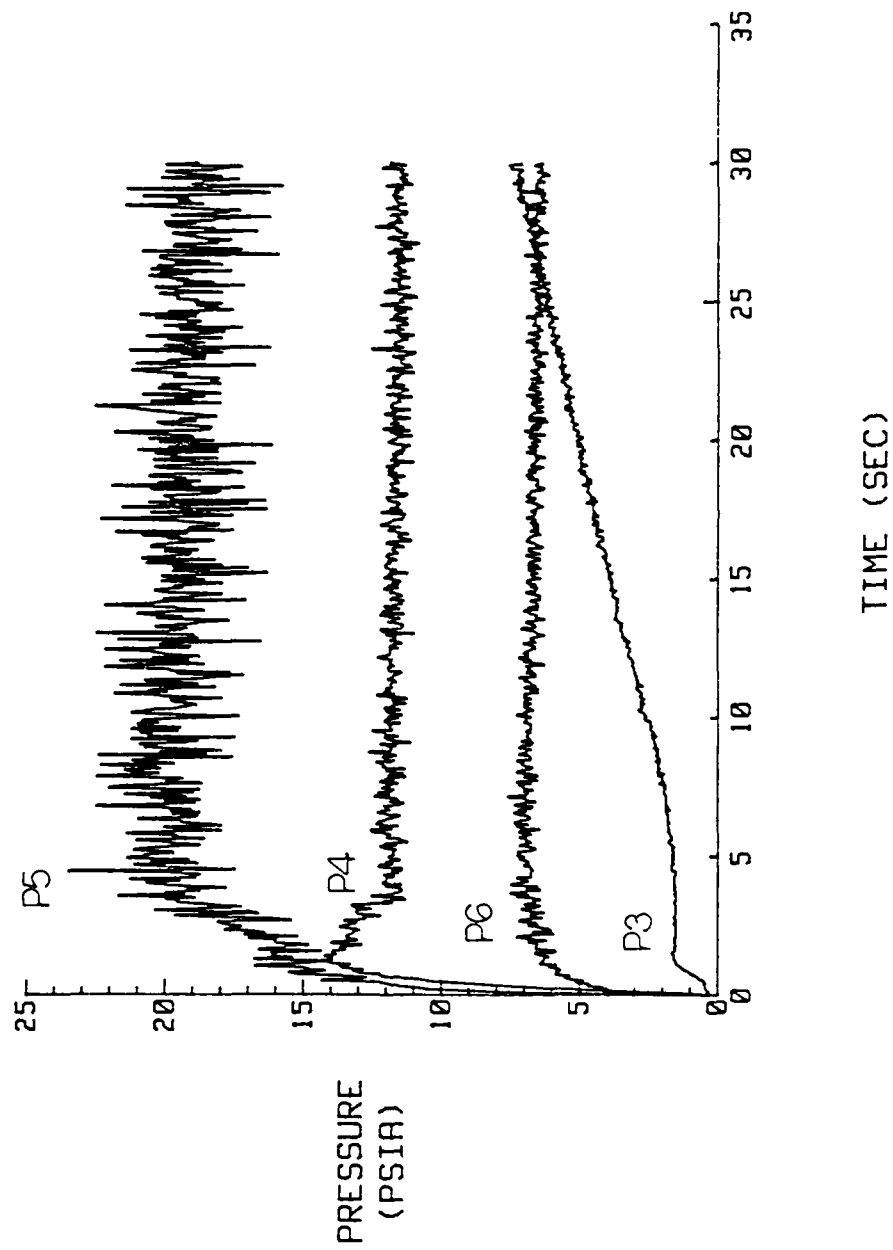


Figure 32. P3, P4, P5 and P6 Vs Time for Unshrouded,
Far Ramjet Nozzle, Low/Low AR; $P_{rjp} = 72$ psia

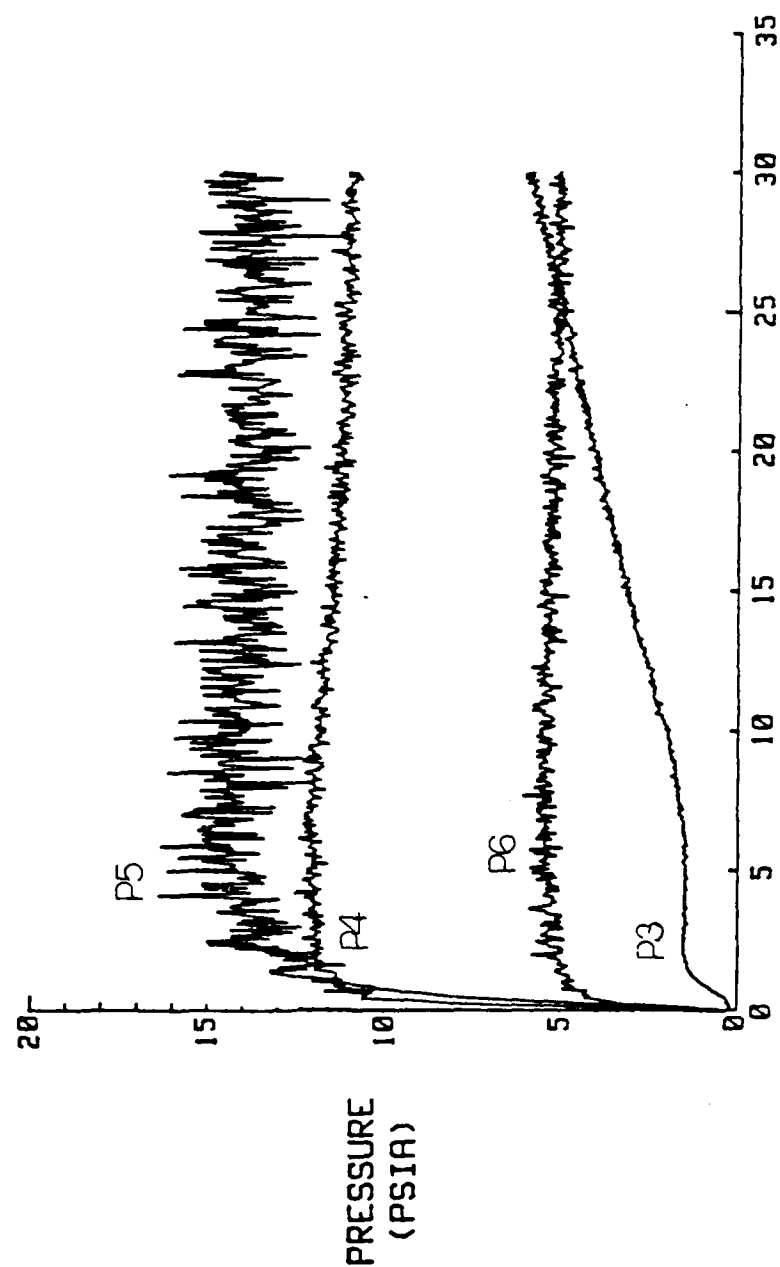


Figure 33. P3, P4, P5 and P6 Vs Time for Unshrouded, Far Ramjet Nozzle, Low/Low AR; $P_{rjp} = 87$ psia

pressure. The slight decrease in P4 with increasing back pressure and at greater ramjet plenum pressures is due to the fact that the ramjet plenum pressure does fall off slightly with time.

Unshrouded, Far Ramjet Nozzle, High/High AR

When the high AR nozzles are used in the unshrouded, far ramjet nozzle model, the base pressures are as shown in Figure 34. In general, the magnitudes of the base pressures decrease as compared to the low AR configuration (see Figure 28). However instead of P5 being greater than P6 as in the low AR model, the opposite occurs. This is presented in Figure 35. The step increase in P5 is due to the back pressure being felt when the back pressure reaches a value nearly equal the base pressure. Compare P5 in Figure 34 to Figure 16 near the end of the experiment. P3 senses the back pressure almost immediately due to the lower exit plane pressures of the high AR nozzles. The pressure differential between the rockets and the ramjet shows the pressure near the rocket base greater than the pressure near the ramjet base. Figures 36, 37, 38 and 39 shows the effect of increasing ramjet plenum pressure on the base pressures of the unshrouded, far ramjet nozzle, high/high AR configuration. In this case, increasing the ramjet plenum pressure has almost no effect on when P3 is affected by the back pressure. This is because the ramjet nozzles are further out from the rockets and hence close to the top of the perimeter of the plexiglass sidewalls and because the exit plane pressures for the high AR nozzles are lower than for the low AR nozzles. P5 and P6 decrease in magnitude slightly due to lessened nozzle exit plane pressures for the high AR nozzles when compared to the low AR nozzles. However, P4 increases significantly. This pressure

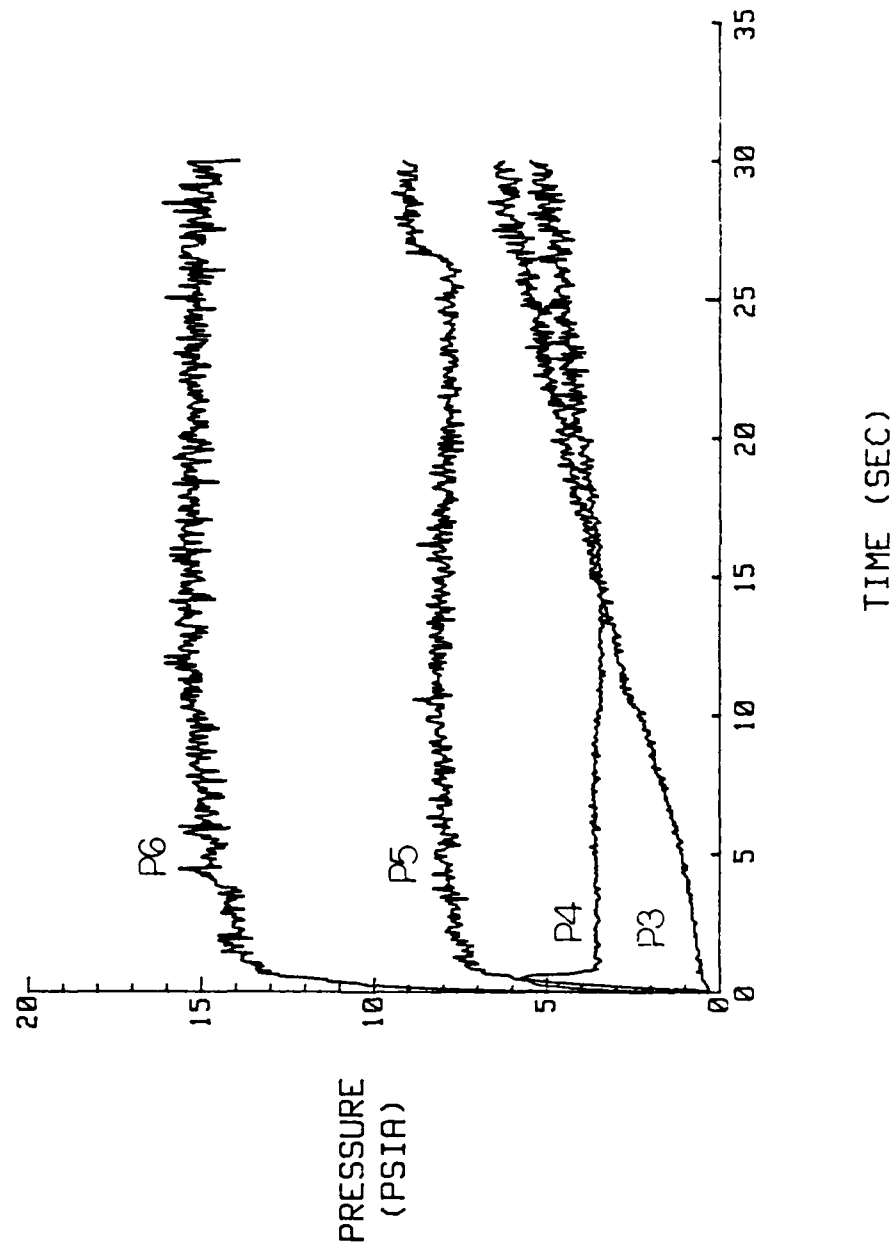


Figure 34. P3, P4, P5 and P6 Vs Time for Unshrouded,
Far Ramjet Nozzle, High/High AR; $P_{rjp} = 42$ psia

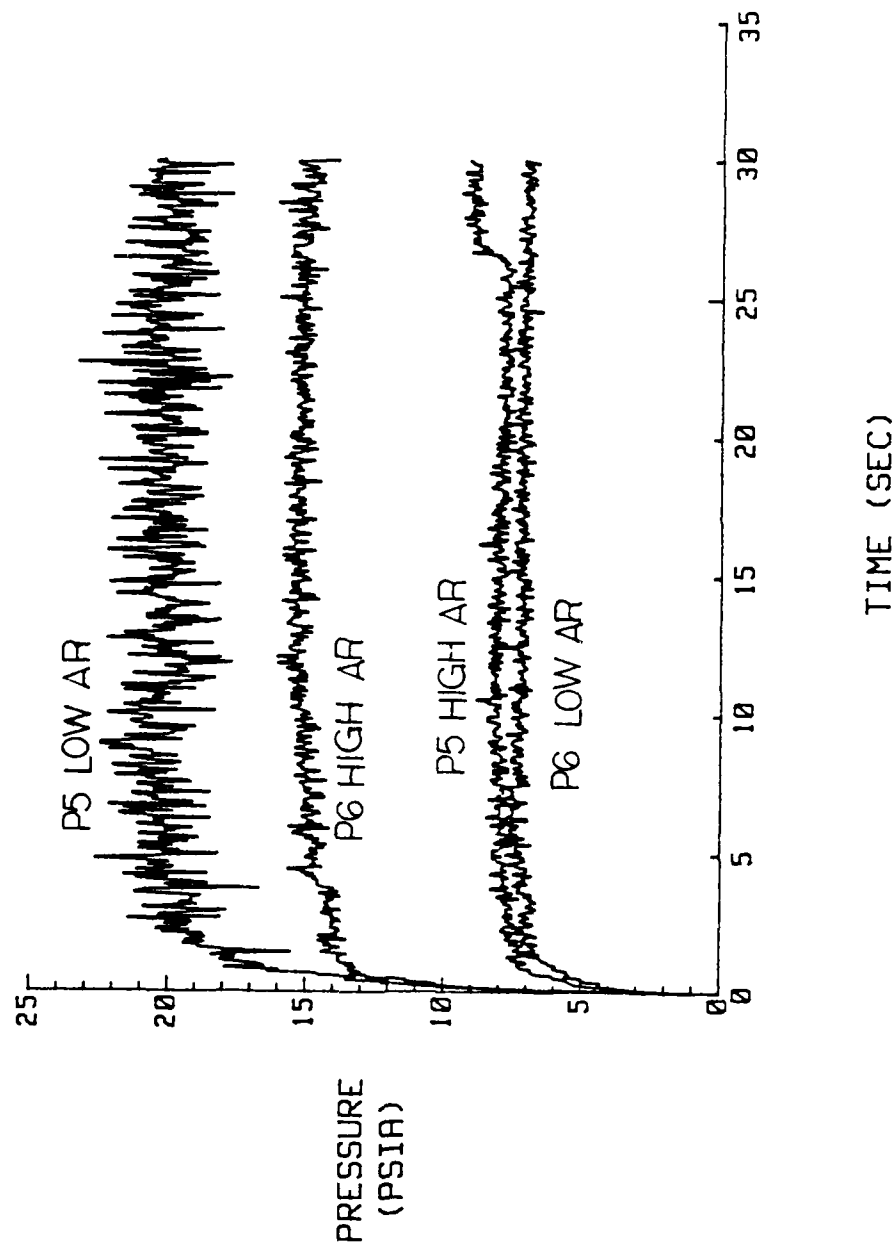


Figure 35. P5 and P6 Vs Time for Unshrouded, Low/Low and High/High AR, Far Ramjet Nozzle; $P_{rjp} = 42$ psia

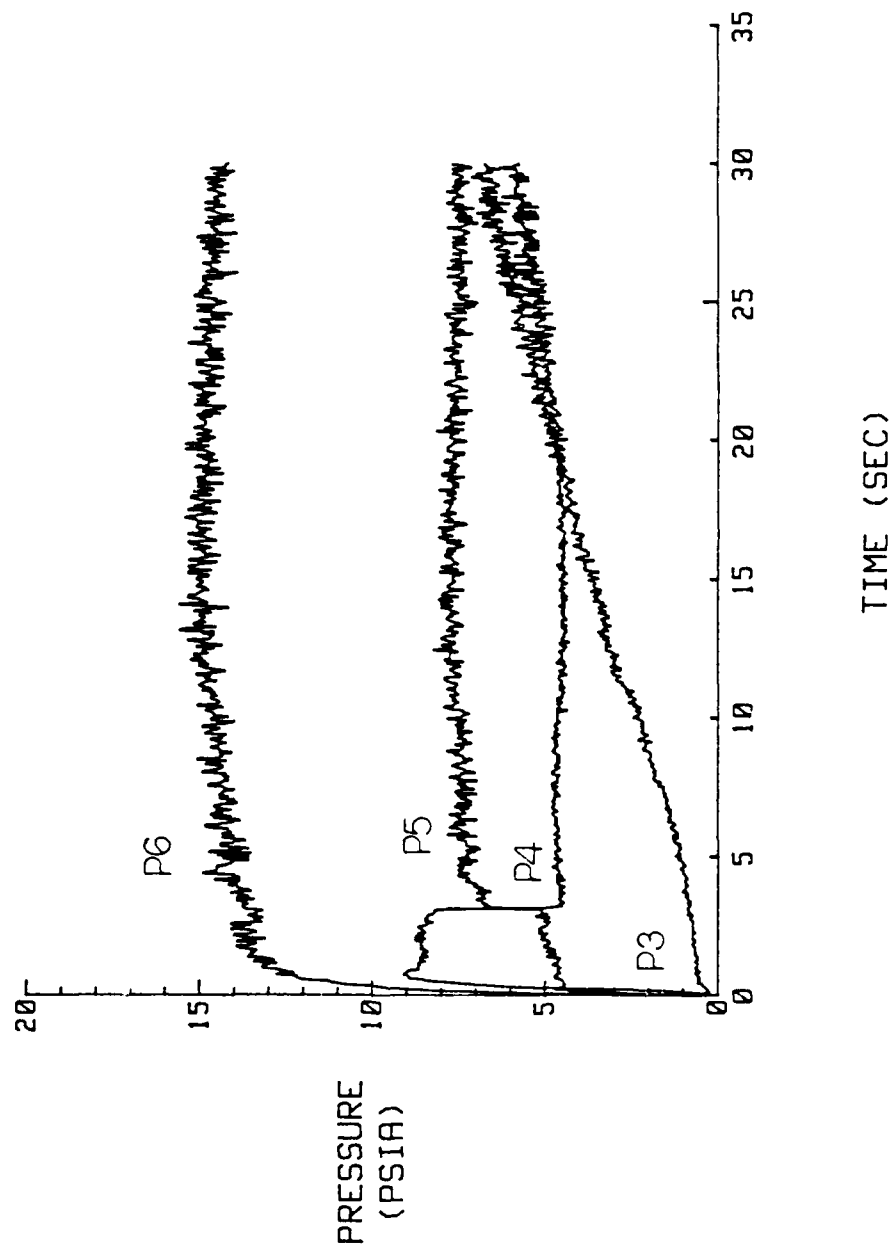


Figure 36. P3, P4, P5 and P6 Vs Time for Unshrouded,
Far Ramjet Nozzle, High/High AR; $P_{rijp} = 52$ psia

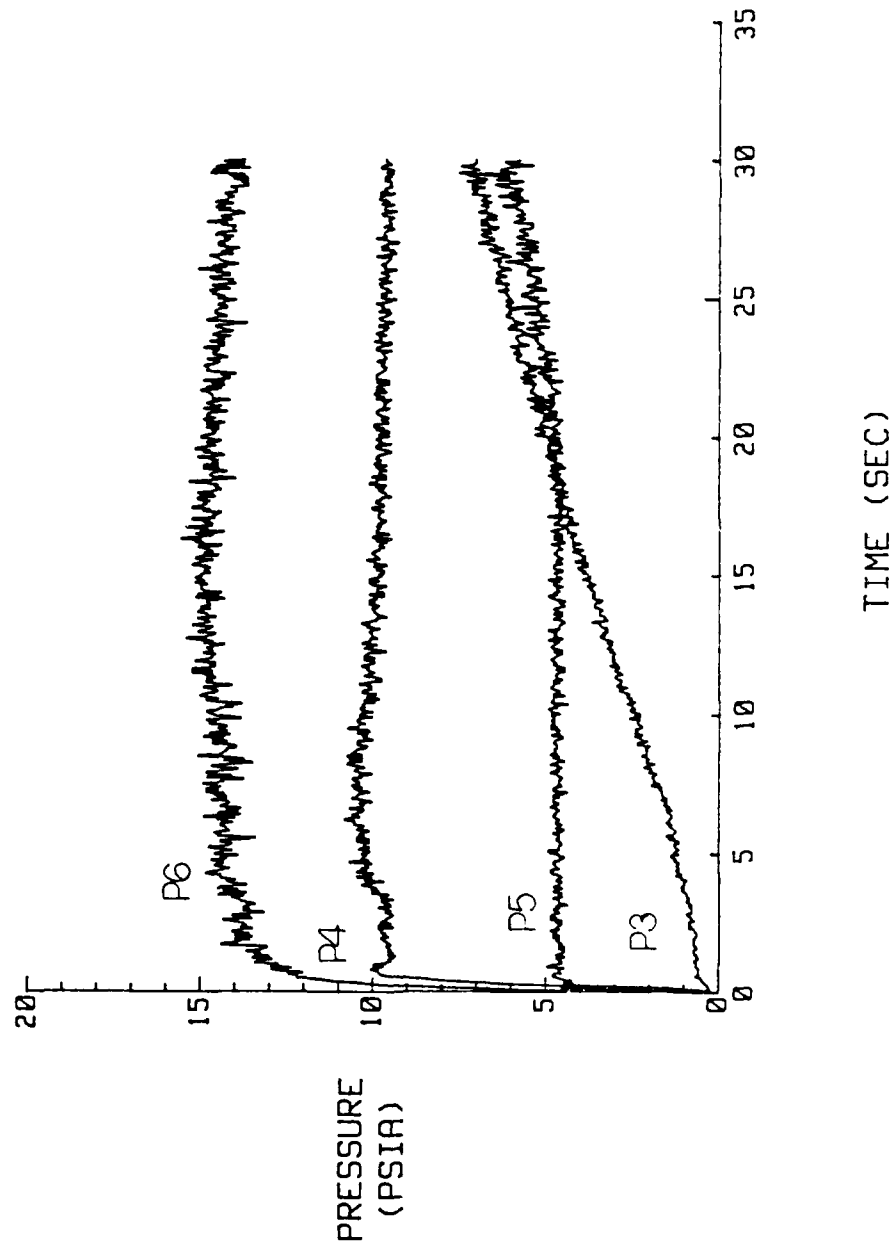


Figure 37. P3, P4, P5 and P6 Vs Time for Unshrouded, Far Ramjet Nozzle, High/High AR; $P_{rjp} = 62$ psia

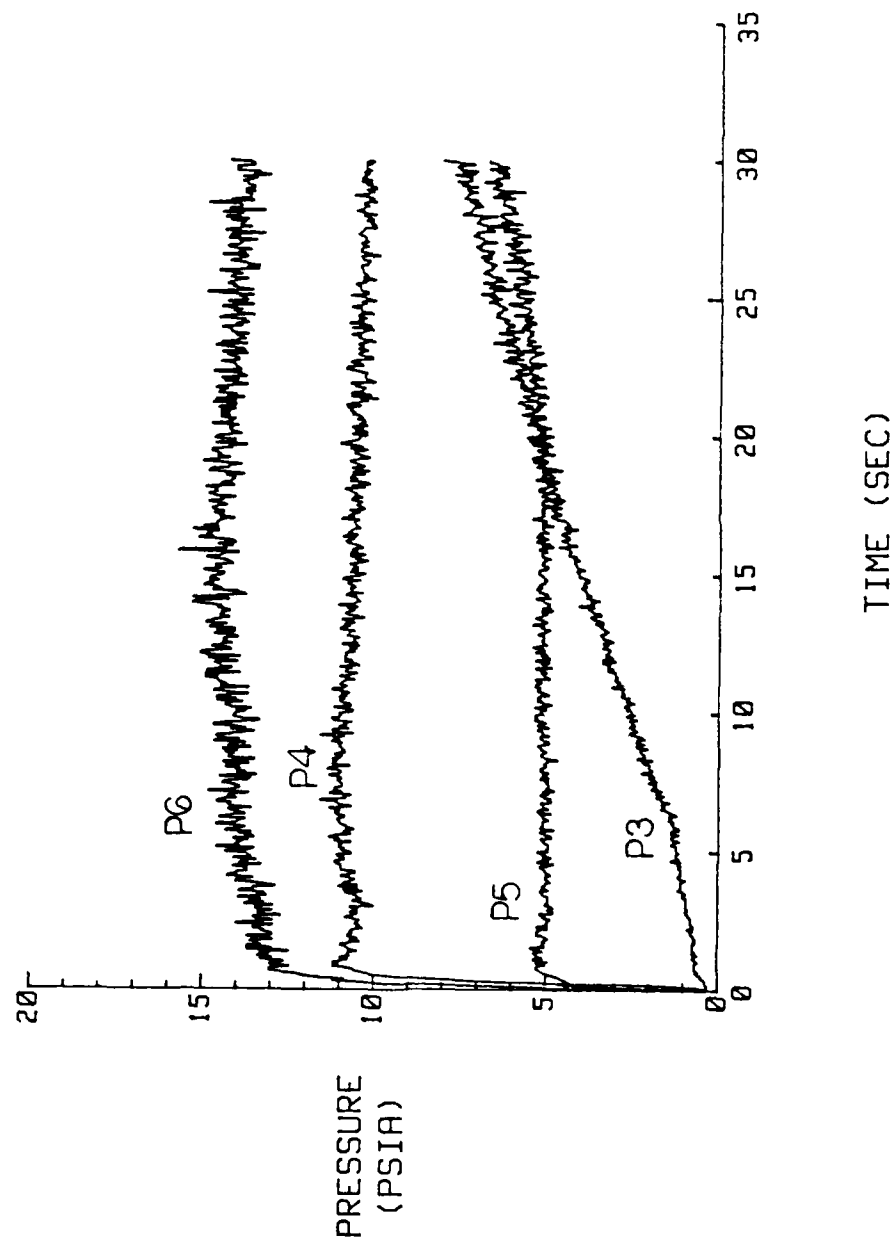


Figure 38. P3, P4, P5 and P6 Vs Time for Unshrouded, Far Ramjet Nozzle, High/High AR; $P_{rjp} = 72$ psia

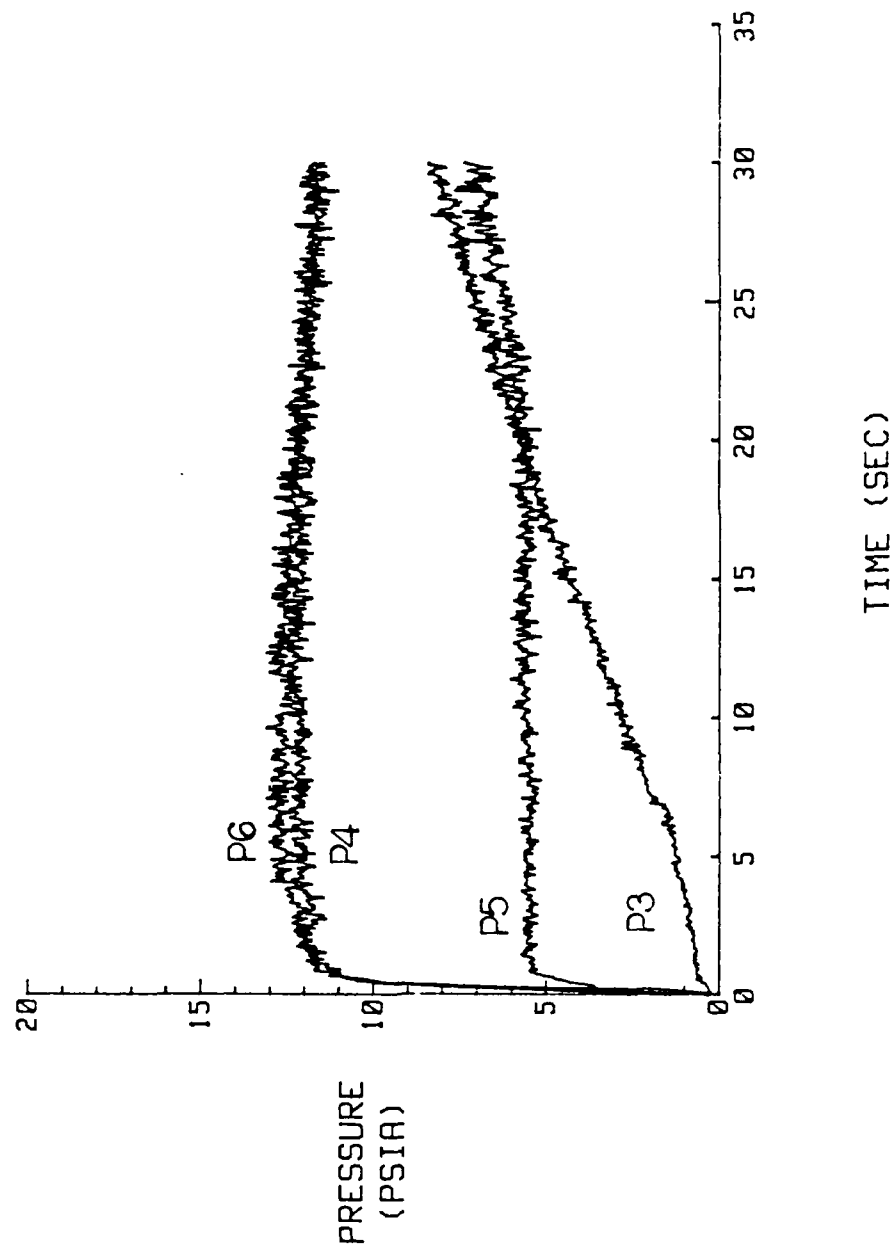


Figure 39. P3, P4, P5 and P6 Vs Time for Unshrouded,
Far Ramjet Nozzle, High/High AR; $P_{rjp} = 87$ psia

between the ramjet and the rockets close to the ramjet goes up with increasing ramjet plenum pressure due to the effects which were noted by Huband (15) and mentioned earlier. The pressure differential between the rockets and the ramjet changes direction as the ramjet plenum pressure increases. This change in direction of the pressure differential is not gradual but it is sudden and can be seen in Figures 36 and 37. P4 and P5 begin as they are in Figures 37, 38, and 39. However, in Figure 36, after the back pressure has increased slightly P4 and P5 suddenly change (P4 drops and P5 rises). This could imply an unstable condition between rocket and ramjet at that ramjet plenum pressure which does not occur at higher ramjet plenum pressures. In Figure 34 (lower ramjet plenum pressure than in Figure 36) P4 and P5 remain as they are after the switch in Figure 36. This can be seen in Figure 40 which shows P4 and P5 for the lowest and highest ramjet plenum pressures. The pressure is greatest near the ramjet and lowest near the rocket for the unshrouded, far ramjet nozzle, high AR at high ramjet plenum pressure. This is opposite to what is seen in Figure 34 for the same model at lower ramjet plenum pressure. This change in pressure differential is due to a combination of lower exit plane pressures lowering the pressure near the rocket and increasing ramjet plenum pressure increasing the base pressure near the ramjet.

Close Shrouded Baseline, Rocket Flow Only

The next phase of experimentation was to use a shroud on the different configurations. The two types of removable shroud used in these experiments were the close shroud and the far shroud (or just shroud). The baseline model for the shroud effects was with rockets only operating with the close shroud. The base pressures for this model are

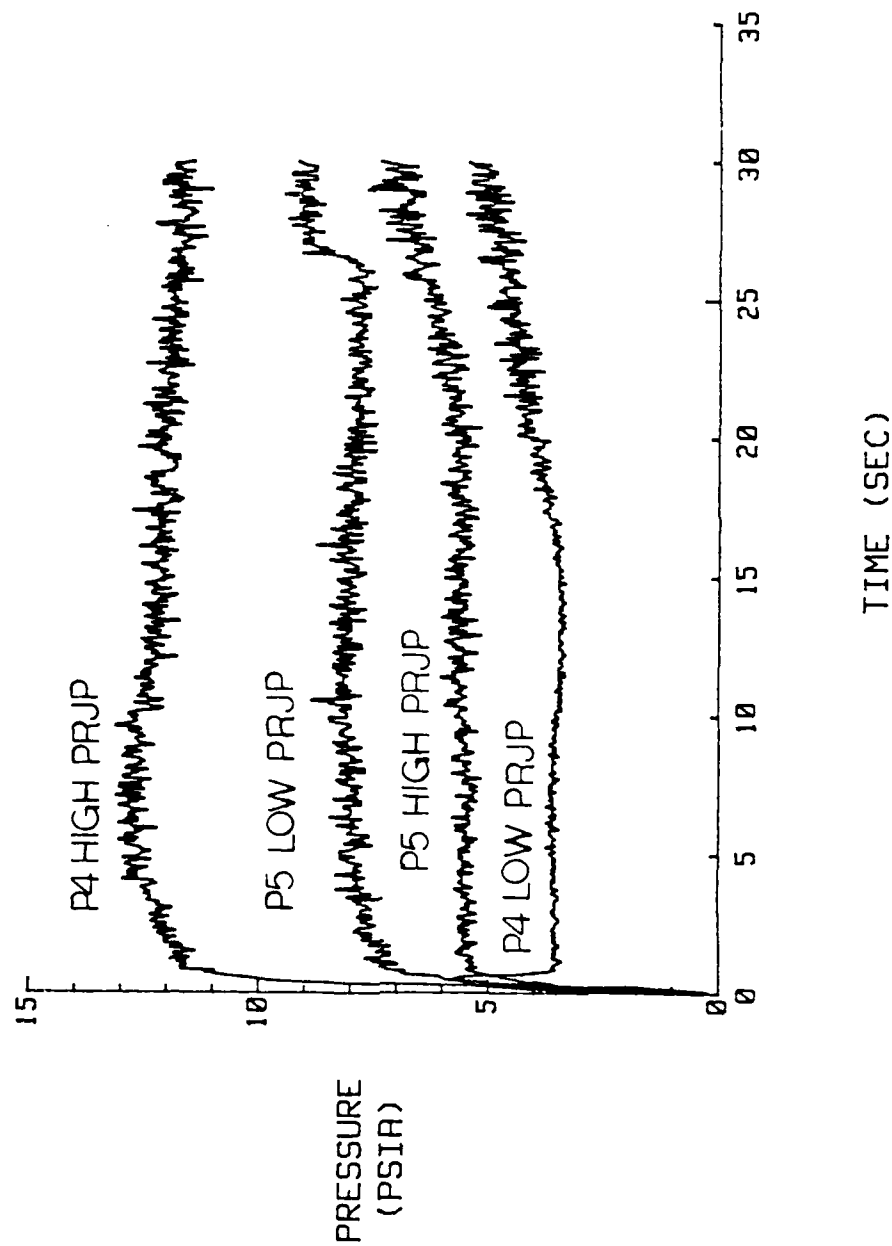


Figure 40. P4 and P5 Vs Time for Unshrouded, Far Ramjet Nozzle, High/High AR, Effect of Increasing Prjp

given in Figure 41. As with the unshrouded case, the pressures P3, P4 and P5 are relatively low compared to P6. The reason for P6 being much greater than the other pressures is the recirculation between the rockets. The back pressure is felt by P3, P4 and P5 almost simultaneously at a back pressure value of nearly 4.5 psia. In comparing the close shrouded baseline to the unshrouded baseline (Figure 15), it can be seen that the back pressure must be higher before it can be felt in the base regions of the close shrouded case. For P3 this effect of working against higher back pressure is plotted for the two baseline cases in Figure 42. This effect is due to the fact that the base area of the close shrouded model is closed off from flow entering either through the top or the bottom of the two dimensional model by the shroud.

Close Shrouded, Close Ramjet Nozzle, Low/Low AR

Conditions change quite markedly when both rockets and ramjets operate in a shrouded mode. For the close shrouded, close ramjet nozzle, low/low AR model the base pressures are shown in Figure 43. The pressure between the rockets and ramjet closer to the ramjet (P4) goes up significantly due to increased recirculation in this area due to the presence of the ramjet flow. P6 between the rockets decreases compared to the shrouded baseline due to rocket-ramjet flow stream interaction and protection in this area by the rocket exhaust waves. P5 is unaffected by the addition of ramjet operation. P3 is increased by, by ramjet operation. A typical flow pattern for this case is in Figure 44.

These base pressures look much like those shown in Figure 17. It can be seen that the same

AD-A189 714

AN EXPERIMENTAL INVESTIGATION OF ROCKET RAMJET NOZZLE
ASSEMBLY BASE PRESSURES(U) AIR FORCE INST OF TECH
WRIGHT-PATTERSON AFB OH T R WESLING DEC 87

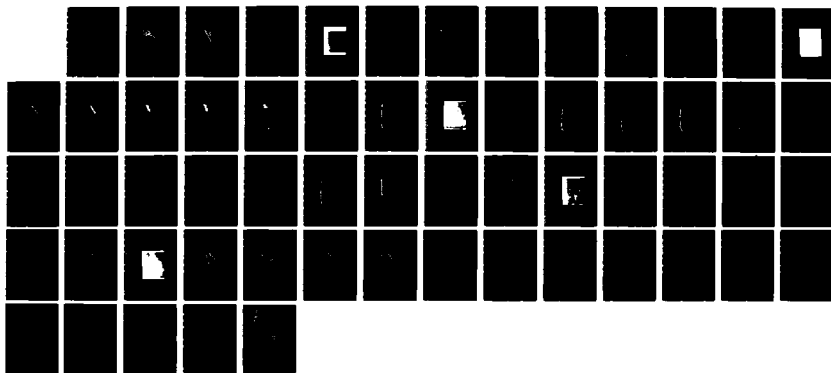
2/2

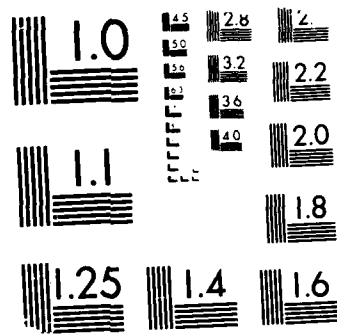
UNCLASSIFIED

AFIT/GA/RA/87D-9

F/G 21/8

NL





MICROCOPY RESOLUTION TEST CHART
NATIONAL BUREAU OF STANDARDS 1963-A

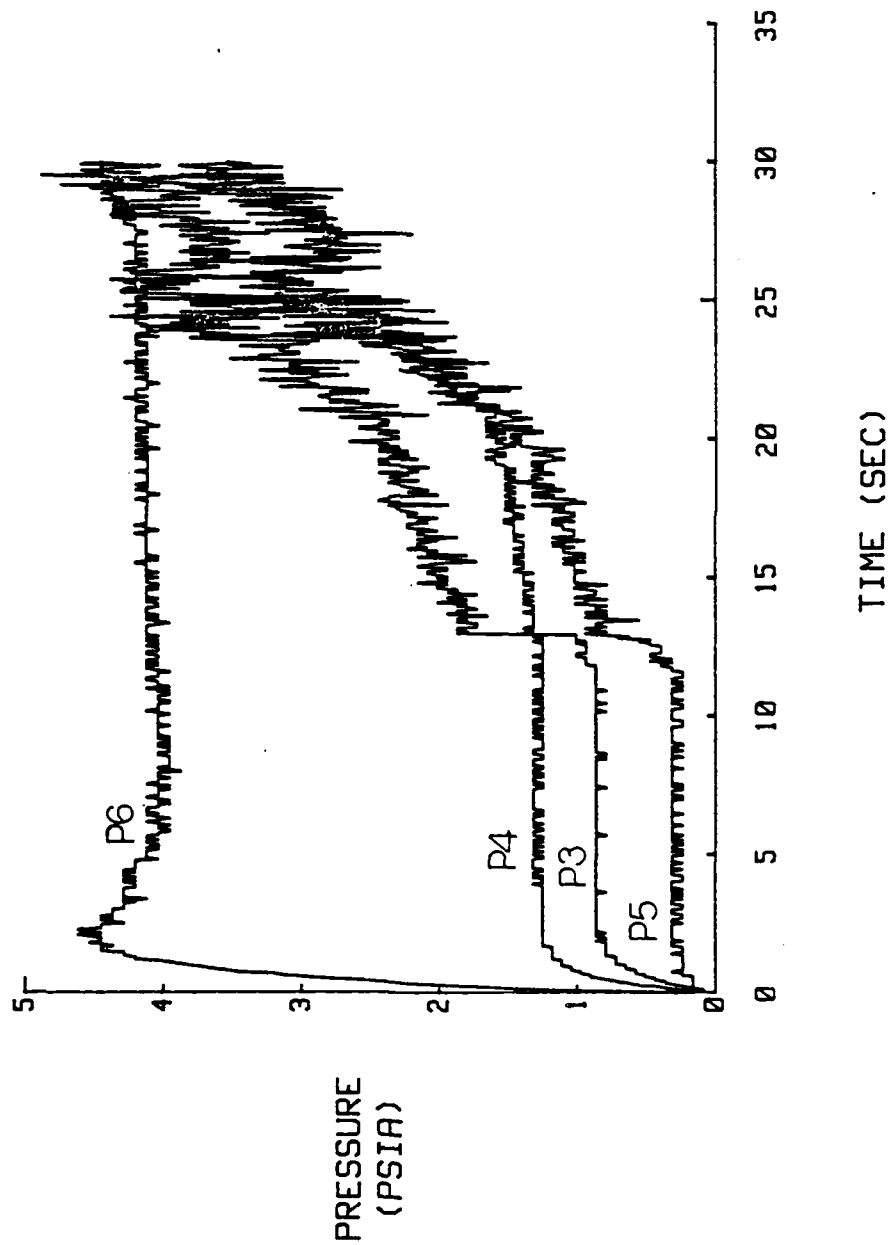


Figure 41. P3, P4, P5 AND P6 Vs Time for
Baseline, Rocket Flow Only, Close Shrouded Base Pressures

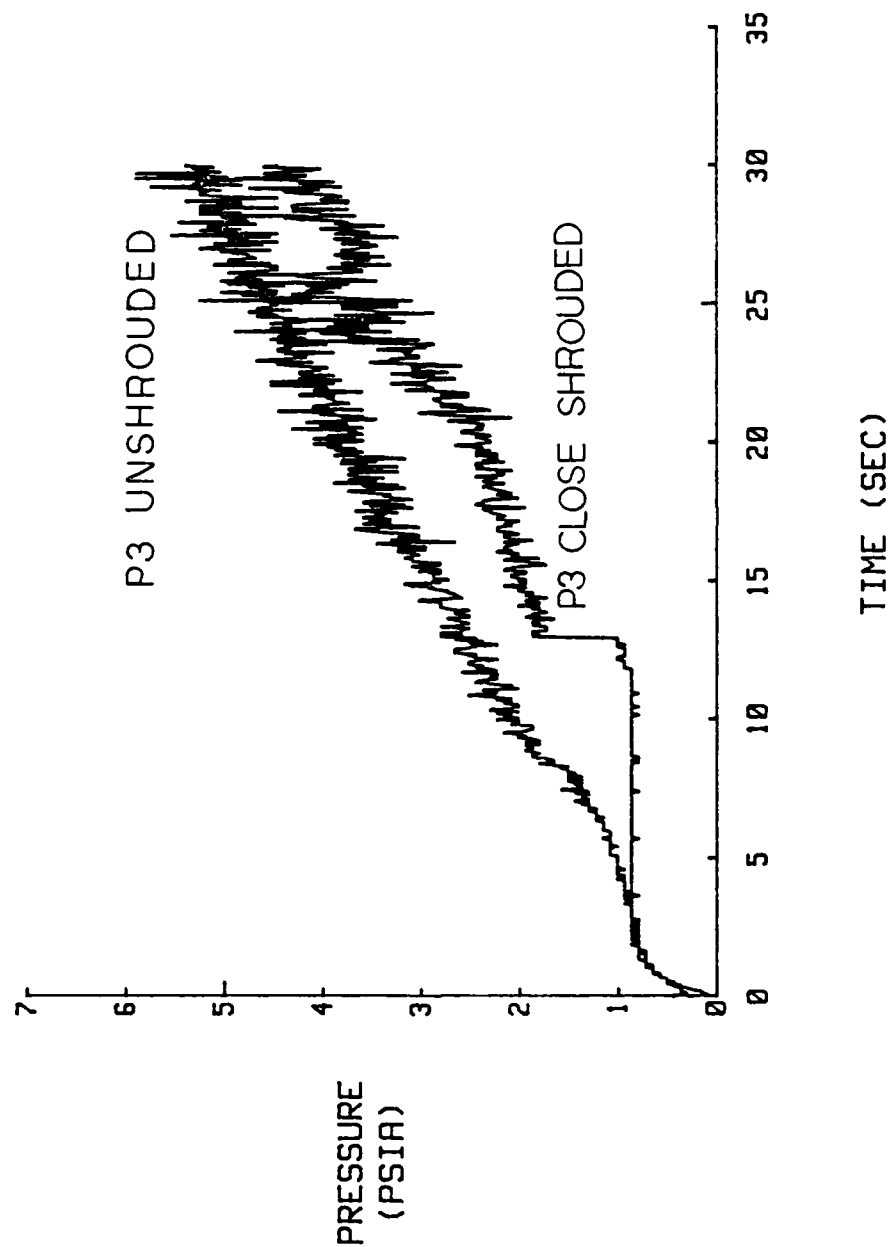


Figure 42. P3 Vs Time for Baseline Unshrouded and Close Shrouded Configurations

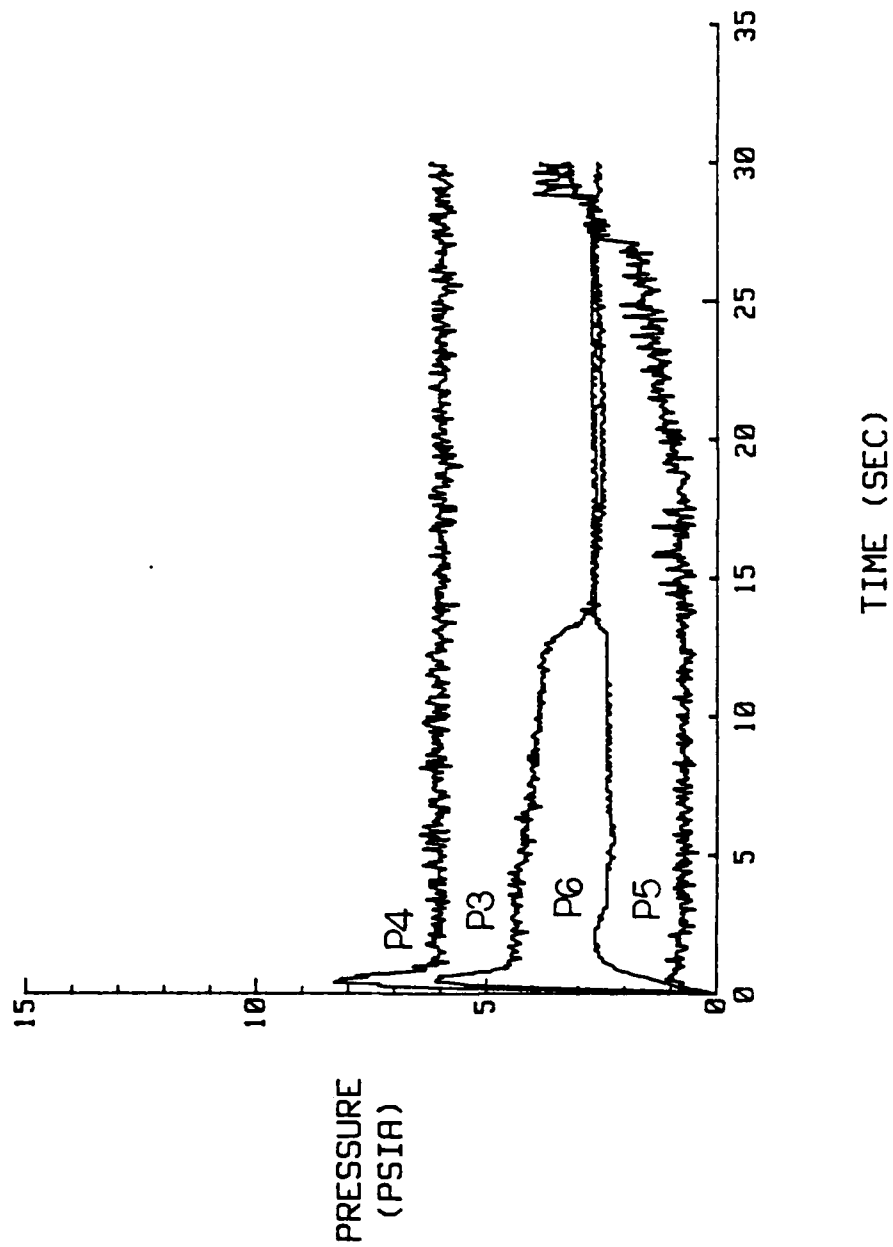


Figure 43. P3, P4, P5 and P6 Vs Time for Close Shrouded, Close Ramjet Nozzle, Low/Low AR; $P_{rjp} = 42$ psia

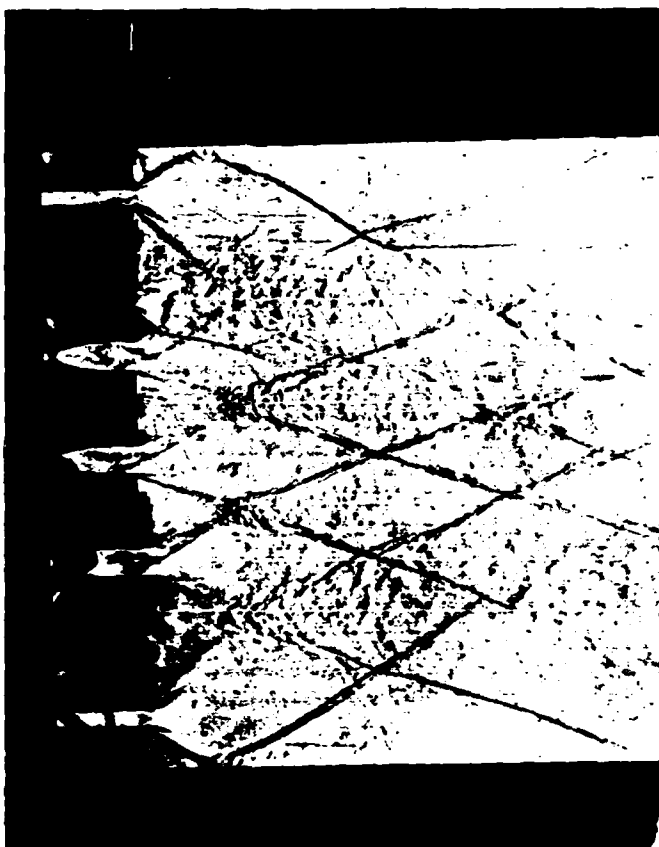


Figure 44. Typical Flow Pattern for Close Shrouded,
Close Ramjet Nozzle, Low/Low AR

considering rocket-ramjet shrouded or unshrouded operation. This can be seen by comparing Figures 17 and 43. There is also little effect on P5 or P6 due to shrouding in this configuration since these pressures are influenced and protected mostly by the rocket exhaust waves. In this shrouded configuration, the pressure differential from rockets to ramjet shows the pressure is greater near the ramjet and lower near the rocket. P3 is significantly affected by the presence of the shroud. P3 gradually decreases instead of increasing due to an increase of the back pressure which is opposite to the unshrouded case (Figure 17). P3 for both the unshrouded and close shrouded, close ramjet nozzle, and low/low AR configurations are shown in Figure 45. This decreasing pressure is due to the ramjet exhaust waves attaching to the shroud and constricting the thickness of the boundary layer as back pressure was increasing. This attachment lessens the pressure communication upstream through the boundary layer. The sharp decrease in P3 in Figure 43 when the back pressure is 3 psia is due to formation of a shock which nearly completely closes off the boundary layer. This phenomenon can be seen in the schlieren motion pictures. This effect gets stronger as the ramjet plenum pressure increases as is shown in Figures 46, 47, 48 and 49. Increasing ramjet plenum pressure for the close shrouded case is nearly the same as what happens in the unshrouded case (compare Figures 46, 47, 48 and 49 to Figures 19, 20, 21 and 22). The pressure differential between rockets and ramjet shows the pressure between rockets and ramjet close to the ramjet going up with increasing ramjet plenum pressure. The pressure between rockets and ramjet close to the rockets stays low even as ramjet plenum pressure increases. P5 changes little with increasing

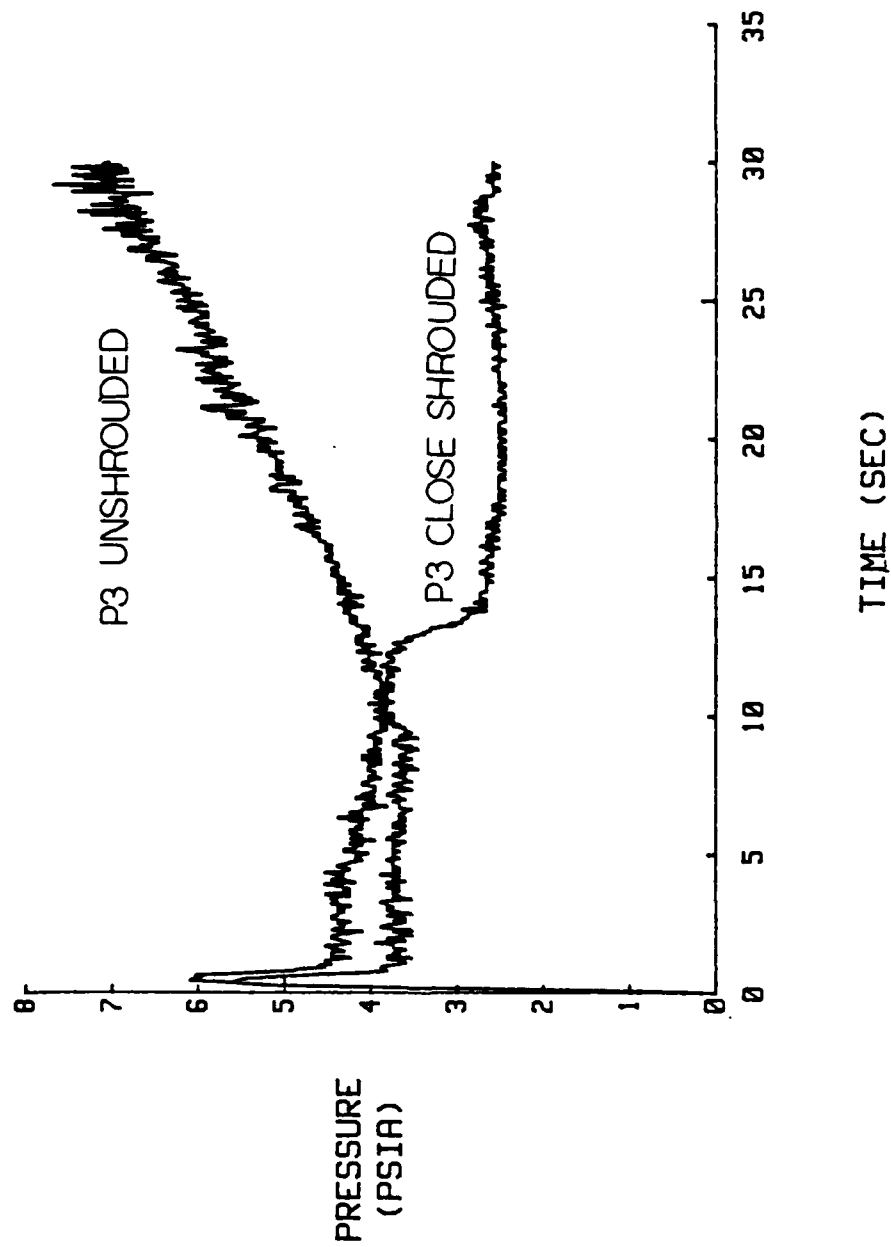
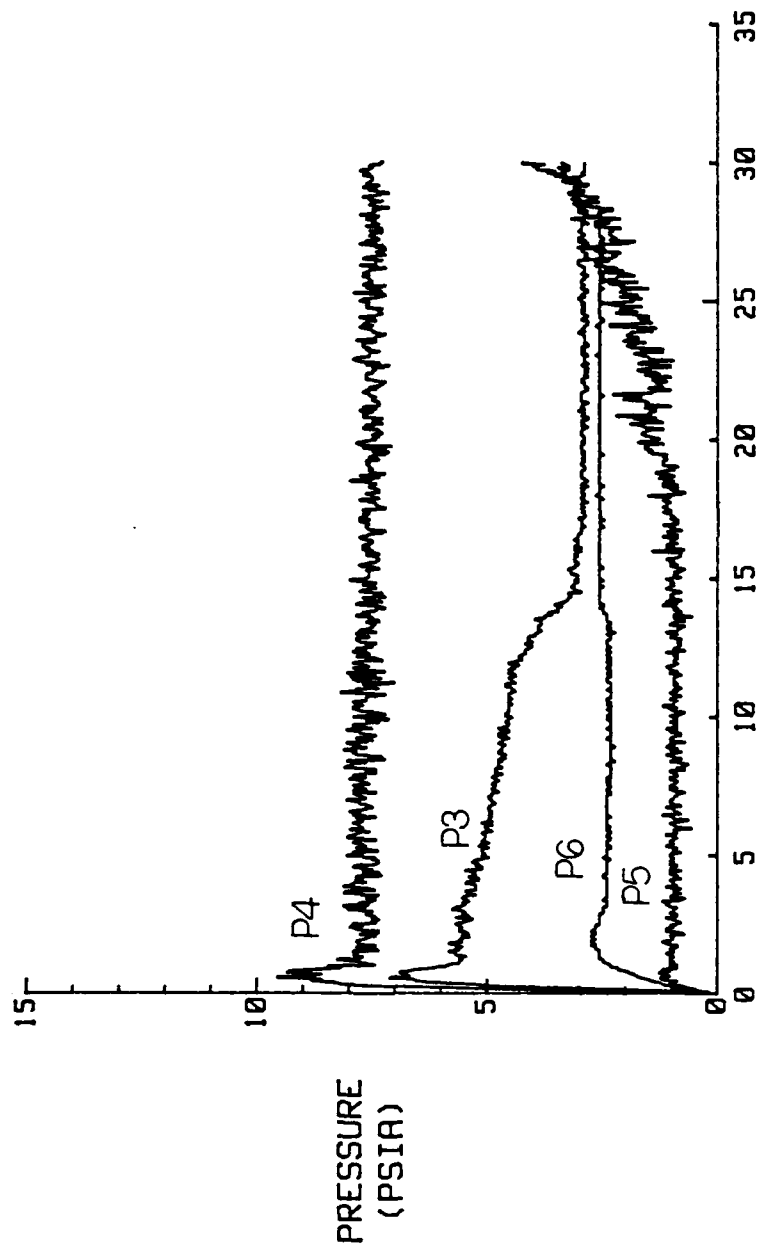


Figure 45. P3 Vs Time for Low P_{rjp} Unshrouded and Close Shrouded Configurations



TIME (SEC)

Figure 46. P3, P4, P5 and P6 Vs Time for Close Shrouded, Close Ramjet Nozzle, Low/Low AR; $P_{rjp} = 52$ psia

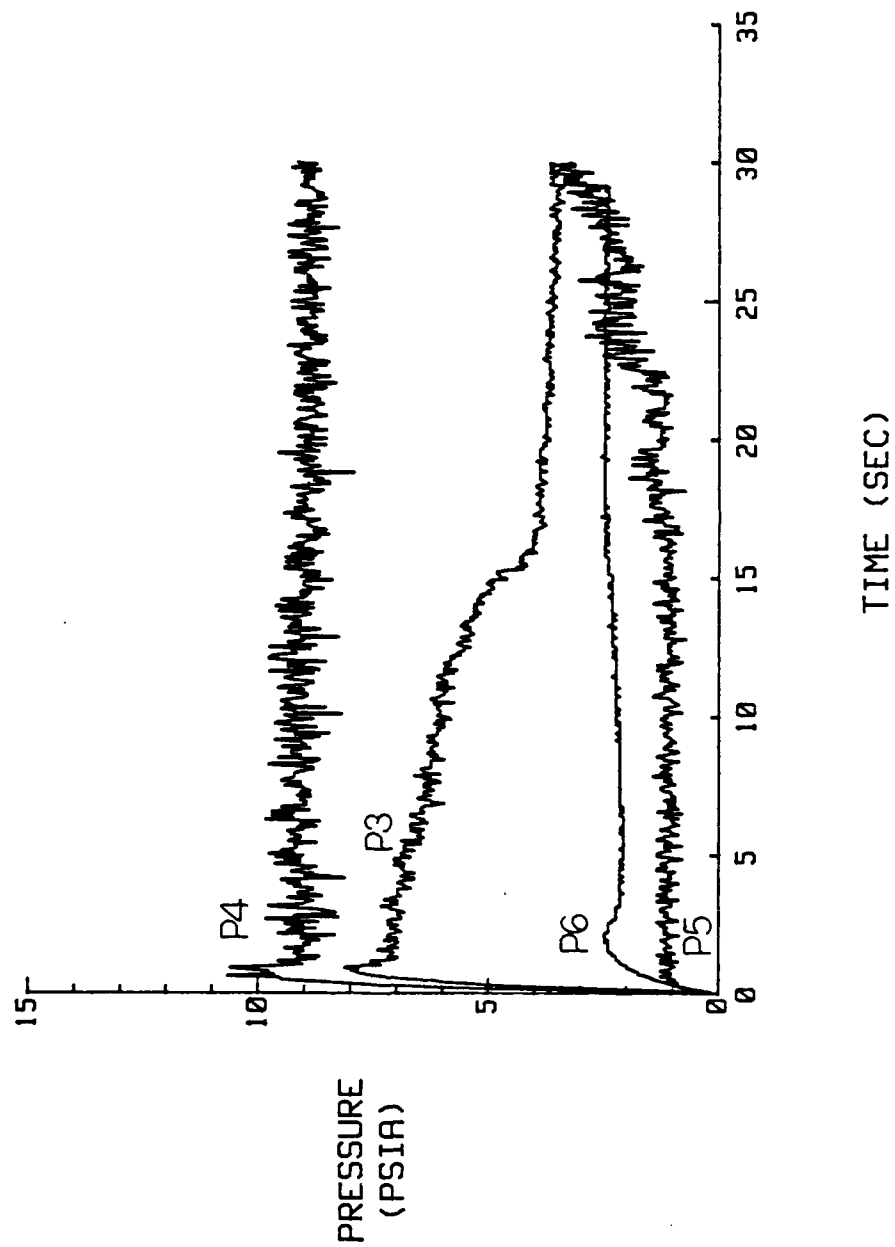


Figure 47. P3, P4, P5 and P6 Vs Time for Close Shrouded,
Close Ramjet Nozzle, Low/Low AR; $P_{rjp} = 62$ psia

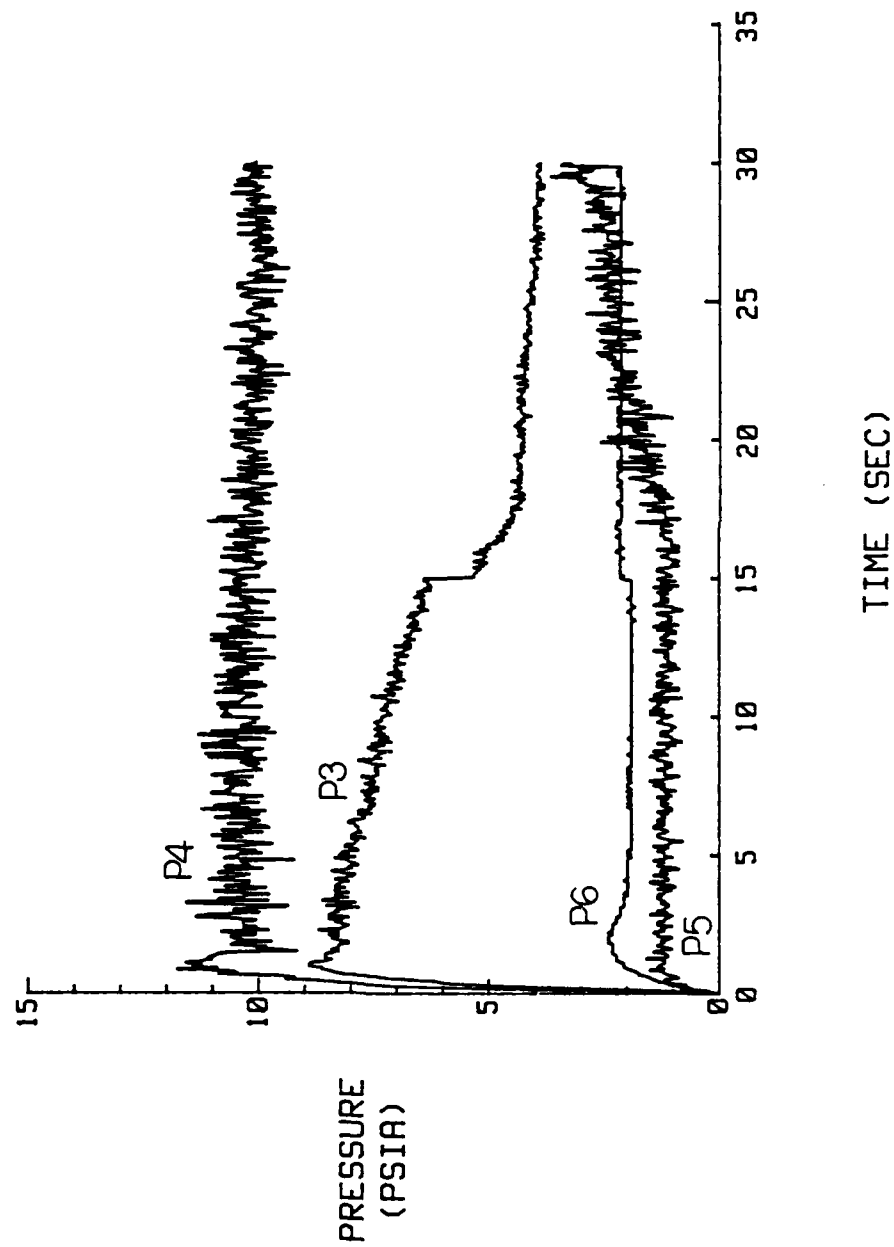


Figure 48. P3, P4, P5 and P6 Vs Time for Close Shrouded, Close Ramjet Nozzle, Low/Low AR; $P_{rjp} = 72$ psia

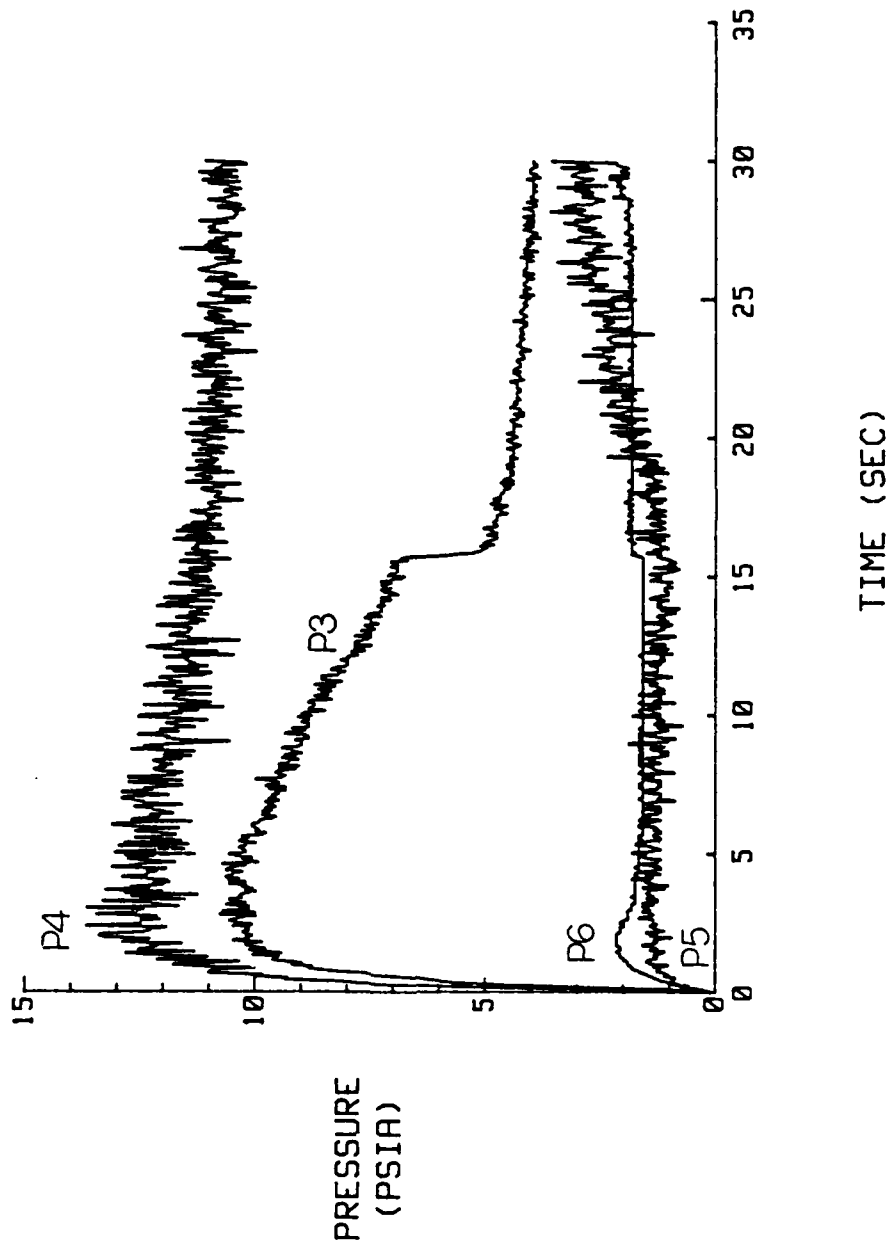


Figure 49. P3, P4, P5 and P6 Vs Time for Close Shrouded,
Close Ramjet Nozzle, Low/Low AR; $P_{rjp} = 87$ psia

ramjet plenum pressure and is small compared to P_4 which grows with increasing ramjet plenum pressure.

Close Shrouded, Close Ramjet Nozzle, High/High AR

As the AR was changed from low to high, the flow patterns change as shown in Figure 50 (compare this to Figure 44). The base pressures for the close shrouded, close ramjet nozzle, high/high AR model are shown in Figure 51. The pressure between the rockets (P_6) is much higher for the high AR nozzles. This is due to greater recirculation effects strong enough to overcome the lower exit plane pressures of the high AR nozzles. The pressure between the rockets and ramjet close to the ramjet (P_4) drops due to the lower exit plane pressure of the ramjet at higher AR. This also accounts for the lower base pressure above the ramjet (P_3). The pressure between rockets and ramjet close to the rockets (P_5) is kept low due to lower exit plane pressures and that area is being well protected by the rocket exhaust waves. The pressure differential between rockets and ramjet shows the pressure is highest by the ramjet and lowest by the rockets. Effects of increasing ramjet plenum pressure are in Figures 52, 53, 54 and 55. The base pressure between the rockets (P_6) decreases slightly due to lessened recirculation occurring as the ramjet plenum pressure increases. P_5 stays low and is relatively unaffected by the increasing ramjet pressure. The area around P_5 is well protected from increasing ramjet plenum pressure by the interaction of the rocket-ramjet exhaust waves. P_4 and P_3 increase with increasing ramjet plenum pressure due to the effects noted by Huband (15) and mentioned earlier. The trend of P_3 decreasing with increasing back pressure, which is more evident at higher ramjet plenum pressures, is due to constriction of the

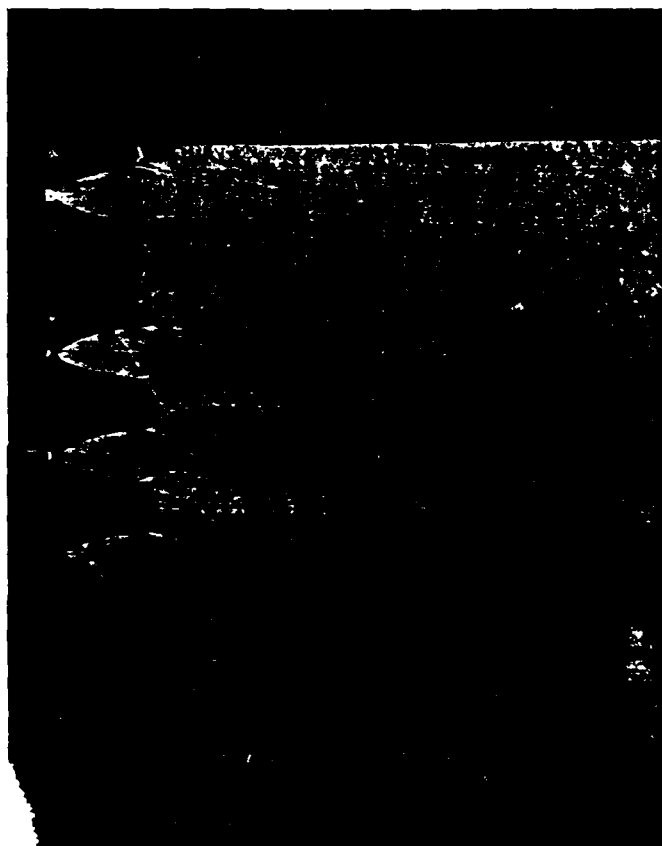


Figure 50. Typical Flow Pattern for Close Shrouded,
Close Ramjet Nozzle, High/High AR

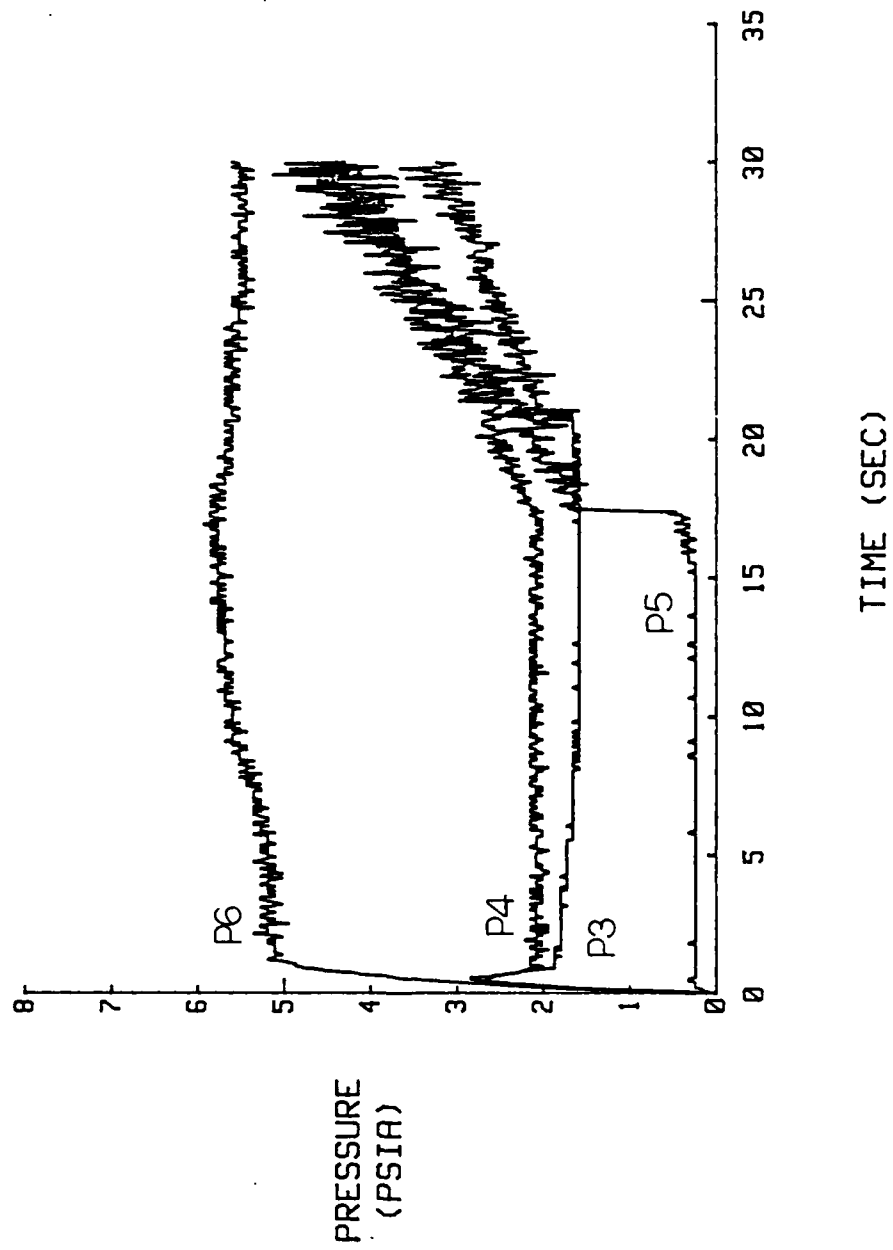


Figure 51. P3, P4, P5 and P6 Vs Time for Close Shrouded,
Close Ramjet Nozzle, High/High AR; $P_{rjp} = 42$ psia

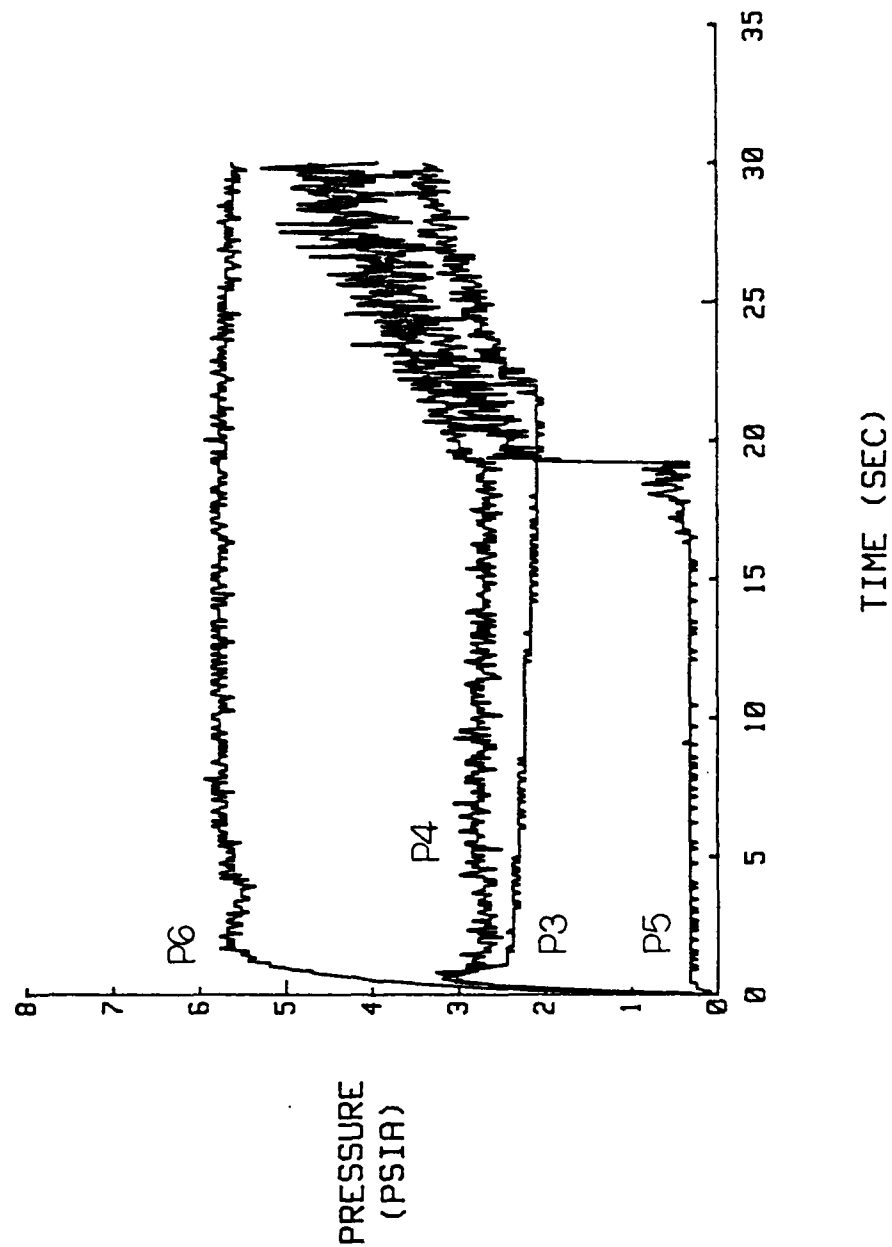


Figure 52. P3, P4, P5 and P6 Vs Time for Close Shrouded,
Close Ramjet Nozzle, High/High AR; $P_{rjp} = 52$ psia

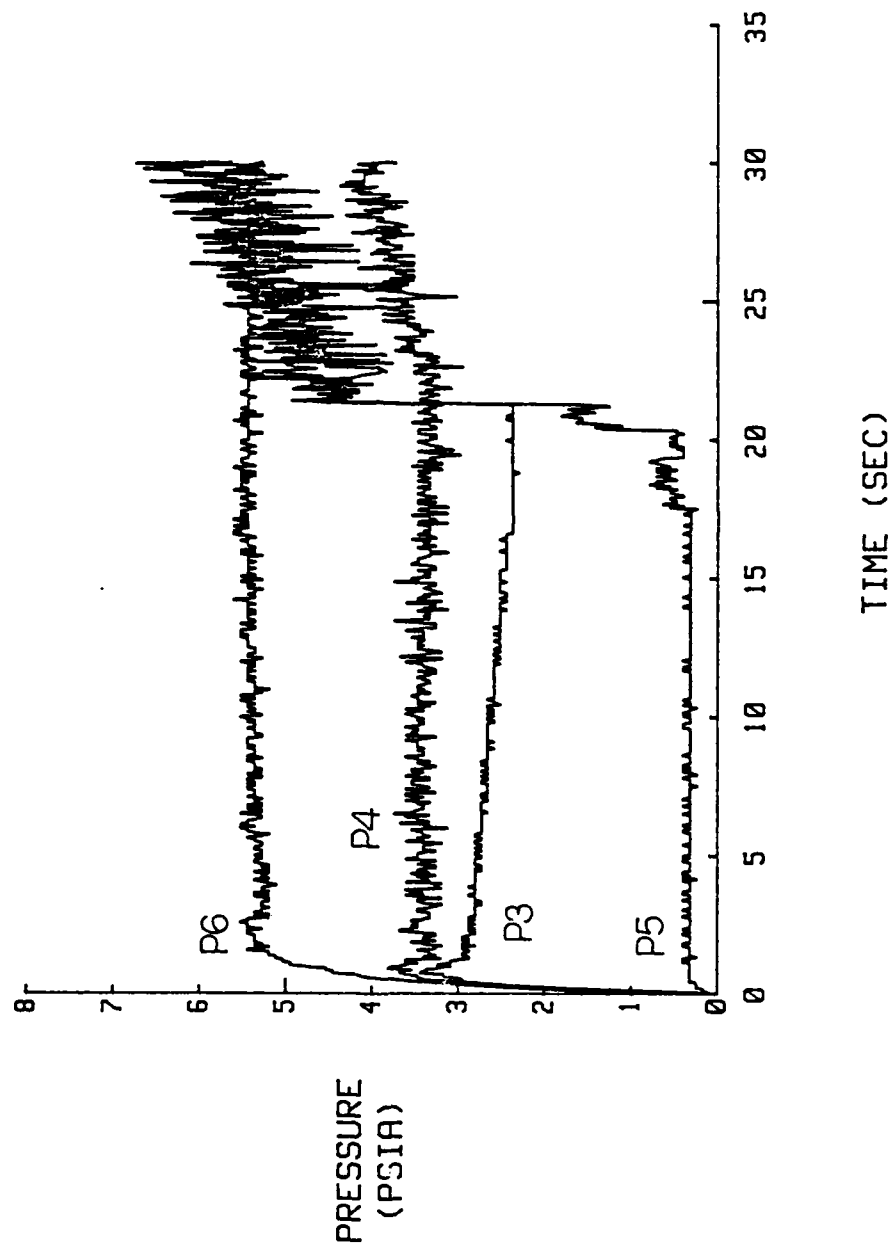


Figure 53. P3, P4, P5 and P6 Vs Time for Close Shrouded,
Close Ramjet Nozzle, High/High AR; $P_{rjp} = 62$ psia

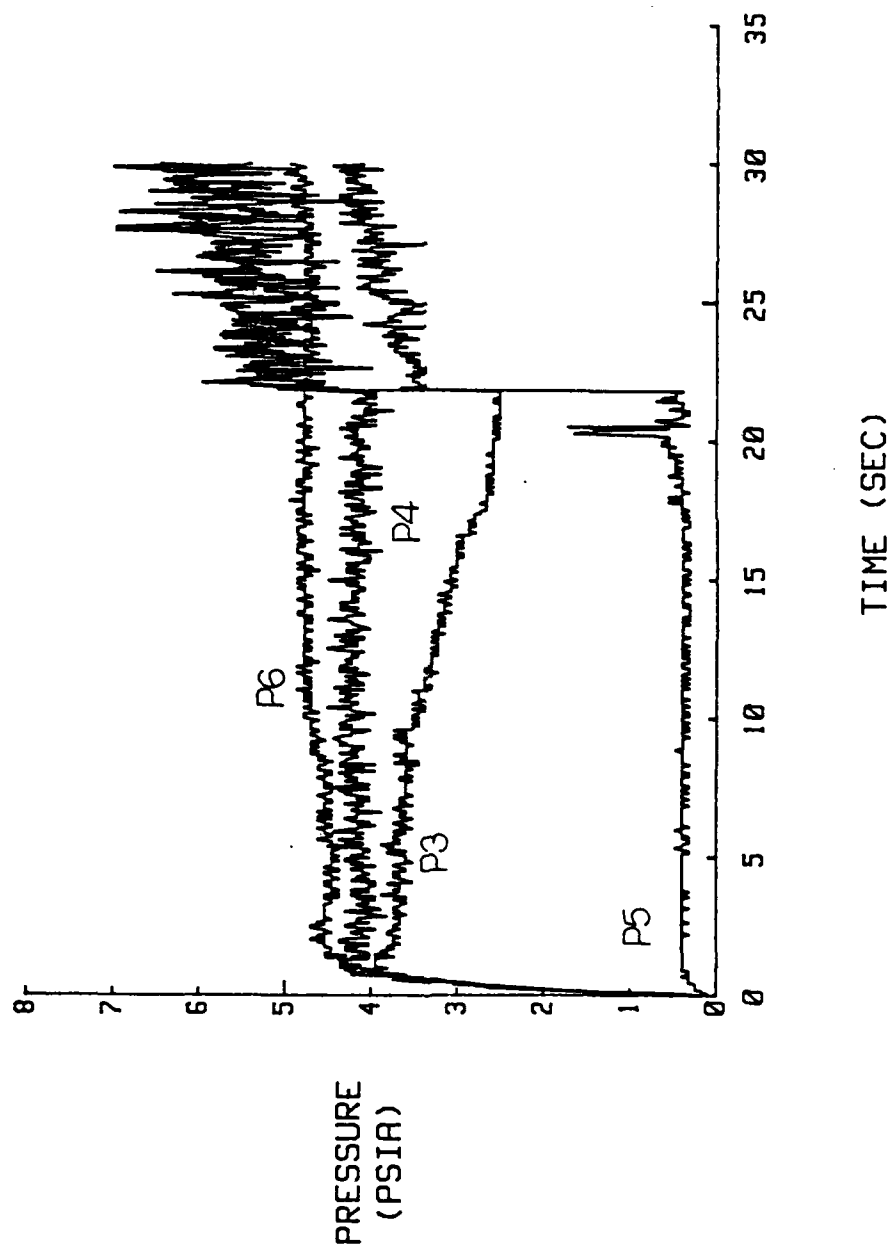


Figure 54. P3, P4, P5 and P6 Vs Time for Close Shrouded,
Close Ramjet Nozzle, High/High AR; $P_{rjp} = 72$ psia

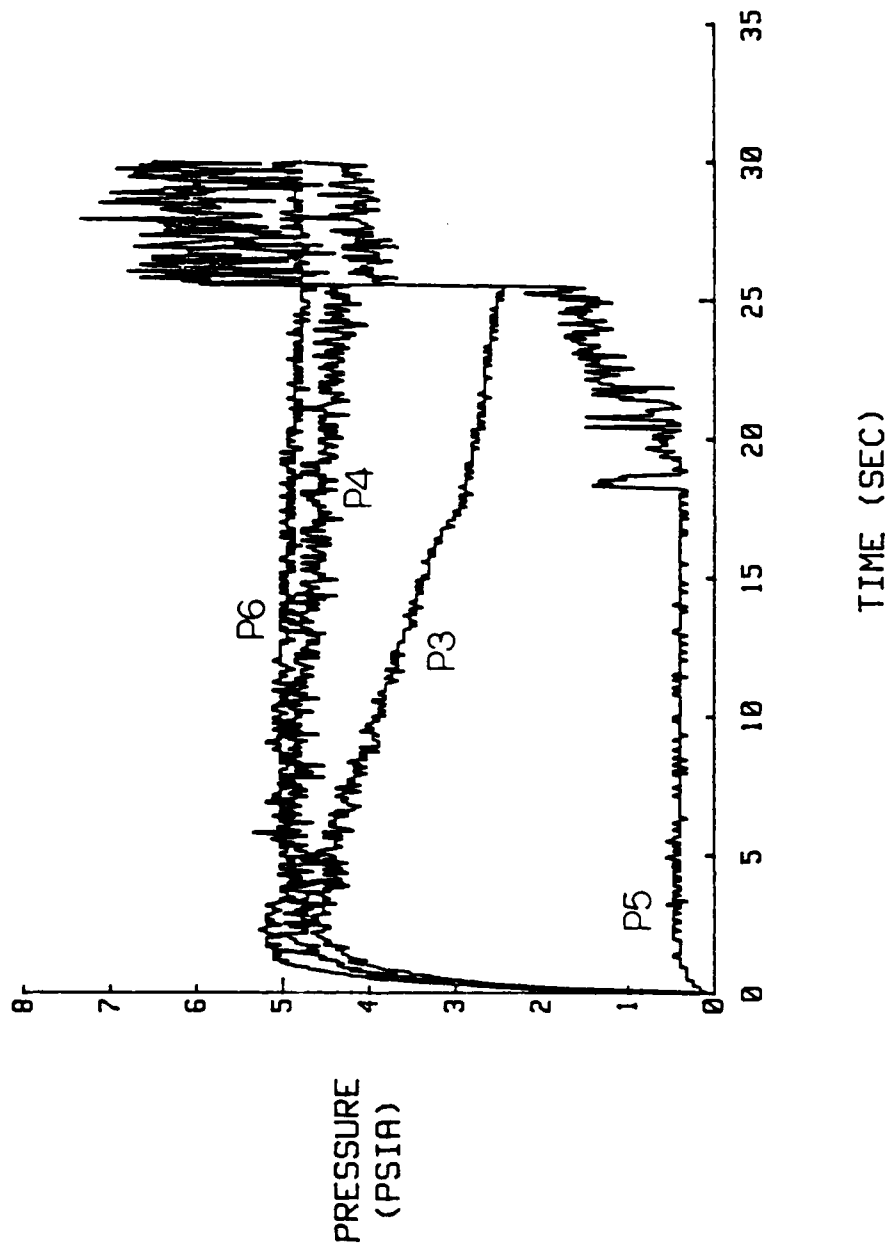


Figure 55. P3, P4, P5 and P6 Vs Time for Close Shrouded,
Close Ramjet Nozzle, High/High AR; $Pr_{jp} = 87$ psia

boundary layer as the back pressure increased during the experimental run. This constriction reduces the pressure communication through the boundary layer. The pressure differential between the rockets and the ramjet shows the pressure between the rockets and the ramjet close to the ramjet increasing with increasing ramjet plenum pressure. The low pressure near the rockets stayed low as ramjet plenum pressure increases. This is true for both the unshrouded and shrouded cases as can be seen by comparing Figures 52, 53, 54 and 55 to Figures 24, 25, 26 and 27.

Shrouded, Far Ramjet Nozzle, Low/Low AR

The next shrouded runs were for the ramjet nozzles far out from the model centerline. This is the shrouded (not close shrouded since the close shroud is not physically possible for the far ramjet nozzle mode), far ramjet nozzle, low/low AR model. The base pressures for this configuration are in Figure 56. A typical flow pattern in the underexpanded regime of operation is shown in Figure 57. The pressure near the rockets between rockets and ramjet (P5) is much higher than in the close ramjet nozzle case. This is due to strong recirculation and the low AR nozzles which have a relatively high exit plane pressure. These base pressures are similar to those in the unshrouded, far ramjet nozzle case (compare Figure 56 to Figure 29). Also, P6 is increased significantly due to recirculation between the rockets. The increase in P5 and P6 when the ramjets are moved far out is also due to the fact that the shroud directs the flow from the ramjet exhaust toward the model center (compare Figure 56 to Figure 43). P4 is relatively undisturbed when moving the ramjet nozzles out in the unshrouded case. P3 is generally lower than when the ramjet nozzles are close in. This is due

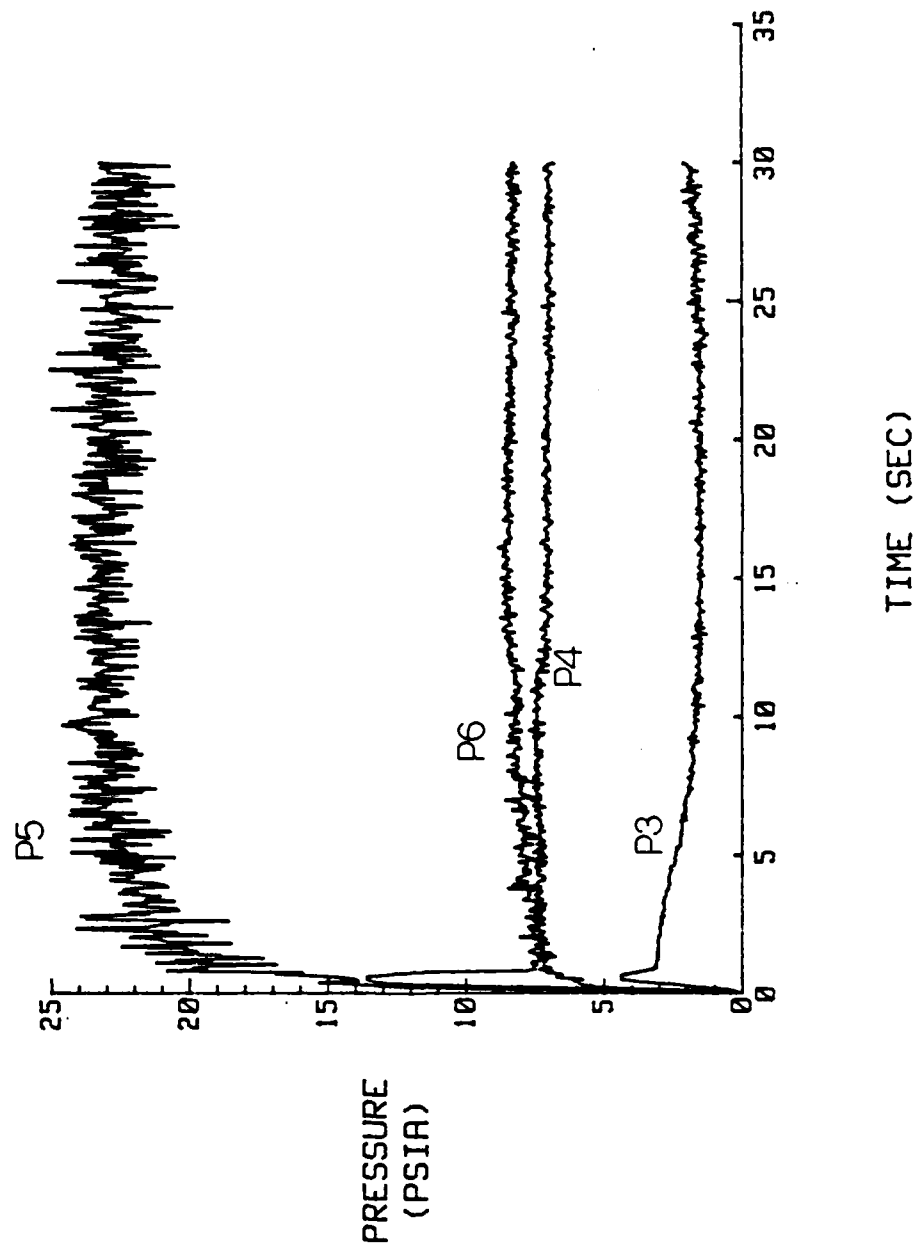


Figure 56. P3, P4, P5 and P6 Vs Time for Shrouded,
Far Ramjet Nozzle, Low/Low AR; $P_{rjp} = 42$ psia



Figure 57. Typical Flow Pattern for Shrouded,
Far Ramjet Nozzle, Low/Low AR

to the ramjet exhaust flow being turned in towards the rocket flow and away from the shroud and the area around P3. The pressure differential between rockets and ramjet is now showing the pressure to be much greater near the rockets than near the ramjet. For the cases of increasing ramjet plenum pressure, the base pressures are shown in Figures 58, 59, 60 and 61. The recirculation around P5 remains strong with increasing ramjet plenum pressure. It does weaken slightly due to the growing strength of the ramjet waves interacting with constant strength rocket exhaust waves. The increasing ramjet plenum pressure goes mostly to increasing the base pressure around the ramjet. P3 and P4 go up quite a bit with the increasing ramjet plenum pressure. As before in shrouded cases, P3 falls off with increasing back pressure at higher ramjet plenum pressures due to the ramjet exhaust waves constricting the boundary layer in that area and restricting the flow communication upstream which would increase P3. P4 also sees a sudden drop as ramjet plenum pressure increases for the same reasons as P3 as seen in Figures 58, 59, 60 and 61. The effects on P4 occur mostly at the highest ramjet plenum pressures. P6 is relatively unaffected by any increases in ramjet plenum pressure since the rocket waves strongly protect that area in this configuration. The pressure differential between the rockets and the ramjet shows the pressures P4 and P5 getting more nearly equal with increasing ramjet plenum pressure. The pressure near the rocket, though is still a little greater than the pressure near the ramjet.

Shrouded, Far Ramjet Nozzle, High/High AR

For the high AR nozzles put in this model, the base pressures for the shrouded, far ramjet nozzles, high/high AR model are in Figure 62.

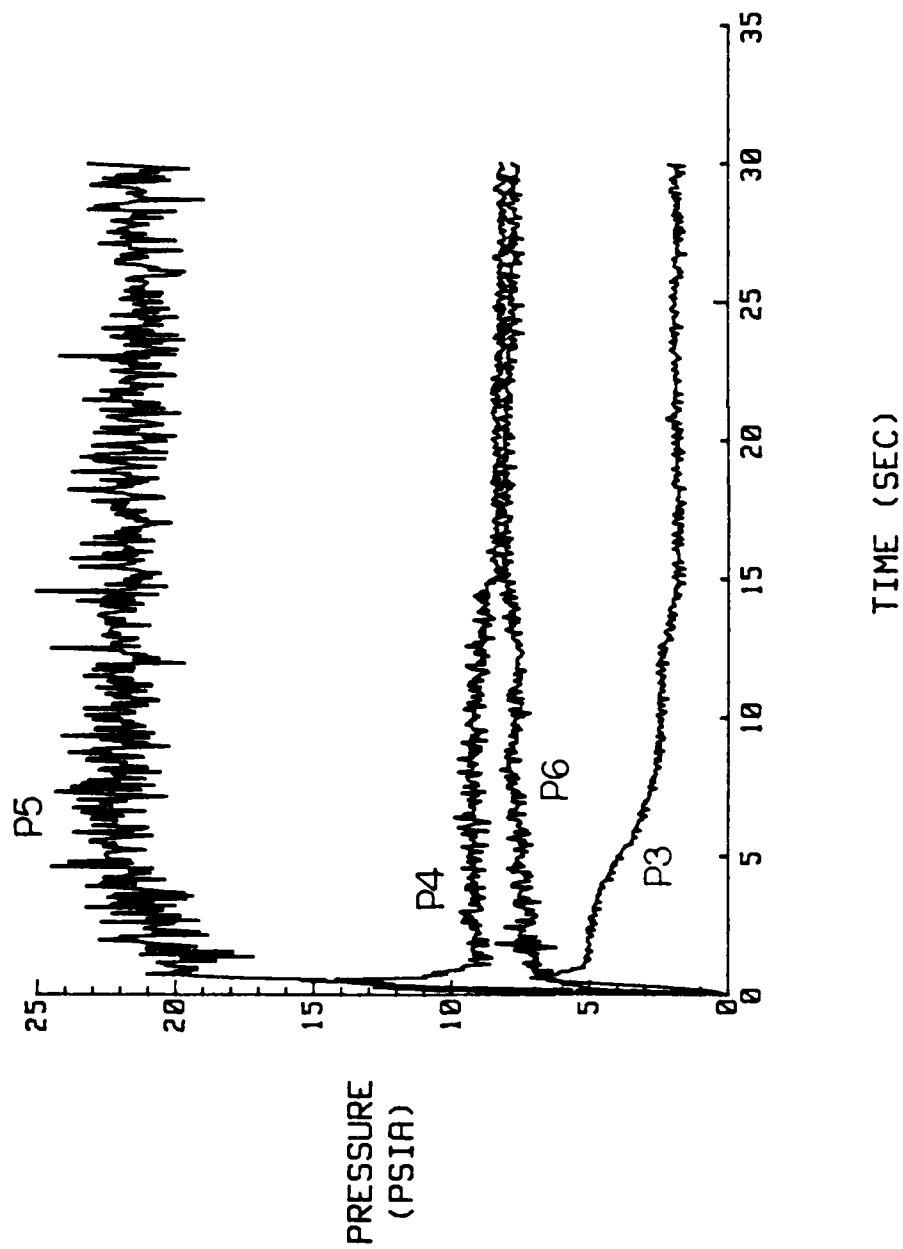


Figure 58. P3, P4, P5 and P6 Vs Time for Shrouded,
Far Ramjet Nozzle, Low/Low AR; $P_{rjp} = 52$ psia

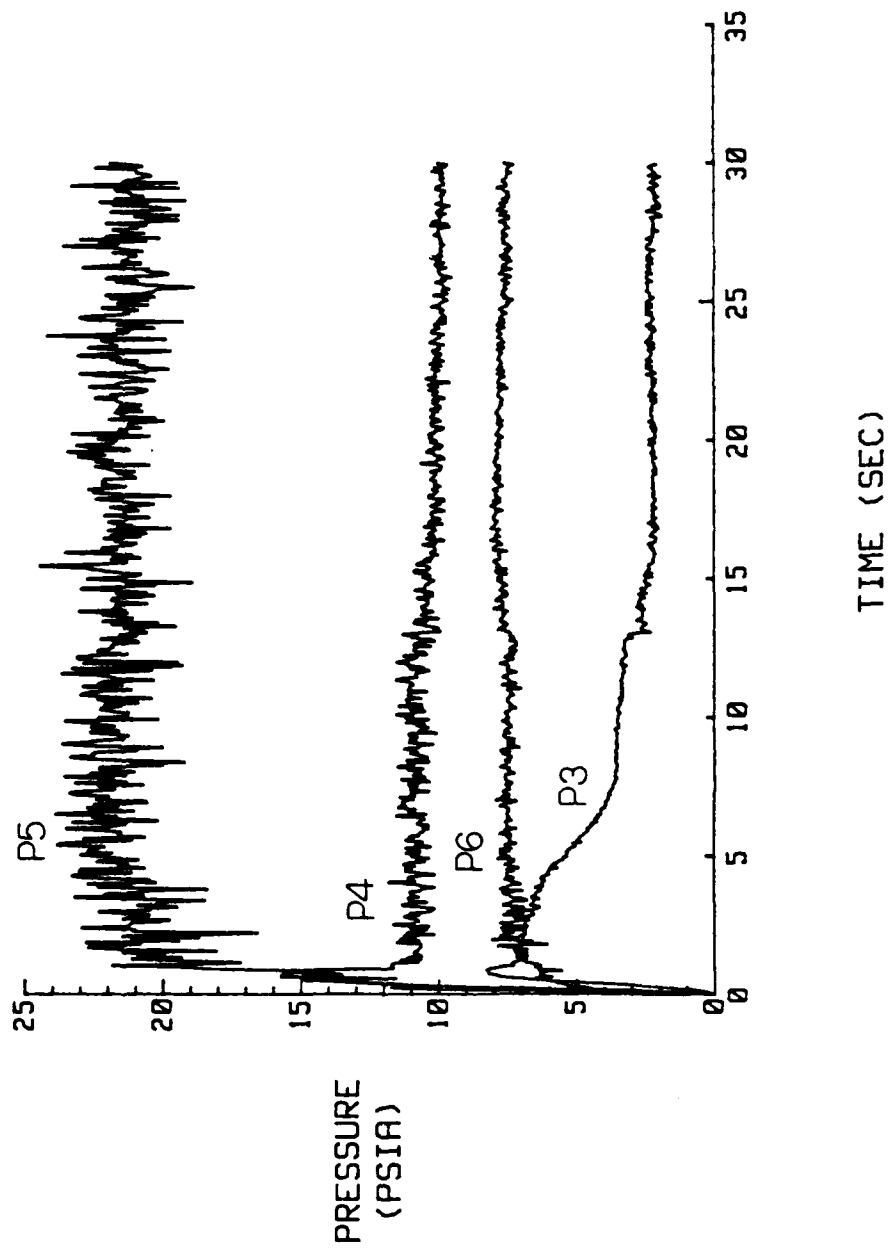


Figure 59. P3, P4, P5 and P6 Vs Time for Shrouded, Far Ramjet Nozzle, Low/Low AR; $P_{rjp} = 62$ psia

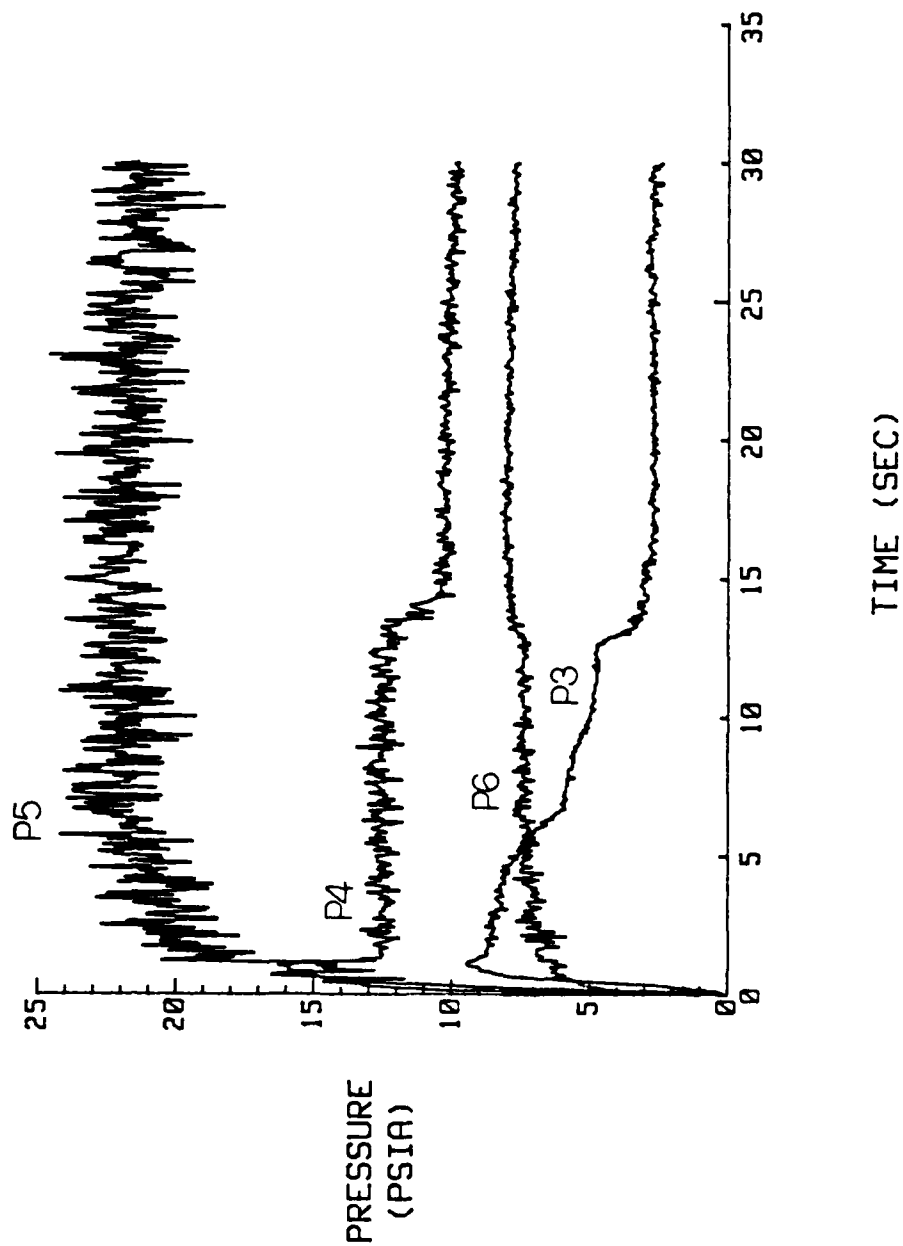


Figure 60. P3, P4, P5 and P6 Vs Time for Shrouded,
Far Ramjet Nozzle, Low/Low AR; $P_{rjp} = 72$ psia

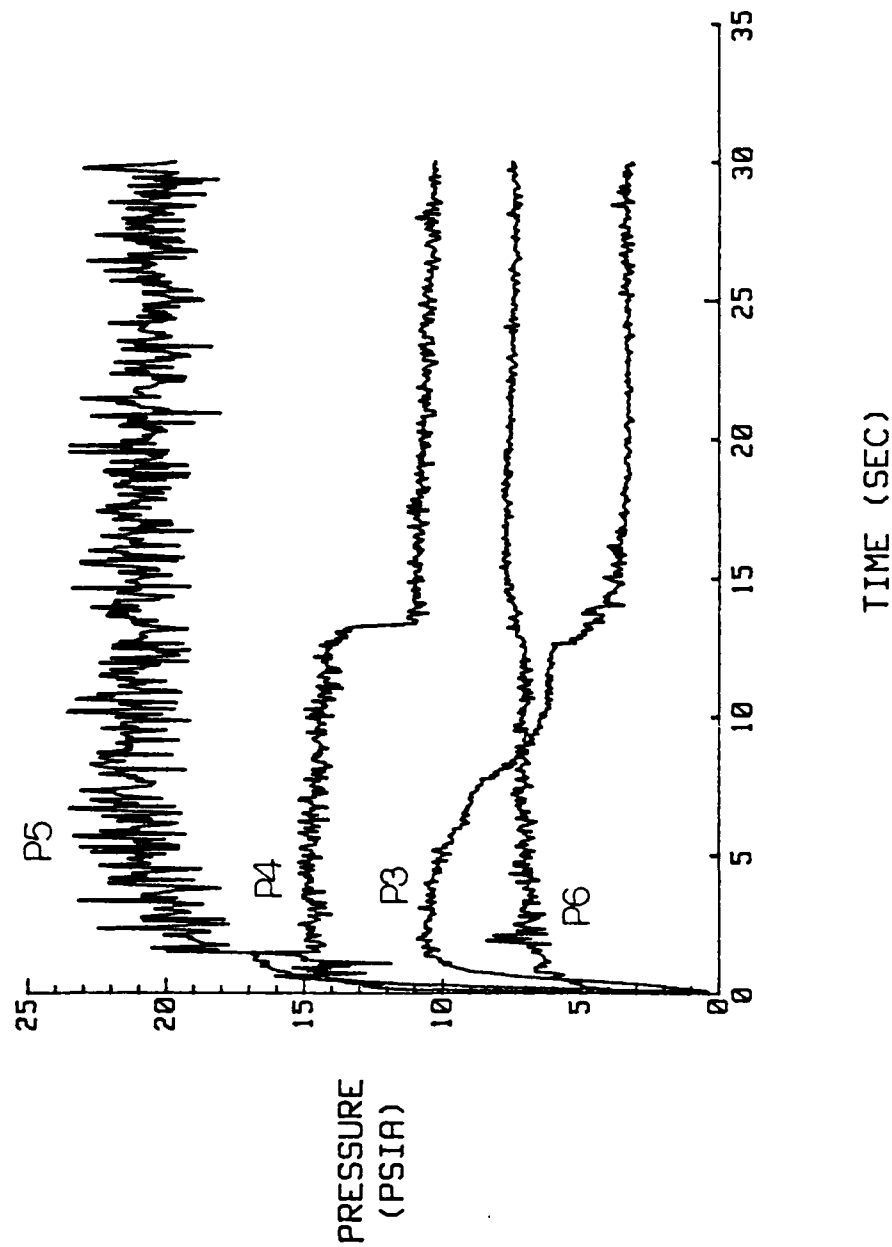


Figure 61. P3, P4, P5 and P6 Vs Time for Shrouded,
Far Ramjet Nozzle, Low/Low AR; $P_{rjp} = 87$ psia

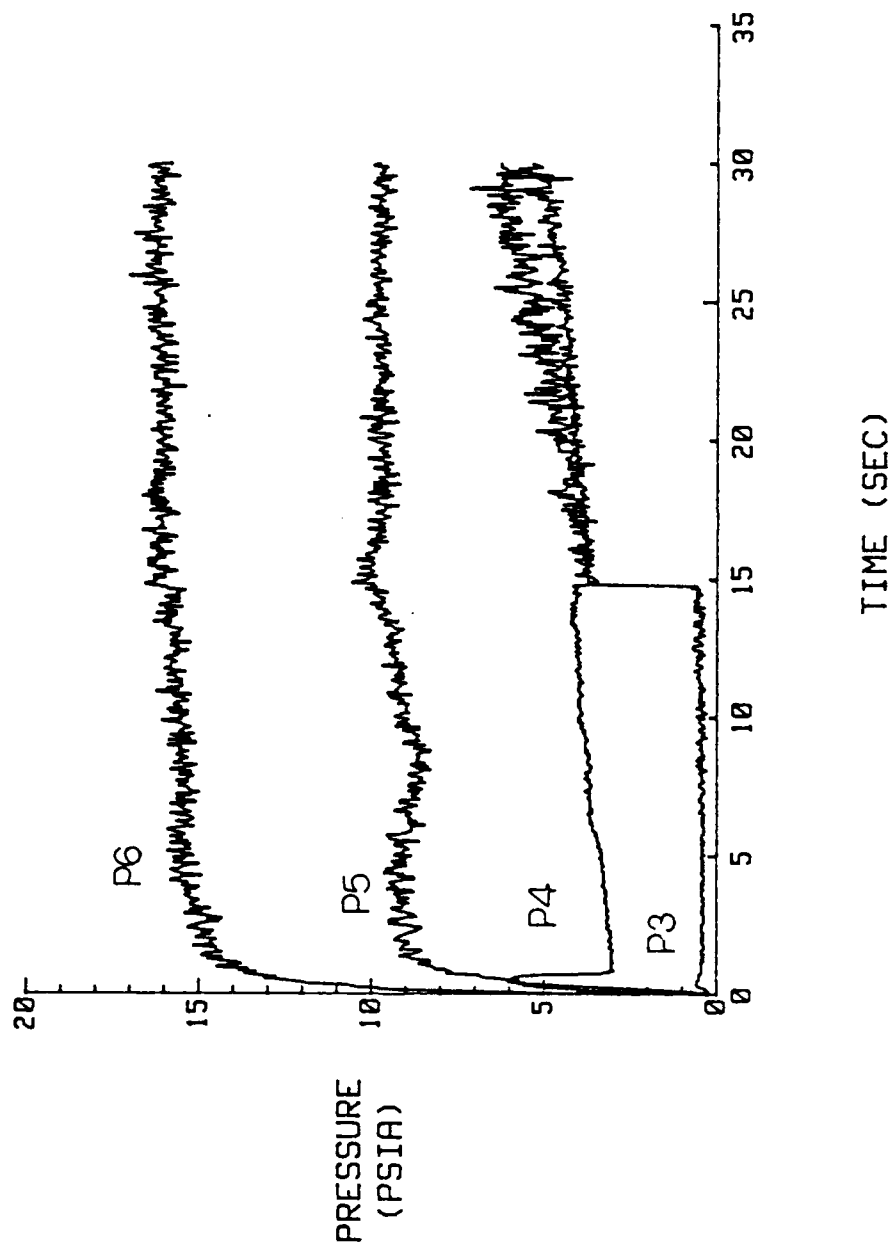


Figure 62. P3, P4, P5 and P6 Vs Time for Shrouded,
Far Ramjet Nozzle, High/High AR; $P_{rjp} = 42$ psia

The base pressures here are similar to those in the unshrouded case (compare Figure 62 to Figure 34). The base pressure between the rockets has gone up dramatically over the low AR case due to greater recirculation. The magnitude of this rise in P6 is shown in Figure 63. This same trend is noted when going from the unshrouded low AR nozzle model to the high AR nozzle model in the far ramjet nozzle mode. This effect can be seen in Figure 64. P5 on the other hand has decreased quite a bit due to the lower exit plane pressures of the high AR nozzles. P3 and P4 are also lower due to the lower exit plane pressures of the high AR nozzles. The sudden jump in P3 near the middle of the experiment is due to the back pressure reaching the area of P3. The pressure differential in this model shows the pressure near the rockets greater than the pressure near the ramjet. The effects of increasing ramjet plenum pressure are shown in Figures 65, 66, 67 and 68. The strong recirculation which was present in three earlier models (see Figure 34, Figures 30, 31, 32 and 33 and Figures 58, 59, 60 and 61) around P5 is again present at higher ramjet plenum pressures. The recirculation effects keep P6 nearly constant as the ramjet plenum pressure increases. As in all previously considered configurations, the main effect of increasing the ramjet plenum pressure is to increase the base pressures around the ramjet (P3 and P4). As before in the case of using a shroud, P3 decreases with increasing back pressure due to constriction of the boundary layer. This reduction of P3 is seen in Figures 43 and 56, Figures 46, 47, 48 and 49, Figures 52, 53, 54 and 55, and Figures 58, 59, 60 and 61. As the ramjet plenum pressure increased, the pressure differential shows the pressures between rockets and ramjet not changing

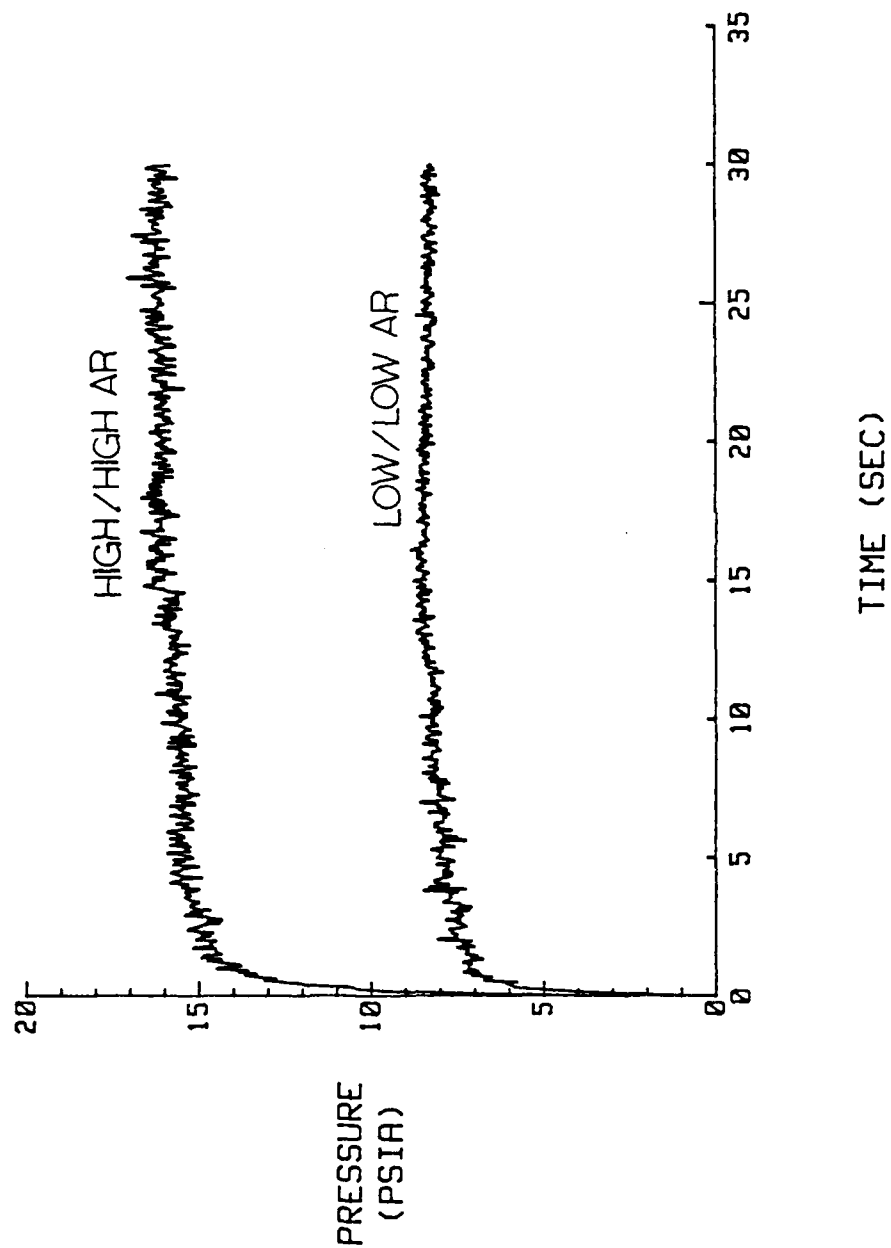


Figure 63. P6 Vs Time for Shrouded, Far Ramjet Nozzle,
Low/Low and High/High AR

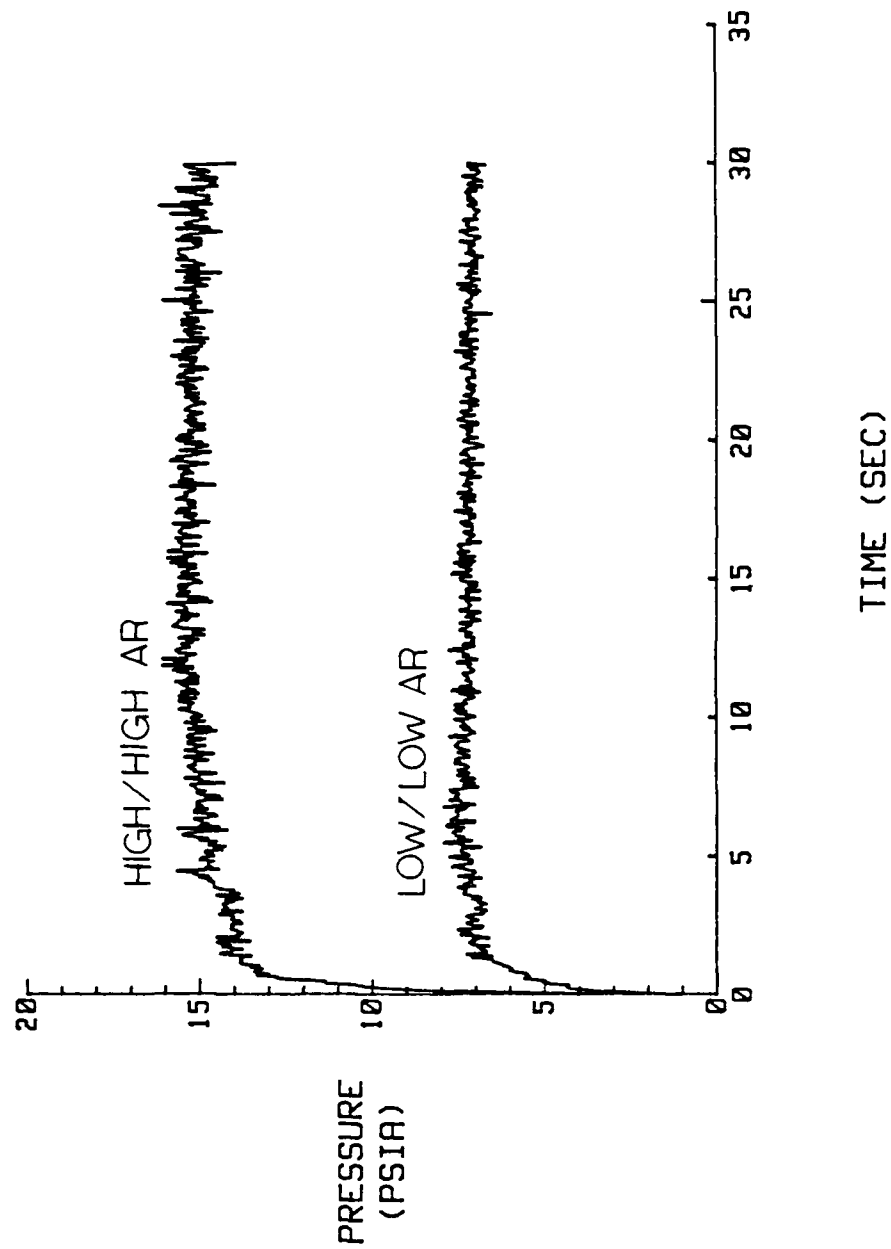


Figure 64. P6 Vs Time for Unshrouded, Far Ramjet Nozzle,
Low/Low and High/High AR

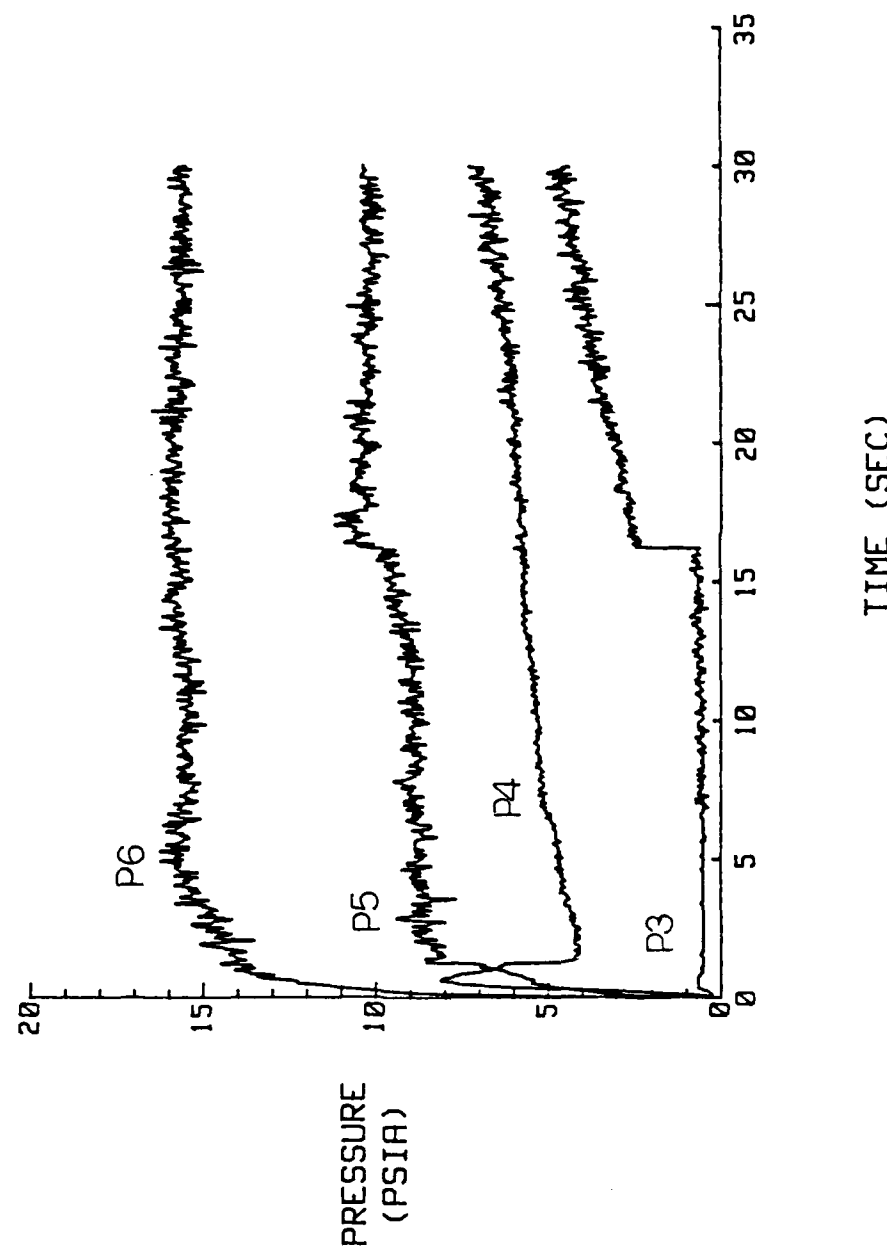


Figure 65. P3, P4, P5 and P6 Vs Time for Shrouded,
Far Ramjet Nozzle, High/High AR; $P_{rjp} = 52$ psia

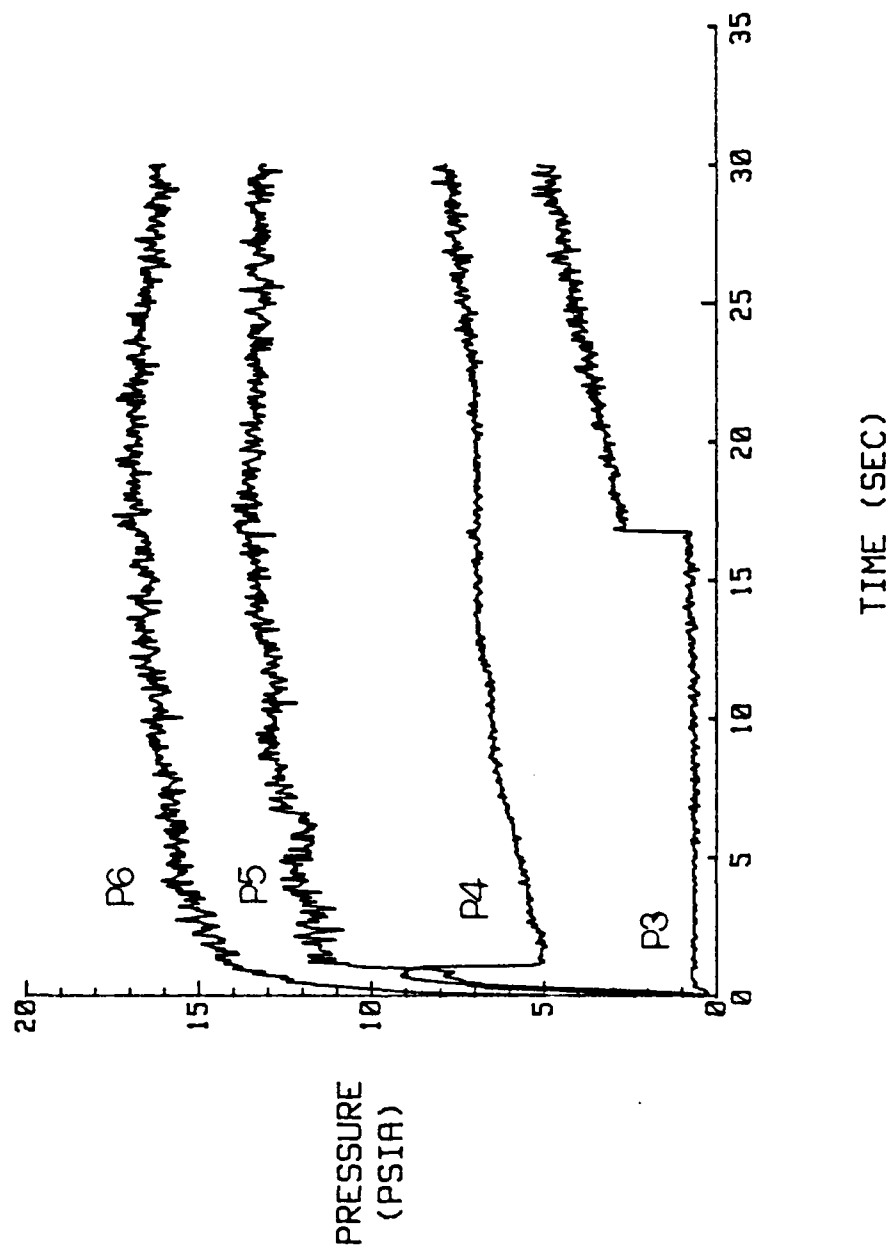


Figure 66. P3, P4, P5 and P6 Vs Time for Shrouded,
Far Ramjet Nozzle, High/High AR; $P_{rjp} = 62$ psia

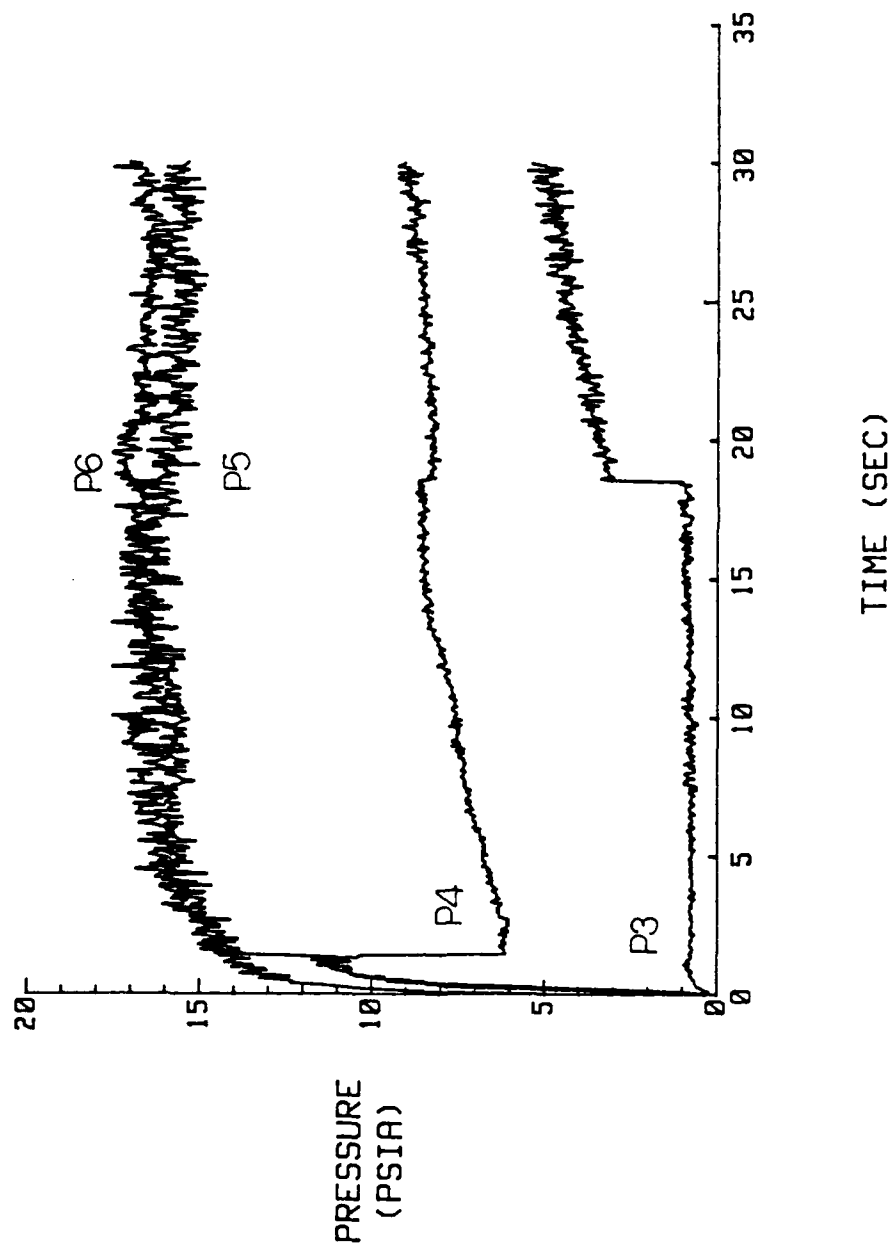


Figure 67. P3, P4, P5 and P6 Vs Time for Shrouded, Far Ramjet Nozzle, High/High AR; $P_{rjp} = 72$ psia

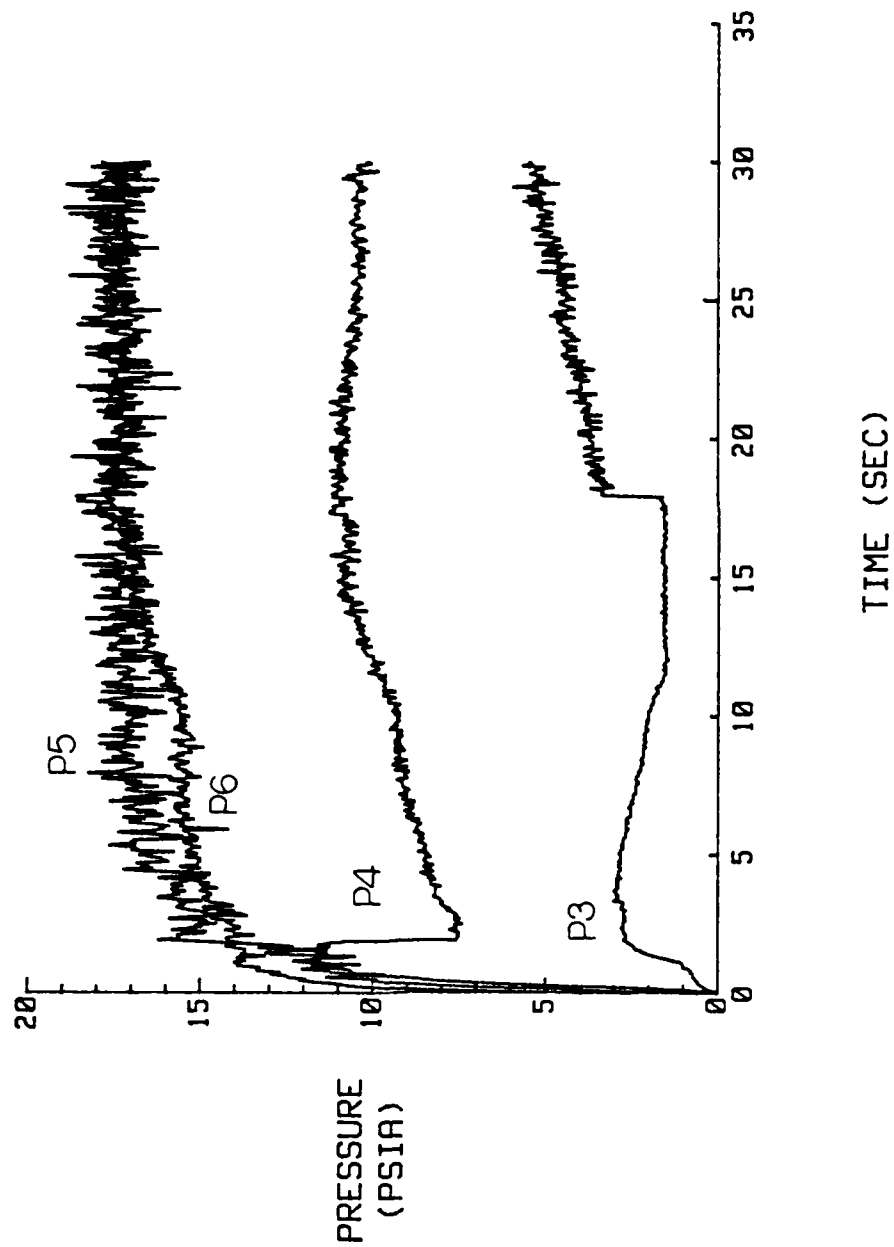


Figure 68. P3, P4, P5 and P6 Vs Time for Shrouded,
Far Ramjet Nozzle, High/High AR; $P_{rjp} = 87$ psia

except that both base pressures in the region between rockets and ramjet (P4 and P5) increase in nearly equal magnitudes at the highest ramjet plenum pressure. As the ramjet plenum pressure increased, P5 changed most first at the middle ramjet plenum pressures, then P4 caught up near the highest ramjet plenum pressure.

Shrouded, Close Ramjet Nozzle, Low/Low AR

The next model investigated was one where the ramjet nozzles were close in to the rockets, but the shrouds were far out from the model centerline. The base pressures for the shrouded, close ramjet nozzle, low/low AR configuration are in Figure 69. The main effect of the shroud being further out is that the back pressure is detected much later (compare Figure 69 to Figure 43). A typical flow pattern for this model is in Figure 70. Compare this flow pattern to the flow pattern of Figure 44 to see the effects of shroud location. Both pictures were taken at approximately the same back pressure and operating conditions. For this model, the pressure differential is nearly the same as for the model with the close in shroud. Compare Figure 69 to Figure 43 to see this. The pressure near the ramjet is higher than the pressure near the rocket. The effects of increasing the ramjet plenum pressure are shown in Figures 71, 72, 73 and 74. As the ramjet plenum pressure increased, the effects of the back pressure are staved off until the back pressure became quite high. In Figure 69, the back pressure is first felt by P3 due to pressure communication traveling upstream in the boundary layer. At the higher ramjet plenum pressures, the waves from the ramjets attach to the shroud until the back pressure forces the ramjet plume to connect to the rocket plumes. This constricts the boundary layer on the shroud and

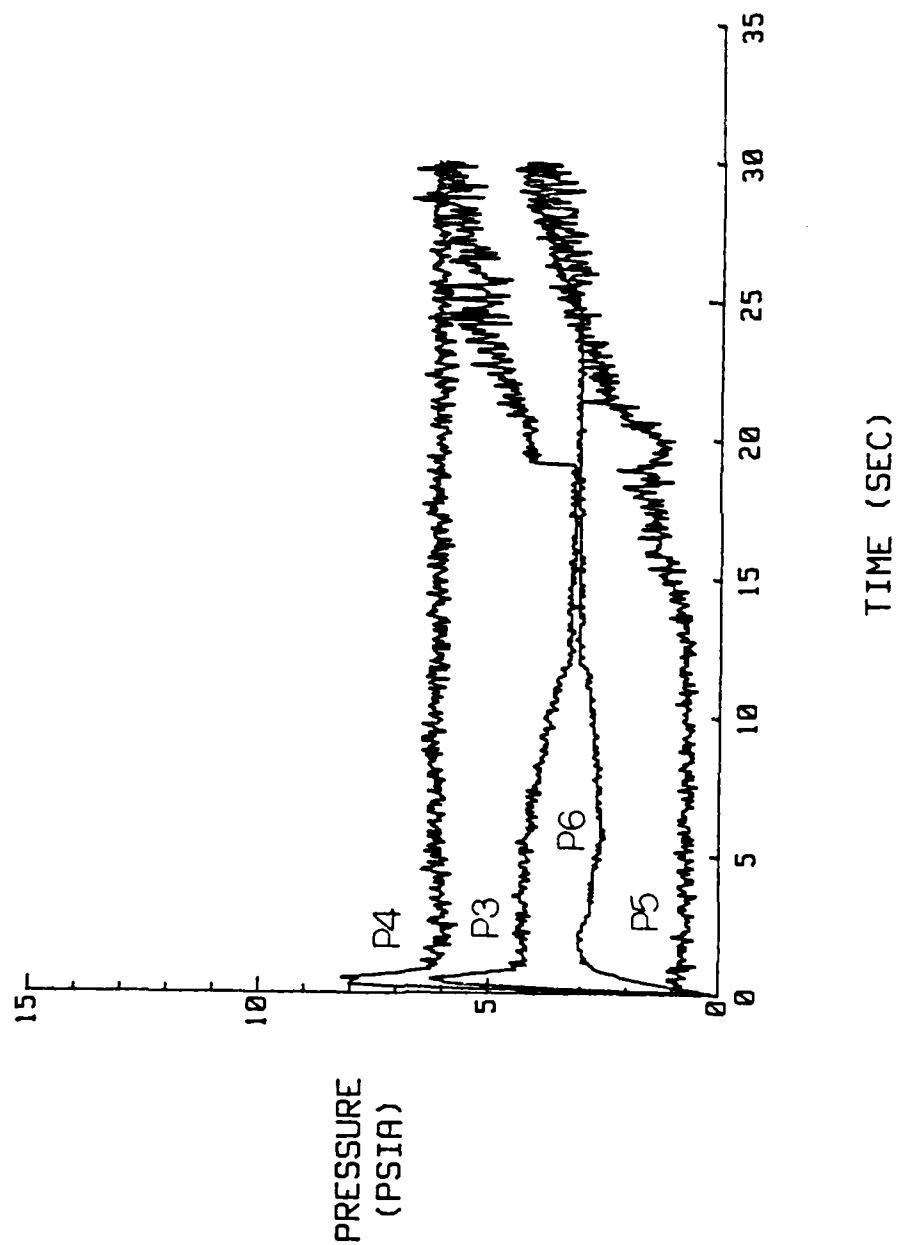


Figure 69. P3, P4, P5 and P6 Vs Time for Shrouded,
Close Ramjet Nozzle, Low/Low AR; $P_{rjp} = 42$ psia

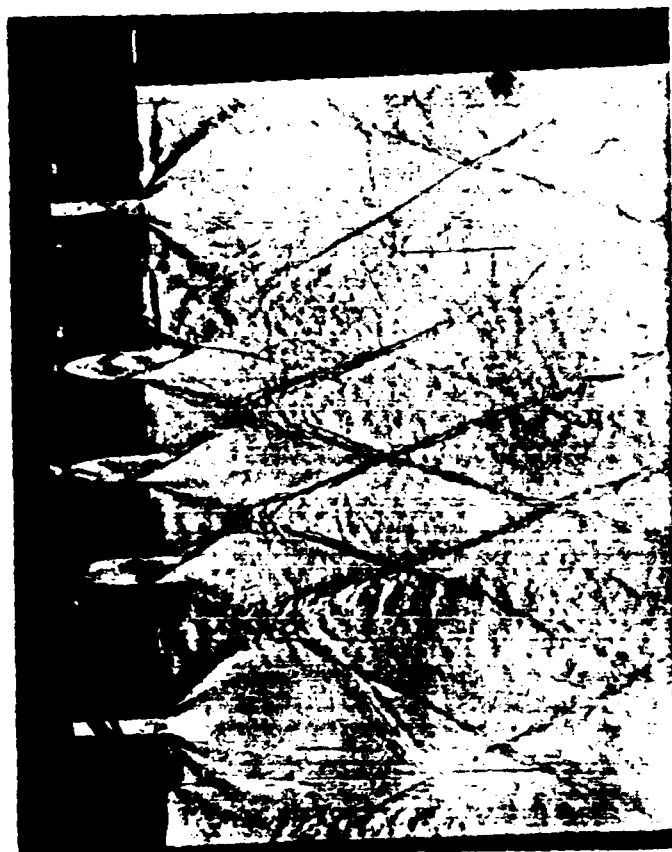


Figure 70. Typical Flow Pattern for Shrouded,
Close Ramjet Nozzle, Low/Low AR

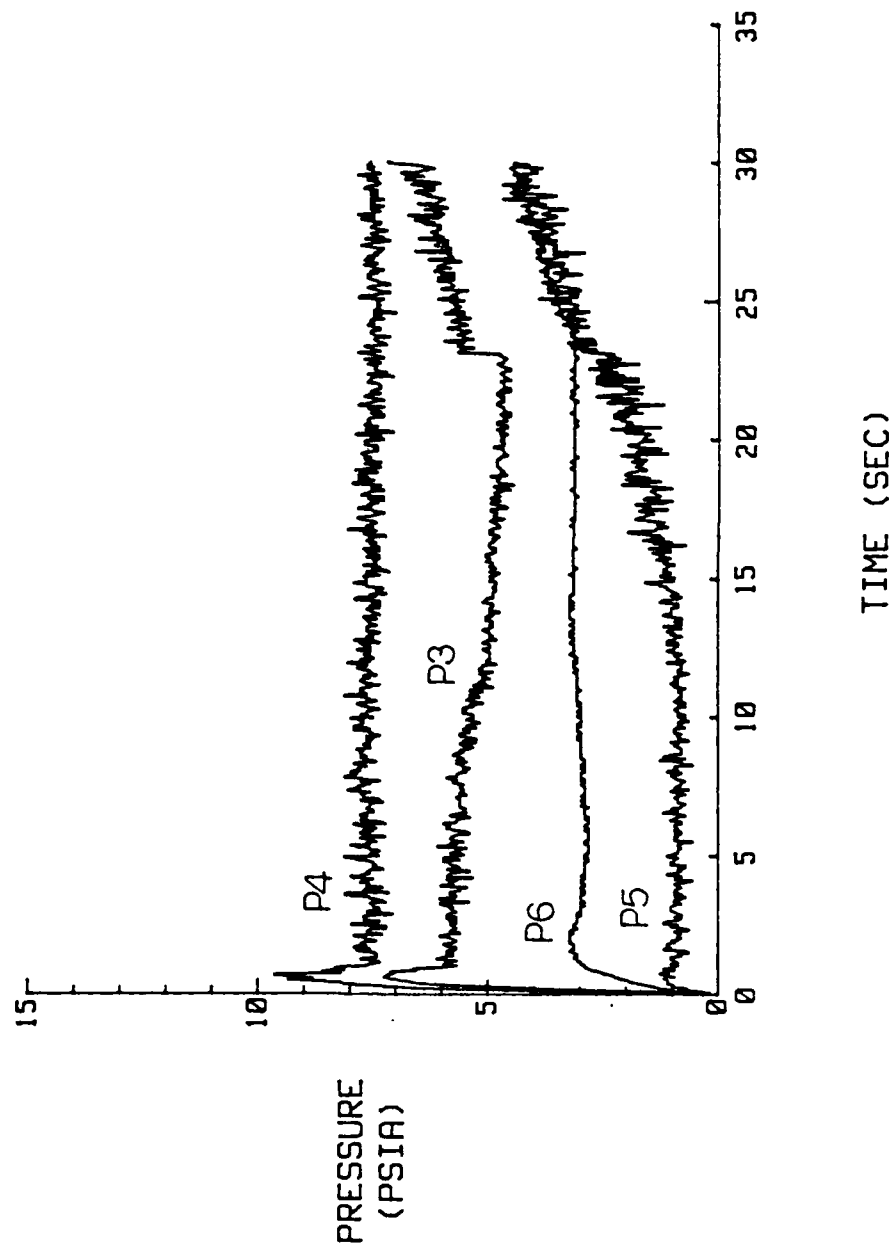
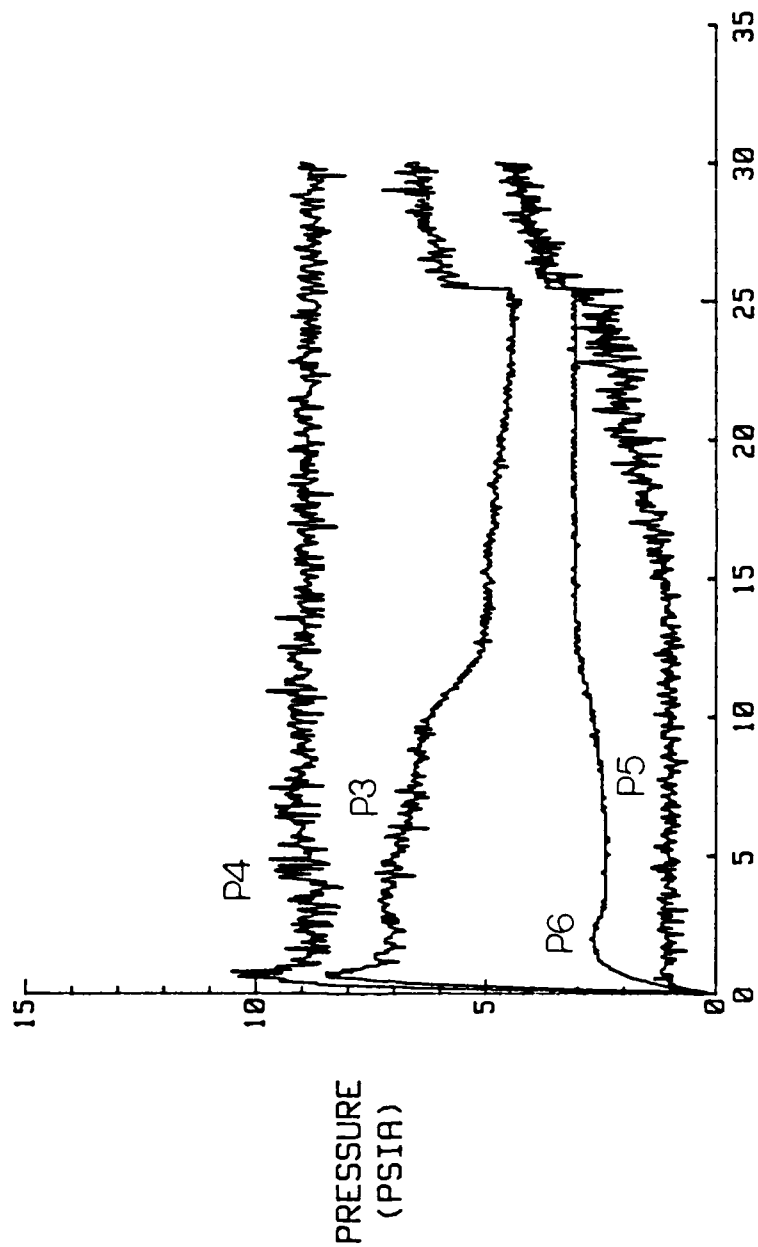


Figure 71. P3, P4, P5 and P6 Vs Time for Shrouded,
Close Ramjet Nozzle, Low/Low AR; $P_{rjp} = 52$ psia



TIME (SEC)

Figure 72. P3, P4, P5 and P6 Vs Time for Shrouded,
Close Ramjet Nozzle, Low/Low AR; $P_{rjp} = 62$ psia

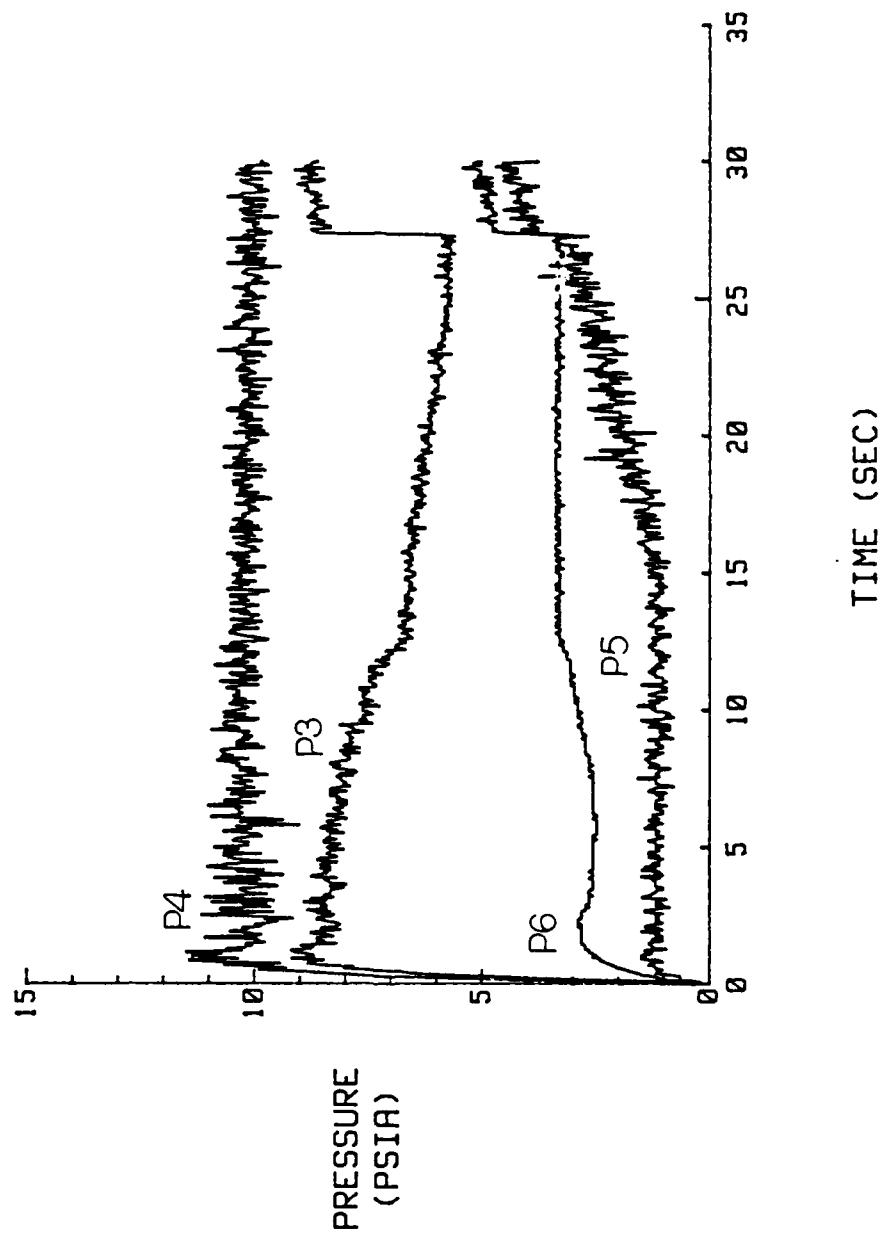


Figure 73. P3, P4, P5 and P6 Vs Time for Shrouded,
Close Ramjet Nozzle, Low/Low AR; $P_{rjp} = 72$ psia

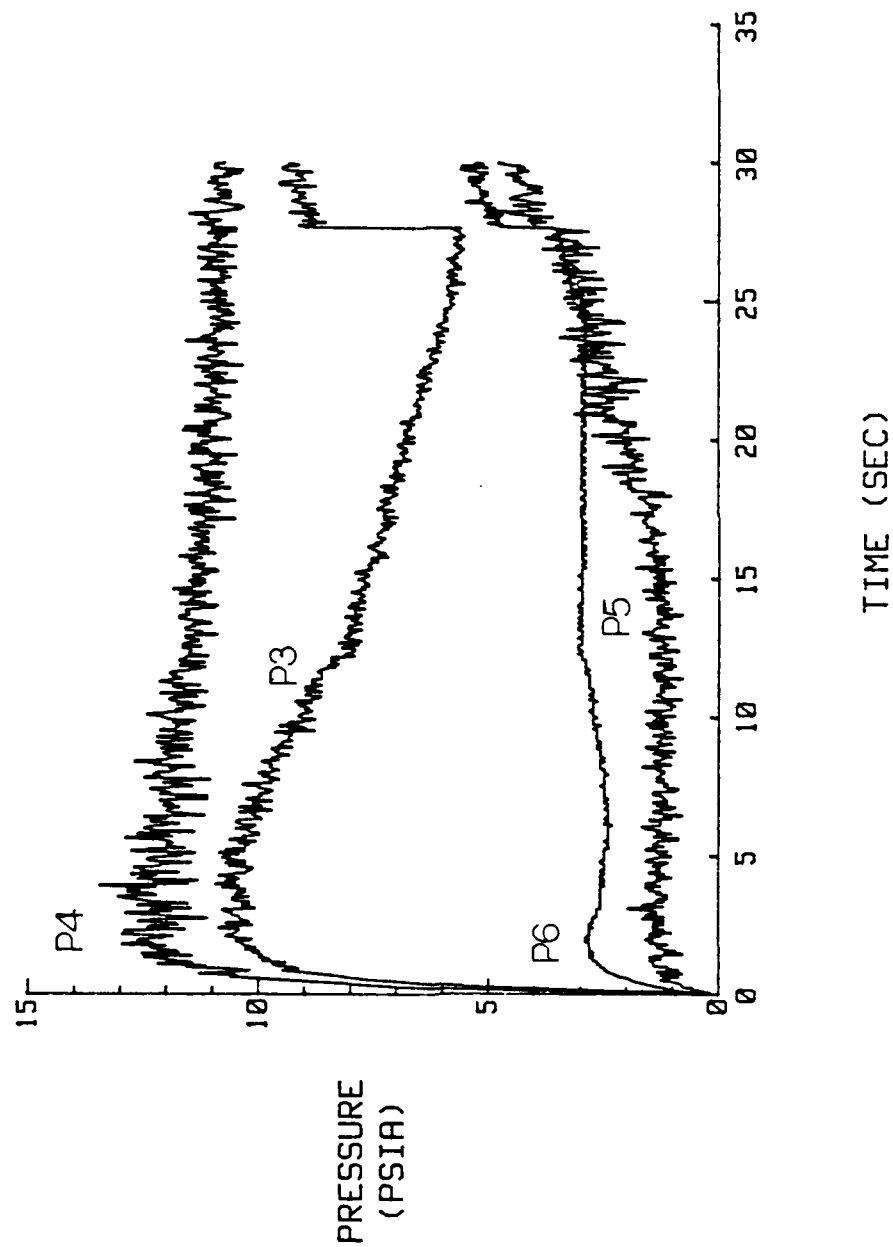


Figure 74. P3, P4, P5 and P6 Vs Time for Shrouded,
Close Ramjet Nozzle, Low/Low AR; $P_{rjp} = 87$ psia

restricts the pressure communication upstream through the boundary layer. This causes P3 to decrease. When the back pressure is strong enough to break the bond between the ramjet flow and the shroud, ramjet flow attaches to the rocket flow, allowing the back pressure to be felt at P3. At the higher ramjet plenum pressures, the pressure differential between the rockets and ramjet shows the low pressure near the rocket stays low and the high pressure near the ramjet gets higher as the ramjet plenum pressure increases.

Shrouded, Close Ramjet Nozzle, High/High AR

The high AR nozzles were installed giving the base pressures for the shrouded, close ramjet nozzle, high/high AR configuration shown in Figure 75. A typical flow pattern for this model is in Figure 76. The high AR model has recirculation in the area of P3 and P4 which is what kept these higher than P5 and P6. But P3 and P4 are lower for this model than for the low AR model due to the high AR nozzles having a lower exit plane pressure. The high AR model keeps the pressures at P5 and P6 relatively low due to the low exit plane pressures of these nozzles. P5 and P6 are also protected by the rocket exhaust wave structure. The pressure differential between the rockets and the ramjet indicates the pressure near the ramjet is higher than the pressure near the rockets. The effects of increasing the ramjet plenum pressure for this model are in Figures 77, 78, 79 and 80. The most noticeable effects of increasing the ramjet plenum pressure are to increase the base pressures around the ramjets and to delay any back pressure effects. These effects are slight, however. The stronger ramjet waves interacting with the rocket waves protects the base regions against higher back pressures. The

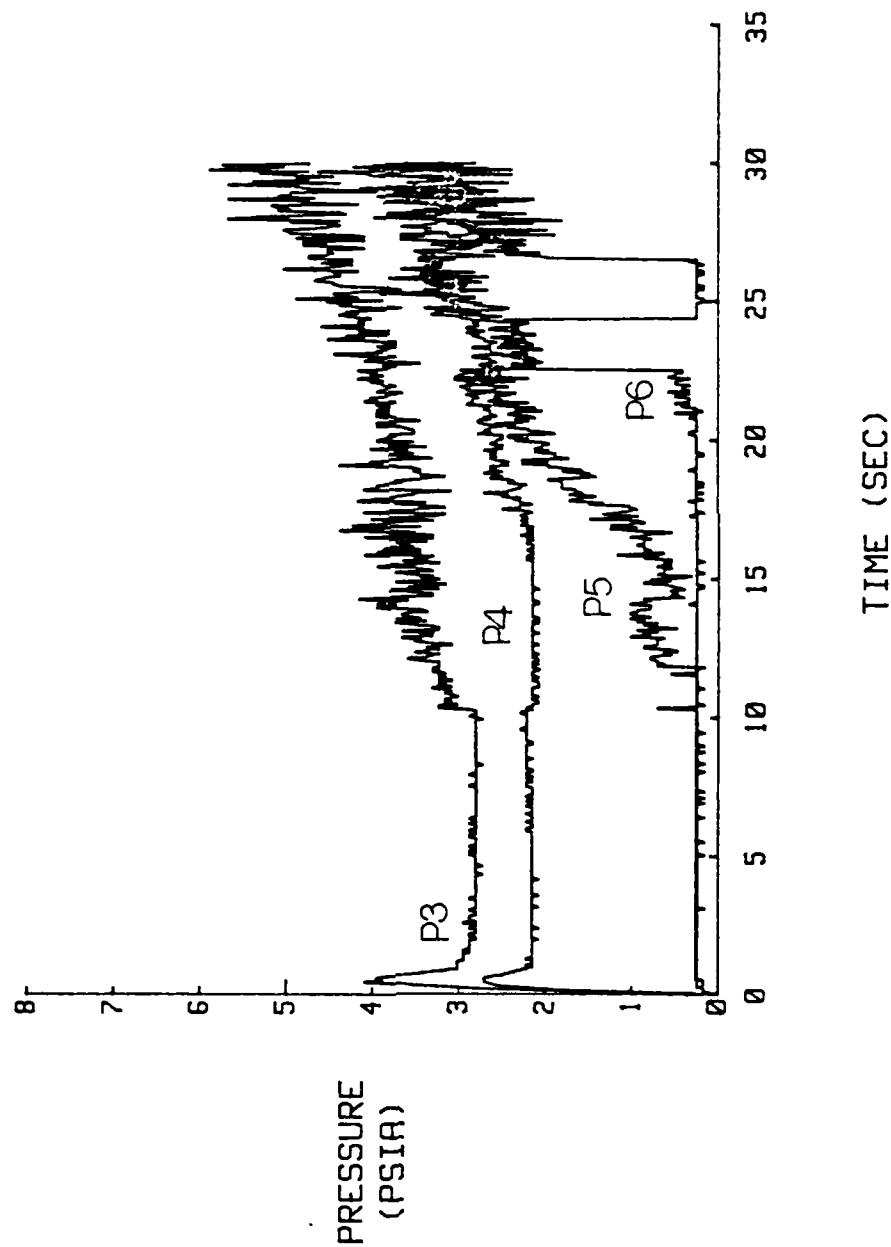


Figure 75. P3, P4, P5 and P6 Vs Time for Shrouded, Close Ramjet Nozzle, High/High AR; $P_{rjp} = 42$ psia

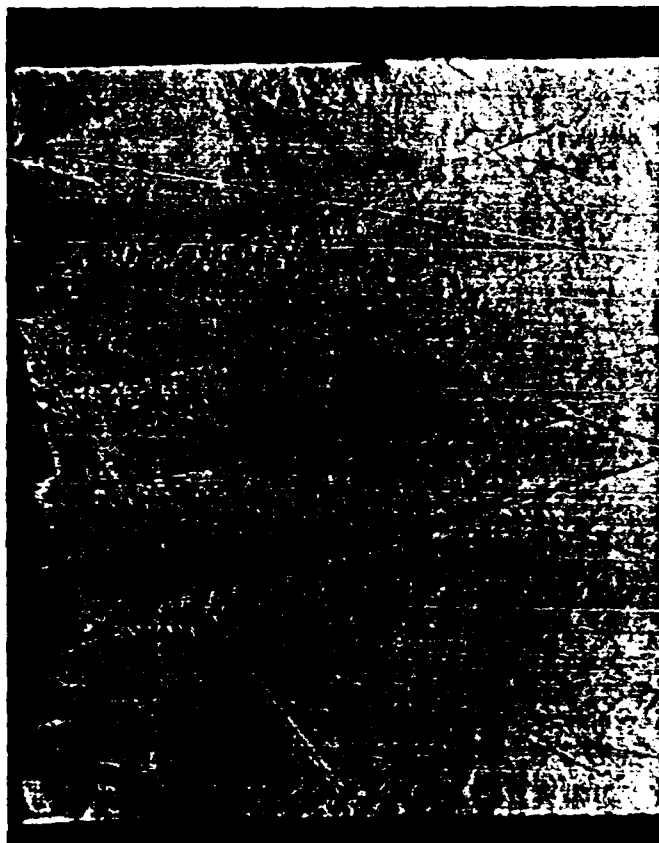


Figure 76. Typical Flow Pattern for Shrouded,
Close Ramjet Nozzle, High/High AR

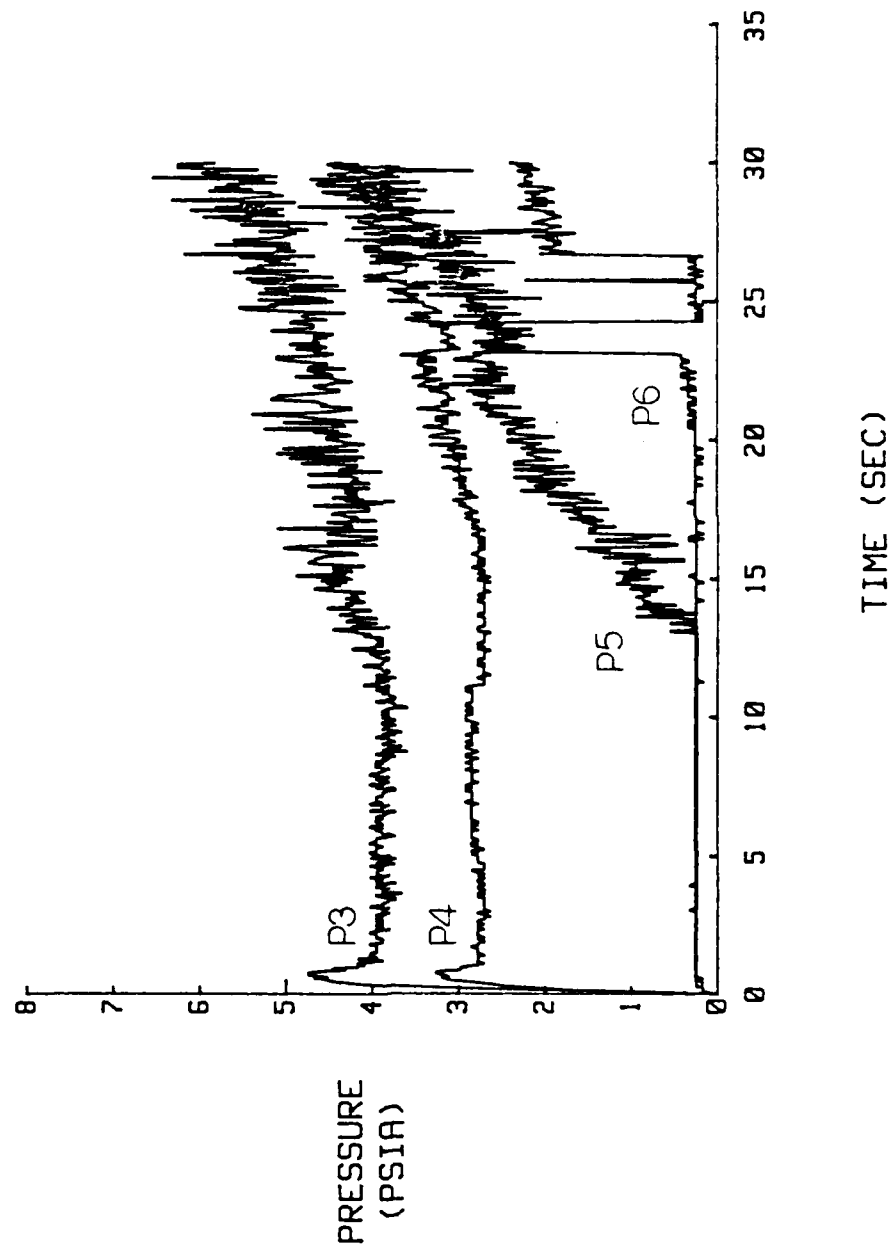


Figure 77. P3, P4, P5 and P6 Vs Time for Shrouded, Close Ramjet Nozzle, High/High AR; $P_{rjp} = 52$ psia

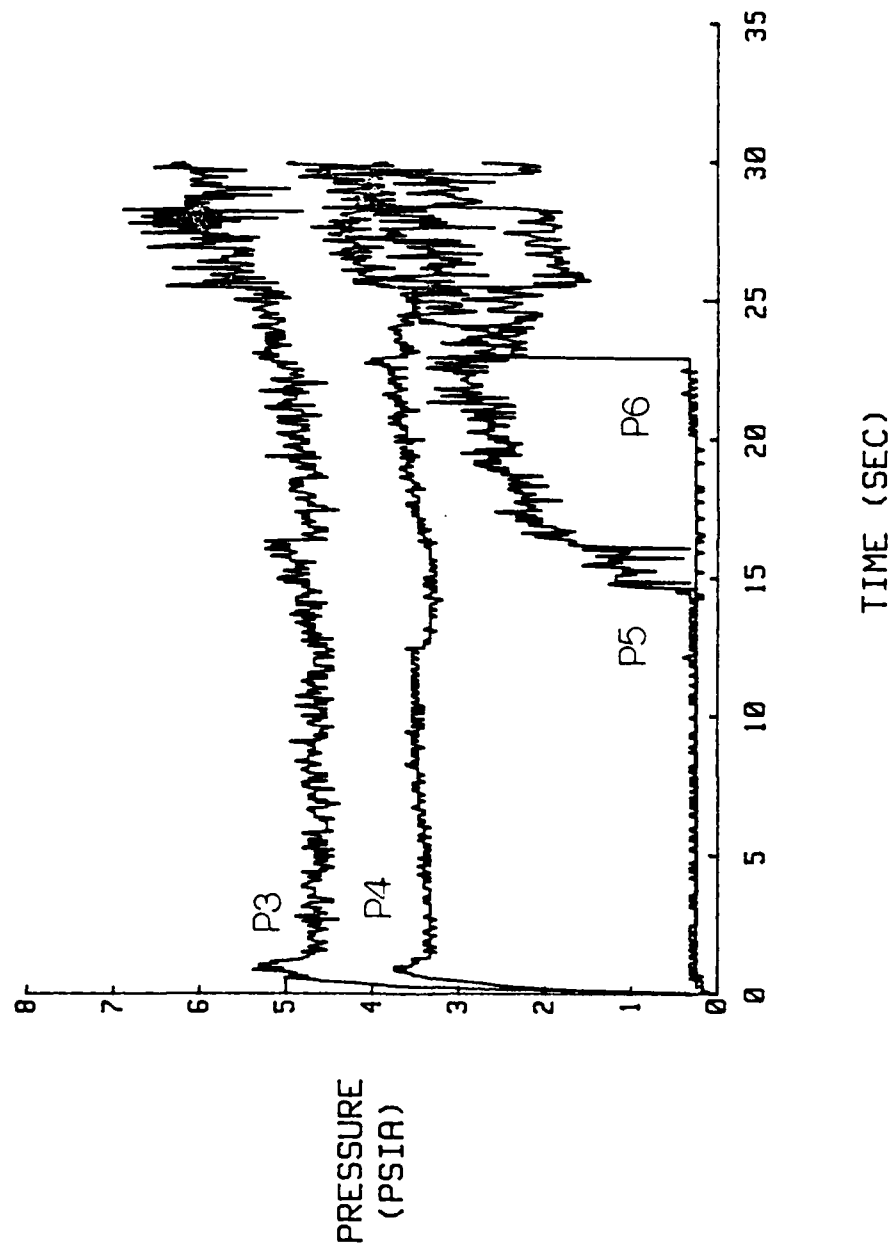


Figure 78. P3, P4, P5 and P6 Vs Time for Shrouded, Close Ramjet Nozzle, High/High AR; $P_{rjp} = 62$ psia

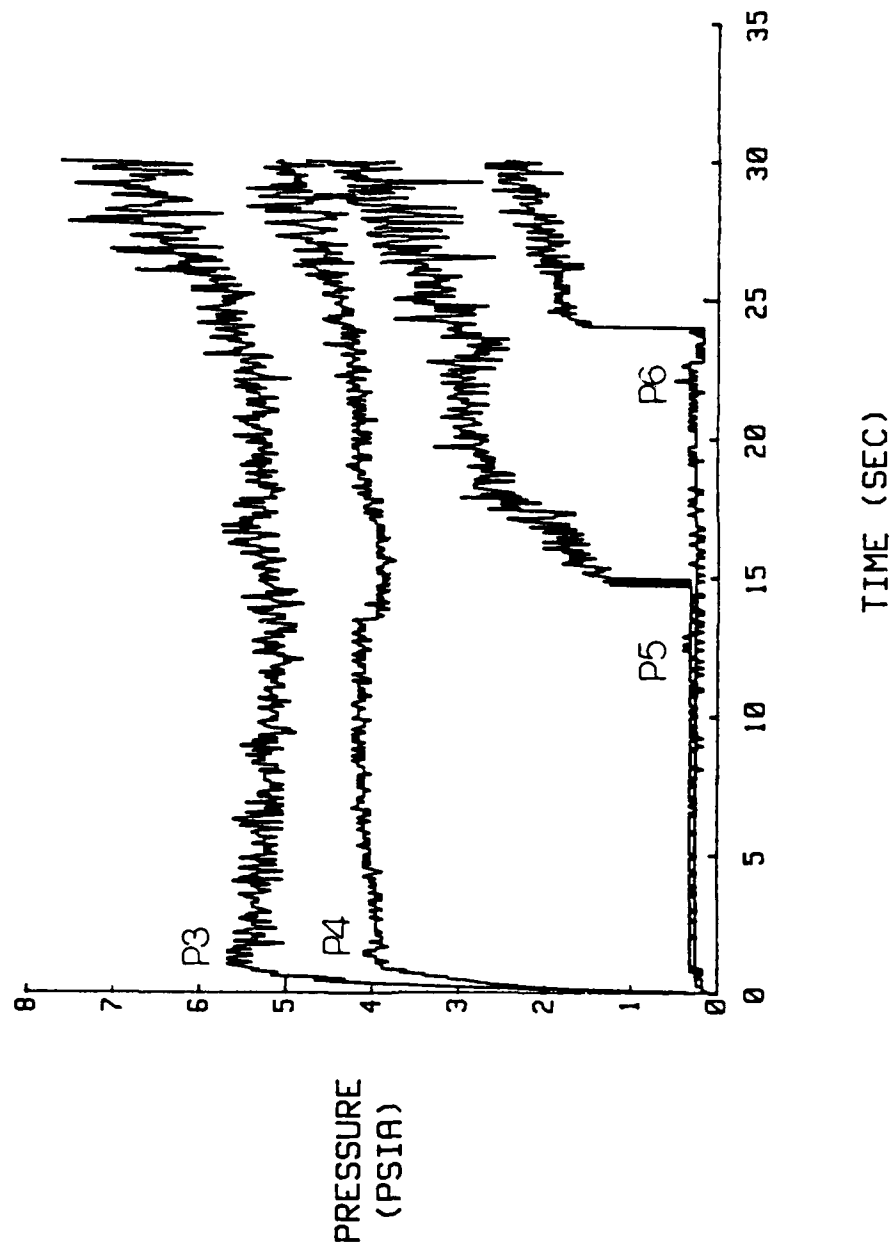


Figure 79. P3, P4, P5 and P6 Vs Time for Shrouded, Close Ramjet Nozzle, High/High AR; $P_{rjp} = 72$ psia

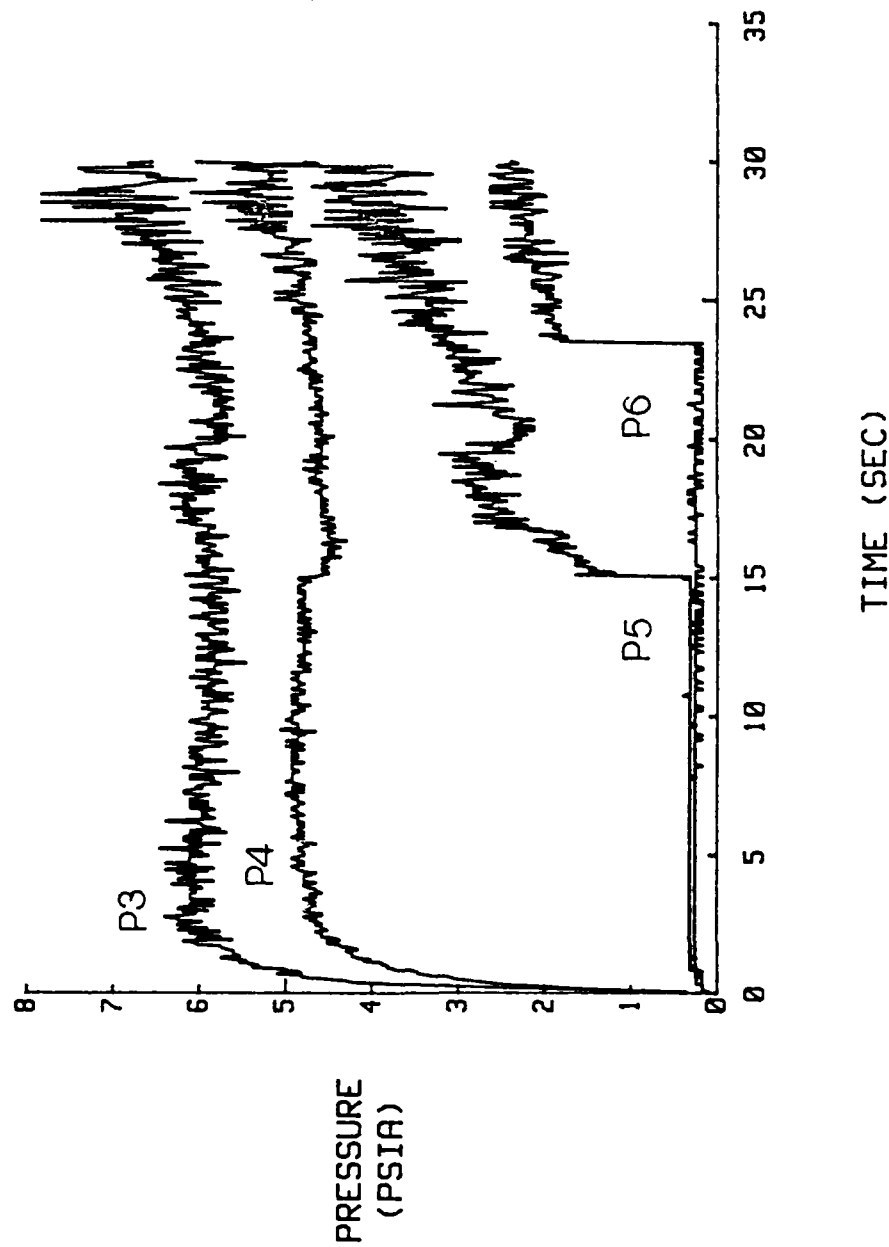


Figure 80. P3, P4, P5 and P6 Vs Time for Shrouded, Close Ramjet Nozzle, High/High AR; $P_{rjp} = 87$ psia

pressure differential between the rockets and the ramjet at increased ramjet plenum pressure indicates the base pressure to be greater near the ramjet and lesser near the rockets.

In summary of the discussions, the effects of adding ramjet flow to rocket only flow are to modify the recirculation zone between the rockets and to increase the base pressure in the area of the ramjets. This is true for both the shrouded and the unshrouded baseline configurations. In the recirculation regions between the ramjet and the shroud and between ramjet and rockets, the base pressures are established by the flow recirculated into the base regions and balanced by flow entrainment across the waves bounding the flow recirculation regions.

There are a number of effects on the base pressures that result from changing the shroud position from 2.5 inches from the model centerline to 2.0 inches from the model centerline for the high AR nozzles. In comparing Figure 51 to Figure 75, the base pressure is reduced significantly when the shroud is moved from its close position to its far position. Also, when the shroud is moved further out from the model centerline, the base pressure between the ramjet and the shroud is increased somewhat. The pressures between rockets and ramjet are relatively unaffected by the shroud position. These same trends hold true even as the ramjet plenum pressure is increased. This can be seen by comparing Figures 52, 53, 54 and 55 to Figures 77, 78, 79 and 80. On the other hand, there are few effects, if any, of the shroud position for the low AR models. Even as ramjet plenum pressure is increased, the effect of shroud placement is small on the low AR models. Figures 43,

69, Figures 46, 47, 48 and 49 and Figures 71, 72, 73 and 74 show the effect of shroud placement.

In two specific cases at high ramjet plenum pressure and in at least part of the overexpanded regime of nozzle operation the base pressure above the ramjet (P_3) is greater than the ambient pressure. Both of these cases are close ramjet nozzle configurations. One has high AR nozzles and the far shrouded configuration. The other has low AR nozzles and no shroud. The fact that the pressure in this area is higher than the ambient pressure could lead to a positive increase in the pressure area term of the momentum equation.

The most noteworthy effect of increasing the ramjet plenum pressure is to increase the base pressures in the areas of the ramjets. In most instances there is little effect on base pressures near the rockets (P_5 and P_6) when ramjet plenum pressure is increased. Another important effect of increasing the ramjet plenum pressure is to enable the various configurations to operate against higher back pressures.

VII. Conclusions

Pressure and flow relationships of 12 combinations of area ratio, shrouds, and ramjet nozzle spacing were investigated over a wide range of experimental conditions. The apparatus and associated instrumentation, including what was present before this experimentation and that which was fabricated solely for this experimentation, were sufficient for this research. The results of this investigation led to the following conclusions:

1. Whenever a shroud is employed and the expansion waves from the ramjet attach to the shroud, as back pressure increases during an experiment, the attachment becomes stronger. This attachment constricts the boundary layer and lessens the pressure communication upstream through the boundary layer. With this constriction the base pressure between the ramjet and the shroud falls. This effect of lowering the base pressure between the shroud and the ramjet is more noticeable for higher ramjet plenum pressures and when the shroud and the ramjet nozzle are close together. This effect is also more apparent in models with the low area ratio nozzles which have a higher exit plane pressure.

2. The shroud has its greatest effect in the experimental mode where the ramjet nozzles are close in to the model centerline. The most effect of the shroud for the high area ratio nozzles is in going from an unshrouded model to a shroud close in to the ramjets. This is due to wave interaction between ramjets, rockets and the shroud. The shroud is able to direct the rocket and ramjet waves together at the center of the model and produce quite a bit of recirculation between the rockets thus

pushing that base pressure up significantly. For the low area ratio nozzles, the effect of the shroud is seen on the pressure between the ramjet and the shroud. Instead of this pressure rising with increasing back pressure as in the unshrouded case, this base pressure falls due to the interaction of the ramjet waves and the shroud.

3. The pressure differential which exists between the rockets and the ramjet is sometimes strong and at other times the two base pressures P_4 and P_5 are nearly equal. When the ramjet nozzles are close in to the rocket nozzles, the pressure differential between the rocket and ramjet exhaust streams is oriented so as to show the base pressure near the ramjet to be greater than the base pressure near the rocket. This occurs regardless of type of shrouding or area ratio. However, when the ramjets are far out from the rockets the pressure differential is oriented so as to show the base pressure between the ramjet and rockets close to the rockets to be the higher pressure. This also occurs regardless of shroud type and area ratio. Therefore, as the ramjets are moved further away from the rockets, the pressure differential between them changes direction.

4. When the ramjet nozzles are at their far position from the rocket nozzles and in the unshrouded configurations, the pressure in the base region of the model between the ramjet and the top of the model was sometimes greater than the ambient pressure. When there is a positive difference between the base pressure above the ramjet and the ambient pressure, this difference in pressure could lead to a somewhat significant increase in thrust. The pressure area term of the momentum thrust equation could be much greater with this additional base pressure.

This increase in thrust, however, must be tempered by the realization that this increase in thrust could come at the expense of added dry weight to a booster vehicle in the form of attachment equipment necessary to keep the ramjet at a large distance from the rockets.

VIII. Recommendations

The following recommendations are made for continuation of this work in the area of clustered rocket-ramjet nozzles:

1. On some occasions, the noise on the data acquisition channels became a hindrance to properly evaluating the data. A method for reducing this noise should be investigated.

2. The plexiglass panes used in this research are ideal for modifications to allow pressure measurements of the flow field on the sidewalls downstream of the nozzle exit planes. Likewise, the shrouds should be instrumented to take pressure measurements along them downstream of the nozzles.

3. A high speed motion picture camera capable of equalling or exceeding the data acquisition system's sampling rate capability should be obtained in order to be able to capture on film any dynamic phenomena. This film could then aid in explaining pressure measurements.

4. More extensive instrumentation of the base region between rockets and ramjet should be accomplished in order to further investigate the pressure differential which exists between these nozzles.

Bibliography

1. Maxwell, J. A. An Experimental Study of a Rocket Ramjet Nozzle Cluster. MS Thesis AFIT/GA/AA/87M-3. School of Engineering, Air Force Institute of Technology (AU), Wright-Patterson AFB OH, March 1987.
2. Rodgers, D. C. Investigation of Shrouded Nozzle Exit Pressure Changes. MS Thesis AFIT/GA/AA/86D-15. School of Engineering, Air Force Institute of Technology (AU), Wright-Patterson AFB OH, December 1986.
3. Moran, J. R. An Experimental Study of Clustered Nozzles with Variable Shrouds. MS Thesis AFIT/GA/AA/85D-1. School of Engineering, Air Force Institute of Technology (AU), Wright-Patterson AFB OH, December 1985.
4. Daley, D. H. "A Nozzle Operating Diagram," Bulletin of Mechanical Engineering Education, Vol. 6, pp. 245-257. Pergamon Press, 1967.
5. Hill, P. G. and C. R. Peterson. Mechanics and Thermodynamics of Propulsion. Reading, Massachusetts: Addison-Wesley, 1970.
6. Lancaster, O. E. Jet Propulsion Engines. Princeton University Press, 1959.
7. Bjurstrom, D.R. An Experimental Study of Clustered, Two-Dimensional Rocket Nozzles. MS Thesis AFIT/GA/AA/84D-1. School of Engineering, Air Force Institute of Technology (AU), Wright-Patterson AFB OH, December 1984.
8. Shapiro, A. H. The Dynamics and Thermodynamics of Compressible Fluid Flow. Vol. 1. New York: John Wiley and Sons, Inc., 1964.
9. Mulenburg, G. M. An Experimental Study of the Effect of Inlet Geometry on Flow and Performance of a Supersonic Nozzle. MS Thesis AFIT/ME69-11. School of Engineering, Air Force Institute of Technology (AU), Wright-Patterson AFB OH, December 1969.
10. Sutton, G. P. and D. Ross. Rocket Propulsion Elements (Fourth Edition). New York: John Wiley and Sons, Inc., 1976.
11. Holmes, B. K. and R. J. Matz. An Investigation of the Multi-Nozzle Rocket Shroud Concept. AEDC-TR-65-249. Arnold AFS, Tennessee: ARO Inc., February 1965 (AD 369808).

12. Franke, M. E. Lecture notes and materials distributed in MENG 630, Fluid Mechanics of Rockets, School of Engineering, Air Force Institute of Technology (AU), Wright-Patterson AFB, Ohio. January to March 1987.
13. Barton, D. L. and D. Taylor. An Investigation of Ejectors Without Induced Flow. AEDC-TN-59-145. Arnold AFS, Tennessee: ARO Inc., December 1959.
14. Hewlett-Packard. Operating Manual for the 6901S Measurement and Analysis System. HP Part Number 06901-90003. October 1983.
15. Huband, G. W. Numerical Study of Supersonic Flows Using Different Techniques. MS Thesis AFIT/GA/AA/86D-8. School of Engineering, Air Force Institute of Technology (AU), Wright-Patterson AFB, OH, December 1986.

Vita

Captain Timothy R. Wesling was born on 16 September 1960 in Palmer, Massachusetts. In June 1982 he received his Bachelor of Aerospace Engineering degree from the Georgia Institute of Technology. Following graduation, he received a commission in the USAF through the ROTC program. His first duty station was the then Air Force Rocket Propulsion Laboratory for three and one half years. He served as a Development Engineer for 16 months and as a Ballistic Missile and Space Propulsion Analyst for 26 months. Captain Wesling entered the Air Force Institute of Technology in May 1986.

Permanent Address: 3550 Pecan Point Drive
Sugarland, Texas 77478

ADA189714

REPORT DOCUMENTATION PAGE

Form Approved
OMB No. 0704-0188

1a. REPORT SECURITY CLASSIFICATION Unclassified			1b. RESTRICTIVE MARKINGS		
2a. SECURITY CLASSIFICATION AUTHORITY			3. DISTRIBUTION/AVAILABILITY OF REPORT Approved for public release; distribution unlimited.		
2b. DECLASSIFICATION/DOWNGRADING SCHEDULE					
4. PERFORMING ORGANIZATION REPORT NUMBER(S) AFIT/GA/AA/87D-9			5. MONITORING ORGANIZATION REPORT NUMBER(S)		
6a. NAME OF PERFORMING ORGANIZATION School of Engineering		6b. OFFICE SYMBOL (If applicable) AFIT-ENY		7a. NAME OF MONITORING ORGANIZATION	
6c. ADDRESS (City, State, and ZIP Code) Air Force Institute of Technology Wright-Patterson Air Force Base, Ohio 45433			7b. ADDRESS (City, State, and ZIP Code)		
8a. NAME OF FUNDING/SPONSORING ORGANIZATION		8b. OFFICE SYMBOL (If applicable)		9. PROCUREMENT INSTRUMENT IDENTIFICATION NUMBER	
8c. ADDRESS (City, State, and ZIP Code)			10. SOURCE OF FUNDING NUMBERS		
		PROGRAM ELEMENT NO.		PROJECT NO.	TASK NO.
				WORK UNIT ACCESSION NO.	
11. TITLE (Include Security Classification) An Experimental Investigation Of Rocket Ramjet Nozzle Assembly Base Pressures					
12. PERSONAL AUTHOR(S) Timothy R. Wesling, Capt, USAF					
13a. TYPE OF REPORT MS Thesis		13b. TIME COVERED FROM _____ TO _____		14. DATE OF REPORT (Year, Month, Day) 1987 December	
15. PAGE COUNT 151					
16. SUPPLEMENTARY NOTATION					
17. COSATI CODES			18. SUBJECT TERMS (Continue on reverse if necessary and identify by block number)		
FIELD	GROUP	SUB-GROUP	Clustered Nozzles, Base Pressures		
			Rocket Ramjet Assemblies		
19. ABSTRACT (Continue on reverse if necessary and identify by block number) Thesis Advisor: Dr. William C. Elrod, Professor Department of Aeronautics and Astronautics ABSTRACT ON BACK					
20. DISTRIBUTION/AVAILABILITY OF ABSTRACT <input type="checkbox"/> UNCLASSIFIED/UNLIMITED <input checked="" type="checkbox"/> SAME AS RPT. <input type="checkbox"/> DTIC USERS			21. ABSTRACT SECURITY CLASSIFICATION Unclassified		
22a. NAME OF RESPONSIBLE INDIVIDUAL Dr. William C. Elrod			22b. TELEPHONE (Include Area Code) 513 255 3517		22c. OFFICE SYMBOL AFIT-ENY

Approved for public release: DAW AIR 180-14.
24K24V
Development
Development

This research project involves the investigation of base pressures of clustered rocket-ramjet nozzles under shrouded and unshrouded conditions. Twelve combinations of expansion ratios and shrouds for rocket-ramjet nozzle clusters in cold flow were investigated. Pressure measurements were made along the base of the rocket-ramjet cluster under simulated conditions ranging in altitudes up to 70,000 feet and flight Mach numbers to just over 3.0. Comparisons were made of the effects on nozzle base pressures of altitude, ramjet plenum pressure, nozzle geometry and shrouding.

Results of this investigation show a potential increase in base pressure thrust for certain nozzle geometries is possible. As the ramjet nozzle exit distance from the centerline of the nozzle assembly increases for unshrouded cases, the base pressure thrust also increases. This appears to be due to recirculation of exhaust gases. There appear to be variations in performance caused by changes in the distance of the shroud from the nozzle assembly centerline. Also, there is a pressure gradient between nozzles in the base region which is affected by configuration and which has an important effect on evaluating the base pressures.

END

DATE

FILMED

4-88

DTIC